Light hadron masses from lattice QCD

Zoltan Fodor* and Christian Hoelbling†

Bergische Universität Wuppertal, Gausstrasse 20, D-42119 Wuppertal, Germany

(published 4 April 2012)

This article reviews lattice QCD results for the light hadron spectrum. An overview of different formulations of lattice QCD with discussions on the fermion doubling problem and improvement programs is given. Recent developments in algorithms and analysis techniques that render calculations with light, dynamical quarks feasible on present day computer resources are summarized. Finally, spectrum results for ground state hadrons and resonances using various actions are summarized.

DOI: 10.1103/RevModPhys.84.449 PACS numbers: 11.15.Ha, 12.38.Gc, 14.20.−c, 14.40.−n

CONTENTS

I. INTRODUCTION

Already at the beginning of the 19th century, it was speculated by Prout (1815) that the hydrogen atom was the basic building block for all other atoms. The mass of the proton, as mass of the hydrogen atom, was known within a factor of 2 accuracy already during the late 19th century (Loschmidt, 1865). Later, the development of mass spectrometry (Goldstein, 1886) allowed a precision measurement of the e/m ratio of the hydrogen nucleus (Wien, 1902; Thomson, 1907) and following the discovery of the atomic nucleus by Rutherford (1911), he showed that hydrogen nuclei were present in other nuclei (Rutherford, 1919) and coined for them the name protons.

The neutron was discovered 13 years later by Chadwick (1932), who also determined its mass with a 2 per mil accuracy. The first meson to be discovered was the pion (Lattes *et al.*, 1947), shortly followed by the kaon (Rochester and Butler, 1947) and the Λ (Seriff *et al.*, 1950), the first strange particles. While these discoveries were made in cosmic ray experiments, the first resonance, the Δ, was discovered by Brueckner (1952) at a cyclotron source. During the following years, these modern accelerators led to a proliferation of hadronic states and it became obvious that they could not all be regarded as elementary.

This large number of hadronic states could first be successfully described by their quark substructure (Gell-Mann, 1961), for which finally quantum chromodynamics (QCD) was found as the dynamical theory by Fritzsch, Gell-Mann, and Leutwyler (1973). With the discovery of asymptotic freedom (Gross and Wilczek, 1973; Politzer, 1973), which built on earlier work regarding the renormalizability of non-Abelian gauge theories by 't Hooft and Veltman (1972), and the qualitative understanding of the confinement phenomenon (Wilson, 1974) a coherent picture of the strong interaction finally emerged. At energies that are large compared to the typical QCD scale $\Lambda_{\mathrm{QCD}} \sim 250$ MeV, the coupling is small and quarks and massless gluons emerge as the fundamental degrees of freedom. At low energies, however, the spectrum of QCD consists of quark-gluon bound states that one would like to identify with the experimentally observed hadrons. Although this qualitative picture is quite compelling, it is nevertheless very difficult to solve QCD in the low energy regime, where it is a strongly coupled theory, and predict, respectively, postdict the hadron spectrum from first principles.

In this review, we summarize the current state of the art of computing the light hadron spectrum, i.e., the spectrum of hadrons with exclusively up, down, and strange valence quarks, directly in QCD. In Sec. II we introduce the primary

*fodor@bodri.elte.hu
†hch@physik.uni-wuppertal.de

tool to study QCD in the nonperturbative regime: lattice QCD. We review various possible discretizations of continuum QCD in view of their usefulness for *ab initio* calculations of light hadron masses with a small and controlled total uncertainty. In Sec. III we review current methods of extracting hadron masses in lattice QCD. We discuss efficient ways of extracting ground state masses as well as current methods to overcome the challenges in singlet and excited state spectroscopy. In Sec. IV we review methods for obtaining predictions at the physical point (the point in parameter space at which the quark masses have their physical values) in the infinite volume continuum theory. Finally in Sec. V we summarize present and notable past results and conclude with an overview of the present understanding of the hadron spectrum from lattice QCD. As a convention when quoting lattice results the first error is statistical and the second one (if given) is systematic unless explicitly noted otherwise.

II. LATTICE TECHNIQUES

Lattice field theory is in most cases the only known systematic way of nonperturbatively computing Green's functions in quantum field theories. It is especially useful in contexts where perturbative treatment is usually inadequate, which is the case in low energy QCD.

Lattice gauge theory was introduced by Wilson (1974)[1] and recent overviews include Montvay and Munster (1994), Gupta (1997), Di Pierro (2000), Smit (2002), Rothe (2005), DeGrand and Detar (2006), and Gattringer and Lang (2010).[2]

In general, a nonperturbative lattice calculation proceeds in three steps. First, one introduces a UV regulator into the theory by means of a finite spacetime lattice. Then, one computes Green's functions in this discretized theory by means of stochastic integration of the path integral, and finally one removes the regulator in order to obtain the continuum result. The last step is possible in theories where the coupling does not diverge in the UV regime. Because of asymptotic freedom, QCD does belong to this class of theories and the cutoff can be removed.

In this section we mainly focus on the first step of the above procedure, the regularization of QCD on a spacetime lattice. This regularization is not unique and the ambiguity is reflected in the wide variety of lattice regularizations of QCD that are in use today, each carrying various advantages and disadvantages. We start with a brief introduction to the path integral formalism in Sec. II.A and the basics of the lattice discretization of QCD in Sec. II.B. We then introduce the basic concepts of the stochastic evaluation of the discretized path integral in Sec. II.C which are necessary to understand the further developments of Secs. II.D and II.E, where we discuss how to obtain efficient lattice regularized theories that actually go over into QCD upon removal of the cutoff. Finally, in Sec. II.F we briefly discuss anisotropic lattice regularizations of QCD that are relevant for excited state spectroscopy.

[1]Independent developments of Smit and Polyakov were never published; see, e.g., Wilson (2005).

[2]See also the classic introductory text by Creutz (1984).

The need for an efficient regularization arises particularly due to the smallness of the light quark masses compared to the intrinsic QCD scale Λ_{QCD}. On the one hand, the physical size of the lattice needs to be much larger than the correlation length of the system which in turn is given by the inverse of the mass of the lightest particle in the spectrum, the pion. On the other hand, the lattice cutoff needs to be much larger than Λ_{QCD} in order to not miss a substantial fraction of the nonperturbative dynamics. These two requirements combined necessitate a large number of lattice points if one wants to perform nonperturbative lattice QCD calculations at physically light quark masses. In connection with the fermion doubling problem the smallness of the light quark masses causes yet further problems that are discussed in detail in Sec. II.D.

Because of these effects, lattice QCD calculations until very recently were restricted to quark masses larger (and in most cases substantially so) than the physical ones. This in turn necessitated an extrapolation in the light quark mass to the physical point in addition to the already necessary continuum extrapolation. The fact that physically light quark masses have been reached by reweighting (Aoki *et al.*, 2010) or directly, at large volumes and several different values of the cutoff (Durr *et al.*, 2011, 2012), is to a large extent due to recent advances in the construction of efficient lattice regularizations that will be reviewed in this section.

A. Basics of the path integral formalism

We start by writing the partition function of a Euclidean quantum field theory using the path integral formalism (Dirac, 1933; Feynman, 1948a, 1948b, 1949; Feynman and Hibbs, 1965) as

$$\mathcal{Z} = \int \mathcal{D}\Phi e^{-S(\Phi)} \tag{1}$$

with the action $S(\Phi)$ and Φ generically denoting all fields of the theory. For bosonic fields one typically introduces periodic boundary conditions, while for fermion fields it is natural to introduce antiperiodic boundary conditions in the time direction [see, e.g., Appendix A of Polchinski (1998)]. While this subtlety usually can be ignored, it does play some role when choosing the parity of interpolating operators as discussed in Sec. III.B. For a gauge theory with fermions one specifically has

$$\mathcal{Z} = \int \mathcal{D}A_\mu \int \mathcal{D}\psi \mathcal{D}\bar{\psi} e^{-(\bar{\psi}M\psi + S_G)} \tag{2}$$

with the Euclidean gauge action

$$\begin{aligned} S_G &= \tfrac{1}{4} F_{\mu\nu} F_{\mu\nu}, \\ F_{\mu\nu} &= \partial_\mu A_\nu - \partial_\nu A_\mu + ig[A_\mu, A_\nu], \end{aligned} \tag{3}$$

and the Euclidean Dirac operator in the case of one fermion flavor

$$M = \gamma_\mu D_\mu + m, \tag{4}$$

where the covariant derivative is given by

$$D_\mu = \partial_\mu + igA_\mu. \tag{5}$$

Note that in the massless case M is anti-Hermitian and, depending on the gauge field configuration, may have exact zero modes. These zero modes of the operator are related to the topology of the underlying gauge field by the Atiyah-Singer index theorem (Atiyah and Singer, 1968).

Using the rules of Grassmannian integration, one can generically rewrite Eq. (2) as

$$\mathcal{Z} = \int \mathcal{D}A_\mu \int \mathcal{D}\psi \mathcal{D}\bar{\psi} e^{-(\bar{\psi}M\psi + S_G)} = \int \mathcal{D}A_\mu \det(M) e^{-S_G}. \tag{6}$$

Averages that correspond to expectation values of time ordered operators in the operator formalism are generically obtained by

$$\langle O \rangle = \frac{1}{\mathcal{Z}} \int \mathcal{D}A_\mu \int \mathcal{D}\psi \mathcal{D}\bar{\psi} O e^{-(\bar{\psi}M\psi + S_G)}, \tag{7}$$

where O denotes a generic observable composed of gauge and fermion fields. The integration over the fermion fields can again be explicitly performed resulting in the replacement of fermion bilinears by propagators on a given gauge field background. For a single fermion bilinear this explicitly reads

$$\int \mathcal{D}\psi \mathcal{D}\bar{\psi} [\psi^{s_f}_{c_f}(y) \bar{\psi}^{s_i}_{c_i}(x)] e^{-\bar{\psi}M\psi} = \det(M)(M^{-1})^{s_f s_i}_{c_f c_i}(y, x), \tag{8}$$

while for a general expression it results in the usual combination of all Wick contractions.

As one can see from Eqs. (2) and (8), virtual fermion effects (“sea fermions”) are contained in the $\det(M)$ factor after the fermion field integration. Ignoring this $\det(M)$ factor results in an uncontrolled approximation to QCD, the quenched approximation (Marinari, Parisi, and Rebbi, 1981b).

B. QCD regularized on a lattice

The path integral (1) has to be performed over all field configurations. In order to make it well defined, we regulate it on a finite spacetime lattice

$$x_\mu = n_\mu a^{(\mu)} \quad \text{with} \quad n_\mu \in \{0, \ldots, N_\mu - 1\}, \tag{9}$$

where the $a^{(\mu)}$ are the lattice spacings in direction μ. Although more general topologies are possible in principle [see, e.g., Jersak, Lang, and Neuhaus (1996)], one usually imposes toroidal boundary conditions $x_\mu + N_\mu a^{(\mu)} = x_\mu$. Here we also specialize to the common isotropic case in which the lattice spacings in all directions are equal $a^{(\mu)} = a$. The anisotropic case will be discussed separately in Sec. II.F.

The fermion field ψ is now a Grassmann vector, defined at the discrete lattice points $x = na$. We write the naive discretization of the free fermionic continuum action as

$$S_F(m) = a^4 \sum_{x=na} \bar{\psi}(x)(\gamma_\mu \mathcal{D}_\mu + m)\psi(x) \tag{10}$$

with

$$\mathcal{D}_\mu = \frac{1}{2a}(V_\mu - V_\mu^\dagger) \tag{11}$$

and

$$(V_\mu)_{xy} = \delta_{x+\hat{\mu},y}. \tag{12}$$

Note that this action was obtained by replacing the continuum derivative operator ∂_μ with the simple lattice finite difference operator $\mathcal{D}_\mu$. This choice is not unique and this nonuniqueness can be exploited to construct efficient fermion regularizations. Another feature of Eq. (10) is that it does not describe a single fermion flavor even in the continuum limit. The latter is known as the fermion doubling problem (Karsten and Smit, 1981) and will be discussed in detail in Sec. II.D. In Sec. II.E.2 we discuss how the ambiguity in the fermion discretization can be utilized to construct numerically efficient lattice fermion regularizations.

The action (10) is invariant under a global symmetry transformation

$$\psi(x) \to \Lambda\psi(x), \qquad \bar{\psi}(x) \to \bar{\psi}(x)\Lambda^\dagger, \tag{13}$$

with $\Lambda \in \mathrm{SU}(3)$ for the case of QCD. This symmetry can be promoted to a local one

$$\psi(x) \to \Lambda(x)\psi(x), \qquad \bar{\psi}(x) \to \bar{\psi}(x)\Lambda^\dagger(x) \tag{14}$$

by including a parallel transport $U_\mu(x)$ to the one-hop term V_μ and thus replacing Eq. (12) with

$$(V_\mu)_{xy} = U_\mu(x)\delta_{x+\hat{\mu},y}. \tag{15}$$

The parallel transport $U_\mu(x)$ is the discretized version of the path ordered product of continuum gauge fields $A_\mu(x)$:

$$U_\mu(x) = \mathcal{P} e^{ig \int_x^{x+\hat{\mu}} dx'_\mu A_\mu(x')} \tag{16}$$

with g being the coupling constant and transforms as

$$U_\mu(x) \to \Lambda(x) U_\mu(x) \Lambda^\dagger(x + \hat{\mu}) \tag{17}$$

under gauge transformations. Note that one could in principle choose different paths than the direct one in Eq. (16). As long as the end points remain fixed, the action will be invariant under local transformations (14). This nonuniqueness will play a role when constructing efficient fermion discretizations in Sec. II.E.2.

In order to construct a kinetic term for the gauge field we first note that the trace over a closed loop of parallel transports is gauge invariant. The simplest of these loops, the plaquette, is defined as

$$U_{\mu\nu}(x) = U_\mu(x) U_\nu(x + \hat{\mu}) U_\mu^\dagger(x + \hat{\nu}) U_\nu^\dagger(x) \tag{18}$$

and has a naive continuum limit

$$U_{\mu\nu} \xrightarrow{a \to 0} 1 + iga^2 F_{\mu\nu} - \tfrac{1}{2} g^2 a^4 F_{\mu\nu}^2 + O(a^6). \tag{19}$$

The simplest discretization of the continuum gauge action therefore reads (Wilson, 1974)

$$S_W = \beta \sum_{x, \mu > \nu} \left(1 - \frac{1}{6} \mathrm{Tr}[U_{\mu\nu}(x) + U_{\mu\nu}(x)]\right), \tag{20}$$

with $\beta = 6/g^2$ which has the continuum limit

$$S_W \xrightarrow{a\to 0} \frac{1}{4}\int d^4x\,\mathrm{Tr}[F_{\mu\nu}(x)F_{\mu\nu}(x)] + O(a^2). \tag{21}$$

We see that Eq. (20) which is known as the Wilson gauge action or plaquette action has discretization errors of $O(a^2)$. Again, this discretization is not unique and one can utilize this ambiguity to find gauge actions with higher order discretization effects. This will be discussed in detail in Sec. II.E.1. By combining Eq. (10) with Eqs. (11), (15), and (20) and introducing the dimensionless quantities $\Psi = a^{3/2}\psi$, $\bar{\Psi} = a^{3/2}\bar{\psi}$, $m = am$, and $D_\mu = a\mathcal{D}_\mu$, we can write the naive lattice QCD action as

$$\begin{aligned} S_n &= S_W + \sum_{q=1}^{N_f} S_F(m_q) \\ &= \beta \sum_{x,\mu>\nu}\left(1 - \frac{1}{6}\mathrm{Tr}[U^\dagger_{\mu\nu}(x) + U_{\mu\nu}(x)]\right) \\ &\quad + \sum_{q=1}^{N_f}\sum_x \bar{\Psi}(x)(\gamma_\mu D_\mu + m_q)\Psi(x), \end{aligned} \tag{22}$$

where we have in addition taken the explicit sum over N_f fermion flavors q.

Before we go into the details of the fermion and gauge field discretization, we mention briefly how in principle the cutoff is removed in lattice QCD. As one can see from Eq. (22), the lattice action exclusively consists of dimensionless quantities. The parameters of the action are the fermion masses m_q and the coupling β. In order to remove the cutoff, i.e., to take the limit $a \to 0$, one therefore has to tune these parameters such that on the one hand the lattice spacing a goes to zero, while, on the other hand, a certain set of dimensionful physical observables that are used to define the physical content of the theory remain constant. These trajectories in parameter space of β and the m_q along which a set of physical observables remains constant as the limit $a \to 0$ is taken are called lines of constant physics. A detailed discussion of how these can be defined is given in Sec. IV.

Along these lines of constant physics it is clear that correlation lengths in physical units will go to a finite limit and therefore will diverge in units of the lattice spacing a. In order to possess a continuum limit it is therefore necessary for a lattice field theory to exhibit a second order phase transition. Problems can arise if the bare coupling constant diverges at a finite cutoff, the so-called Landau pole (Landau, 1955). In that case the only line of constant physics that does not show a divergence at finite cutoff is the one with vanishing coupling, i.e., the trivial theory. In order for theories with a Landau pole problem to have a nonvanishing renormalized coupling (i.e., to be nontrivial) one must retain a finite cutoff which prevents one from taking the continuum limit. Such theories can, however, still serve as effective theories. Consequences for the lattice formulation of this class of theories are discussed, e.g., by Gockeler *et al.* (1998a), Arnold *et al.* (2003), Espriu and Tagliacozzo (2003), and Kogut and Strouthos (2005).

Because of asymptotic freedom (Gross and Wilczek, 1973; Politzer, 1973), however, no such problems are expected to arise in lattice QCD. The perturbative expectation of the vanishing of the QCD coupling constant at large scales has been confirmed by nonperturbative lattice calculations in various settings (Bowler *et al.*, 1986; Gupta *et al.*, 1988; Luscher *et al.*, 1994; Bode *et al.*, 2001; Della Morte *et al.*, 2003; Sommer, Tekin, and Wolff, 2010; Tekin, Sommer, and Wolff, 2010). The most recent result for $N_f = 4$ QCD is plotted in Fig. 1.

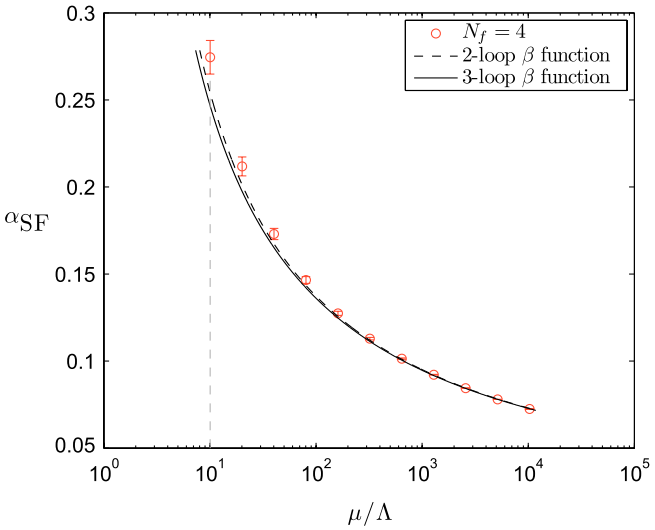

FIG. 1 (color online). Nonperturbative running coupling constant of four flavor QCD in units of the QCD scale Λ from a lattice calculation of Sommer, Tekin, and Wolff (2010) compared to perturbative calculation. Figure courtesy of Rainer Sommer.

C. Numerical evaluation of the path integral

Before we return to the task of constructing a lattice regularization of QCD, we need to discuss some basics of the numerical evaluation of the path integral (7). In terms of dimensionless lattice quantities, Eq. (7) can be written as

$$\langle O\rangle = \frac{1}{\mathcal{Z}}\int \mathcal{D}U_\mu \int \mathcal{D}\Psi\mathcal{D}\bar{\Psi} O e^{-[\bar{\Psi}M(U)\Psi + S_G(U)]}, \tag{23}$$

with a generic gauge action $S_G(U)$ and fermion operator $M(U)$, which in general depends on the gauge field U. We now perform the integration over both the fermion fields $\bar{\Psi}$ and Ψ and the gauge field U. Using Eq. (8) and its generalization for fermion multilinears, we explicitly perform the integration over fermion fields. With the understanding that we have to replace fermion multilinears by the sum over all Wick contractions, we may thus cast Eq. (23) into the form

$$\langle O\rangle = \frac{1}{\mathcal{Z}}\int \prod_{x,\mu} dU_\mu(x)\,\mathrm{det}M(U) O e^{-S_G(U)}. \tag{24}$$

Generally and for QCD, in particular, it is not possible to perform the remaining integration over the gauge fields U_μ in closed form. While both strong (Wilson, 1974) and weak [see, e.g., Capitani (2003)] coupling expansions are possible, neither allows for a detailed quantitative understanding of the nonperturbative dynamics of the system.

From a numerical perspective, Eq. (24) is a high dimensional integral over $4 \times \prod_\mu N_\mu$ copies of the gauge group, which in the case of QCD is SU(3). The only categories of numerical methods that are suitable to perform such a high

dimensional integral are stochastic or Monte Carlo (MC) methods in which the space to be integrated over is randomly sampled, i.e., where observables are averaged over on randomly drawn gauge field configurations $U_\mu(x)$. As Monte Carlo integration is stochastic in nature, there is always a statistical error associated with it. This error has to be estimated in a lattice calculation, which is typically achieved via the jackknife or bootstrap methods [see, e.g., Press *et al.* (2007)].

A straight Monte Carlo integration of Eq. (24) in which the gauge configurations U_μ are randomly produced with equal weight is, however, extremely inefficient. For interesting parameter choices, all but a very small subset of relatively smooth configurations are exponentially suppressed by the exponent of the gauge action $S_G(U)$ and the fermion determinant $\det M(U)$. In order to circumvent this problem, one can produce gauge field configurations with a probability that is proportional to $\det M(U) \times e^{-S_G(U)}$ and compute the expectation value of an observable as an unweighted average over these configurations. This technique, known as importance sampling, requires an algorithm that produces gauge field configurations with the proper weight. Typically this is achieved via a Markov chain process, where a time series of gauge field configurations is produced in which the nth configuration $U_\mu^{(n)}$ depends on the previous one $U_\mu^{(n-1)}$.

A Markov chain is characterized by the transition probability

$$p(m,n) = P(U^m|U^n), \tag{25}$$

where the U^i are all possible gauge configurations, and the conditional probability $P(U^m|U^n)$ is understood in the sense that it denotes the probability of the system to go over from a configuration U^n to U^m in one time step. The transition probability p acts on the space of all gauge configurations. It fulfills the two basic relations

$$\forall\ m,n:\ p(m,n) \geq 0, \qquad \int dm\, p(m,n) = 1, \tag{26}$$

where $\int dm$ denotes the integration over all possible gauge field configurations. If in addition the transition probability (25) fulfills the detailed balance condition

$$\forall\ m,n:\ p(n,m)\rho_m = p(m,n)\rho_n \tag{27}$$

with the desired equilibrium distribution $\rho_n = \det M(U^n) \times e^{-S_G(U^n)}/\mathcal{Z}$, then one can easily show the following two properties:

(1) The transition probability maps the equilibrium distribution onto itself

$$\rho_m = \int dn\, p(m,n)\rho_n. \tag{28}$$

(2) Defining a distance $d(w,v) = \int dn |w_n - v_n|$ in the space of probability distributions, the application of the transition probability moves every probability distribution closer to the equilibrium distribution

$$d(pw,\rho) \leq d(w,\rho). \tag{29}$$

If in addition to Eqs. (28) and (29) the system is ergodic, i.e., if any configuration U^i may be reached from any other configuration U^j with nonvanishing probability in a finite number of time steps, then it is guaranteed that starting from an arbitrary initial probability distribution we end up with the desired equilibrium distribution ρ.

The time until the equilibrium distribution ρ is reached (in the sense that no statistically relevant drift toward the equilibrium expectation value can be seen in any monitored observable) is usually called the thermalization phase and its shortness is an important quality criterion of an algorithm. Once the system is thermalized, i.e., the equilibrium distribution has been reached, it is advantageous if consecutive configurations have as little correlation as possible. In order to have a quantitative handle, it is customary to monitor the autocorrelation time of certain observables within a Markov chain.

In the case of a pure gauge theory or the quenched approximation where the fermion determinant factor $\det M(U)$ is missing and the weight factor is proportional to the exponent of the gauge action $e^{-S_G(U)}$, the update algorithms that produce the next element in the Markov chain usually exploit the locality of the gauge action $S_G(U)$. As pioneered by Creutz, Jacobs, and Rebbi (1979a, 1979b), one can pick a certain gauge link $U_\mu(x)$ from the current gauge configuration U and produce a suggested new gauge configuration U' by multiplying $U_\mu(x)$ with an element of the gauge group. Since the gauge action $S_G(U)$ is a sum of local terms, the change in the action $\delta S = S_G(U') - S_G(U)$ is readily evaluated by recomputing those few terms that contain the flipped gauge link. One can then perform a Metropolis (Metropolis *et al.*, 1953) step, i.e., accept the gauge configuration U' as the next gauge configuration in the Markov chain with probability $e^{-\delta S}$ if the action has increased $\delta S > 0$ or with probability 1 otherwise. It is readily seen that this algorithm satisfies the detailed balance condition (27). Another frequently used local update algorithm for pure gauge theories is the heat bath (Creutz, 1980b; Kennedy and Pendleton, 1985). Supplemented by overrelaxation steps (Adler, 1981, 1988; Brown and Woch, 1987; Creutz, 1987; Fodor and Jansen, 1994), these algorithms are still the state of the art for pure gauge theories.

Because of the nonlocal nature of the fermion determinant $\det M(U)$ an update in a theory with dynamical fermions is substantially more complex and computationally demanding. For a lattice with $N = \prod_\mu N_\mu$ sites, $M(U)$ is typically a $(12 \times N)^2$ matrix[3] and therefore a direct computation of $\det M(U)$ is prohibitively expensive for even moderately sized lattices. Although alternative suggestions have been made (Berg and Forster, 1981; Fucito *et al.*, 1981; Scalapino and Sugar, 1981; Kuti, 1982; Polonyi and Wyld, 1983; Montvay, 1984; Luscher, 1994; Slavnov, 1996), one usually proceeds by introducing a bosonic (complex scalar) pseudofermion field Φ (Weingarten and Petcher, 1981). The fermion determinant may thus be written as

$$\det M(U) = \int \mathcal{D}\Phi^\dagger \mathcal{D}\Phi e^{-\Phi^\dagger M(U)^{-1}\Phi}. \tag{30}$$

[3]Note that in the staggered fermion formulation the size of the matrix is reduced to $(3 \times N)^2$. For a detailed discussion, see Sec. II.D.1.

The catch here is of course the appearance of the inverse fermion matrix $M(U)^{-1}$ in Eq. (30) which is again a nonlocal object. In addition, the kernel operator $M(U)^{-1}$ has to exist [i.e., the matrix $M(U)$ needs to be invertible] and be positive definite Hermitian in order to ensure the convergence of all Gaussian integrals over the pseudofermion field in Eq. (30). From Eq. (22) we see, however, that the naive fermion operator is not Hermitian and neither will be the fermion operators we construct later on. As long as $\det M$ is real and positive definite, however, one may use the identity $\det M = \sqrt{\det(M^\dagger M)}$ to rewrite an arbitrary power of the fermion determinant as

$$\det M(U)^{2\alpha} = \int \mathcal{D}\Phi^\dagger \mathcal{D}\Phi e^{-\Phi^\dagger [M^\dagger(U)M(U)]^{-\alpha}\Phi}. \tag{31}$$

The path integral can now be formulated in terms of bosonic variables only with an additional term in the action

$$S_F = \Phi^\dagger [M^\dagger(U)M(U)]^{-\alpha/2}\Phi. \tag{32}$$

Note that for actions where $M^\dagger(U)M(U)$ does not couple even and odd lattice sites one may choose to keep the pseudofermion fields Φ_e on even lattice sites only and thereby obtain

$$\det M(U)^{\alpha} = \int \mathcal{D}\Phi_e^\dagger \mathcal{D}\Phi_e e^{-\Phi_e^\dagger [M^\dagger(U)M(U)]^{-\alpha}\Phi_e}. \tag{33}$$

In order to efficiently integrate the system of pseudofermions and gauge fields we follow the work of Callaway and Rahman (1982, 1983); Polonyi and Wyld (1983); Batrouni *et al.* (1985); Duane (1985); Duane and Kogut (1985, 1986); and Duane *et al.* (1987) and reinterpret the total action of the system

$$S = S_G + \Phi^\dagger [M^\dagger(U)M(U)^{-\alpha/2}]\Phi \tag{34}$$

as the potential part of a fictitious Hamiltonian

$$\mathcal{H} = \tfrac{1}{2}\pi^2 + S(\phi) \tag{35}$$

with conjugate momenta π, where ϕ collectively denotes all pseudofermion and gauge fields. One can then proceed to choose some initial momenta and integrate the canonical equations of motion

$$\dot{\phi} = \pi, \qquad \dot{\pi} = -\frac{\partial S}{\partial \phi}, \tag{36}$$

numerically in a fictitious time τ along a "classical" path. The classical partition function corresponding to the set of all such classical trajectories is given by

$$Z = \int \mathcal{D}\pi \mathcal{D}\phi e^{-H} = \int \mathcal{D}\pi e^{-(1/2)\pi^2} \int \mathcal{D}\phi e^{-S}. \tag{37}$$

As the Gaussian integration over the momenta π gives only an irrelevant prefactor, Eq. (37) reproduces the correct probability distribution in the original theory. Assuming ergodicity, one can obtain the correct distribution of classical paths (37) by periodically refreshing the momenta π with a random value from a Gaussian distribution. The expectation value of an observable can thus be obtained by averaging it along all classical trajectories in the update chain. The inexact nature of the numerical integration introduces a systematic error, which, however, can be corrected by a final Monte Carlo accept or reject step of the complete trajectory [see Duane *et al.* (1987)]. This is known as the hybrid Monte Carlo (HMC) algorithm.

The Hamiltonian in Eq. (35) is readily constructed in the case where α in Eq. (31) or (33) is a positive integer. For a general fractional power α one can resort to a polynomial (Frezzotti and Jansen, 1997; de Forcrand and Takaishi, 1997) or rational (Clark and Kennedy, 2004; Clark, Kennedy, and Sroczynski, 2005) approximation of the desired fractional power of $M^\dagger(U)M(U)$. These versions of the HMC algorithm are known as polynomial HMC (PHMC) and rational HMC (RHMC) algorithms, respectively.

In order to integrate the equations of motion (36) numerically, one has to compute the derivative of the action (34) with respect to the gauge field

$$\frac{\partial S}{\partial U_\mu(x)} = \frac{\partial S_G}{\partial U_\mu(x)} + \Phi^\dagger \frac{\partial [M^\dagger(U)M(U)]^{-\alpha}}{\partial U_\mu(x)}\Phi. \tag{38}$$

This derivative is commonly known as the force term. The computationally expensive part of Eq. (38) is the second term, the fermionic force term. In the special case $\alpha = 1$ and using the shorthand notation $\mathcal{M}(U) = M^\dagger(U)M(U)$ it can be written as

$$\Phi^\dagger \frac{\partial \mathcal{M}(U)^{-1}}{\partial U_\mu(x)}\Phi = -\Phi^\dagger \mathcal{M}(U)^{-1}\frac{\partial \mathcal{M}(U)}{\partial U_\mu(x)}\mathcal{M}(U)^{-1}\Phi. \tag{39}$$

We see that a single inversion of $\mathcal{M}(U)$ on a pseudofermion vector is required to compute Eq. (39). For general fractional exponents α one can introduce a rational approximation

$$r(\mathcal{M}(U)) \simeq \mathcal{M}(U)^{-\alpha}, \tag{40}$$

with

$$r(x) = \sum_i \frac{\alpha_i}{x + \beta_i}. \tag{41}$$

In this case, the fermion force can be written as

$$\Phi^\dagger r(\mathcal{M}(U))\Phi = -\sum_i \Phi^\dagger \alpha_i [\mathcal{M}(U) + \beta_i]^{-1}\frac{\partial \mathcal{M}(U)}{\partial U_\mu(x)}[\mathcal{M}(U) + \beta_i]^{-1}\Phi, \tag{42}$$

which can be computed using one single multilinear matrix inversion (Frommer *et al.*, 1995; Glassner *et al.*, 1996; Jegerlehner, 1996; de Forcrand, 1996) on a single vector.

An alternative integration scheme, the hybrid molecular dynamics R algorithm, was proposed by Gottlieb *et al.* (1987b). Although it has seen considerable use in the past, it has largely been replaced by the RHMC algorithm. It is a pure molecular dynamics algorithm that, in contrast to pseudofermion algorithms, does not allow for a final MC step to correct for finite step size errors accumulated along the integration trajectory. Because of this feature, detailed balance is fulfilled by the R algorithm only in the limit of a vanishing step size in contrast to HMC-type algorithms that are exact even at finite step size.

An efficient HMC algorithm has to simultaneously satisfy two criteria: On the one hand, the acceptance rate should be high (one typically aims for ~80%–90%), and, on the other hand, the autocorrelation time should be small. The autocorrelation between successive configurations can be decreased by a longer integration trajectory separating them. This, however, leads to larger numerical integration errors and consequently to a lower acceptance rate. A trivial remedy consists of decreasing the time step in the numerical integration, which, however, is computationally expensive because the fermion force has to be computed more often. It is therefore advantageous to use higher order integration schemes (Omelyan, Mryglod, and Folk, 2002a, 2002b, 2003; Takaishi and de Forcrand, 2006) that allow a larger time step in the numerical integration while keeping the acceptance rate high.

Another method for speeding up HMC-type algorithms consists of introducing different time steps for pseudofermions and gauge fields (Sexton and Weingarten, 1992). Splitting off the UV modes of the spectrum by mass preconditioning (Hasenbusch, 2001; Hasenbusch and Jansen, 2003) or via domain decomposition (Luscher, 2003, 2004, 2005) and integrating IR and UV parts with different time steps leads to a substantial additional speedup. This speedup is especially large if combined with the suppression of UV modes and other improvements of the fermion regularization that will be discussed in Sec. II.E.2.

As noted in Sec. II.A, ignoring the effects of the fermion determinant results in the quenched approximation. Since it bypasses the most computationally demanding part of the ensemble generation, it was extensively used in the early years of lattice QCD and is still useful for certain conceptual studies. Although it is an uncontrolled approximation, it may be justified by noting that it becomes exact in the large N_c limit. Furthermore, by choosing the proper scale setting observable (see Sec. IV) a large part of the dynamical fermion corrections might cancel and effectively be absorbed into a redefinition of the coupling constant.[4]

D. The fermion doubling problem and its solutions

We now return to the free, naive fermion action (22)

$$\bar{\Psi}(\gamma_\mu D_\mu + m)\Psi. \tag{43}$$

The fermion operator reads

$$M = \gamma_\mu D_\mu + m, \tag{44}$$

which in Fourier space becomes

$$M(p) = \frac{i}{a}\sum_\mu \gamma_\mu \sin(a p_\mu) + m. \tag{45}$$

The momentum space propagator is consequently given by

$$D(p) = M^{-1}(p) = \frac{-(i/a)\sum_\mu \gamma_\mu \sin(a p_\mu) + m}{[(1/a)\sum_\mu \sin(a p_\mu)]^2 + m^2}, \tag{46}$$

which in addition to the physical pole at $p^2 = -m^2$ has 15 additional poles located at the edges of the Brillouin zone. The poles are located at $(p - \Pi)^2 = -m^2$, where Π is any of the 16 four-momenta

$$\Pi = (p_0, p_1, p_2, p_3), \quad \text{with} \quad p_\mu \in \{0, \pi/a\}. \tag{47}$$

This rather fundamental obstacle of putting fermion fields on the lattice is known as the doubling problem. Physically, we can trace this problem back to the well-known axial anomaly of a continuum theory. In the massless limit, a classical fermionic theory is invariant under the chiral transformation

$$\begin{aligned} \Psi(x) &\to \Psi'(x) = e^{i\phi\gamma_5}\Psi(x), \\ \bar{\Psi}(x) &\to \bar{\Psi}'(x) = \bar{\Psi}(x)e^{i\phi\gamma_5}. \end{aligned} \tag{48}$$

As demonstrated by Adler (1969) and Bell and Jackiw (1969), the conservation of the corresponding Noether current, the axial vector current, is destroyed by quantum fluctuations. In a lattice regulated theory however the existence of a classical symmetry implies a conserved current. The anomaly of the physical fermion axial vector current is canceled by the anomaly of unphysical doublers as demonstrated by Karsten and Smit (1981).[5]

It was later shown by Nielsen and Ninomiya (1981a, 1981b, 1981c), that no lattice fermion regularization exists that fulfills all of the following conditions at the same time:

(i) absence of doubler fermions,
(ii) continuum chiral symmetry in the massless case,
(iii) locality in a sense that $M(x, y) \to 0$ vanishes exponentially as $x - y \to \infty$, and
(iv) correct continuum limit.

This result can be understood by noting that a general lattice fermion operator M which anticommutes with γ_5 in the $m = 0$ case can be written as

$$M(p) = m + i\sum_\mu \gamma_\mu P_\mu(ap) + \sum_\mu \gamma_\mu\gamma_5 R_\mu(ap). \tag{49}$$

The requirement that it reproduces the correct continuum theory implies that for small a the lattice momentum P_μ goes over into the continuum momentum p_μ while $R_\mu \to 0$. Additionally, P_μ is periodic in every direction with period $2\pi/a$. As shown in Fig. 2, these restrictions on P_μ imply either that it has a second root in the first Brillouin zone, which gives an additional pole in the propagator, i.e., a doubler fermion, or that it has at least one discontinuity, which makes the fermion operator $M(x, y)$ nonlocal. Note that in comparison the discretized version of the continuum action of a scalar field

$$S_\phi = \tfrac{1}{2}\phi^\dagger(\partial_\mu\partial_\mu - m^2)\phi \tag{50}$$

in momentum space reads

[4]Another attempt to justify the use of the quenched approximation was made by Anthony, Llewellyn Smith, and Wheater (1982) and Duffy, Guralnik, and Weingarten (1983). They suggested to extrapolate to a positive number of quark flavors by computing observables in the quenched approximation and at an effective negative number of quark flavors.

[5]See also Chodos and Healy (1977) and Kerler (1981).

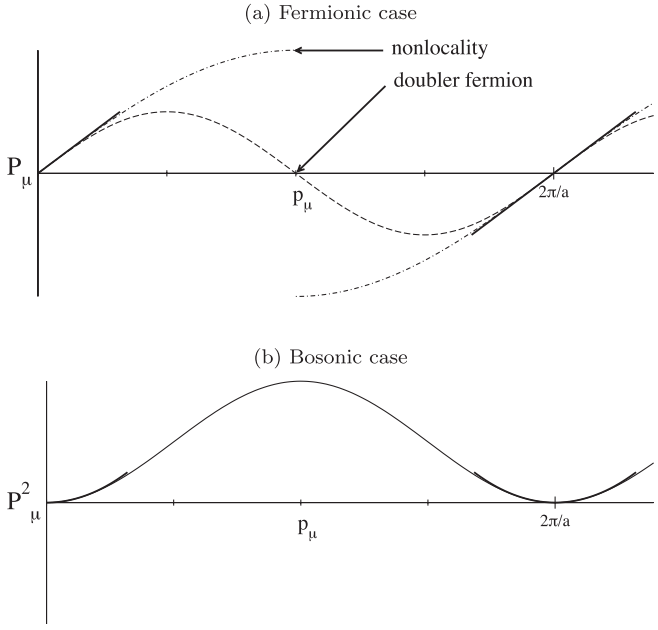

FIG. 2. (a) In the fermionic case, periodicity of the lattice momentum P_μ requires a second root (doubler) or jump within the Brillouin zone (nonlocality). (b) In the bosonic case, only the squared lattice momentum is required to be periodic which can be fulfilled without a jump or an additional root.

$$S_\phi = -\frac{1}{2}\phi^\dagger\left(m^2 + \sum_\mu (P^2)_\mu\right)\phi, \tag{51}$$

which only depends on the discretized momenta squares

$$(P^2)_\mu = \frac{2}{a^2}(1 - \cos ap_\mu). \tag{52}$$

These are naturally periodic with a period of $2\pi/a$ as displayed in Fig. 2(b).

One therefore has to give up on any one of the above requirements for lattice regularizations of fermions. Obviously, one cannot give up the requirement (iv) of a correct continuum limit. Giving up the locality requirement (iii), on the other hand, was suggested, among others, by Drell, Weinstein, and Yankielowicz (1976) who proposed

$$P_\mu = p_\mu \tag{53}$$

by Rebbi (1987), who suggested

$$P_\mu = \sin ap_\mu \frac{2\sum_\nu \sin(ap_\nu/2)}{a\sum_\nu \sin ap_\nu}, \tag{54}$$

and by Gross, Lepage, and Rakow (1987) whose construction involves nonsymmetric difference operators and contains nonrenormalizable terms in the continuum limit. However, all of these approaches turned out to be problematic and have been abandoned.

Among the remaining two options, we first discuss lattice fermion regularizations that give up on the requirement (i) and therefore describe more than a single flavor in the continuum limit. Among these, Karsten (1981), Wilczek (1987), Borici (2008), and Creutz (2008) suggested different implementations of minimally doubled fermions, i.e., lattice fermions which have one single doubler only. As this single doubler has to be placed somewhere within the Brillouin zone, all of these formulations share the characteristic that in Fourier space there is a distinguished direction, namely, the direction from the physical particles pole to the pole of the single doubler fermion. Therefore, a number of discrete lattice symmetries are broken (Bedaque *et al.*, 2008) resulting in a more complicated renormalization pattern and, generically, in a fine-tuning of the parameters of the action (Capitani *et al.*, 2010). Currently fundamental properties of minimally doubled fermions are still being clarified and applications to hadron spectroscopy or other phenomenologically relevant computations are not yet available in the literature.

1. Staggered fermions

A less minimal but more symmetric way of putting doublers on the lattice is given by the staggered fermion formulation that was developed in a series of papers by Kogut and Susskind (1975), Banks, Susskind, and Kogut (1976), and Susskind (1977). Staggered fermions are obtained from the naive fermion action (43) by noting a fourfold exact degeneracy (in the interacting theory) that can be exposed by a spin diagonalization

$$\Psi(x) = \Gamma(x)\chi(x), \qquad \bar{\Psi}(x) = \bar{\chi}(x)\Gamma^\dagger(x), \tag{55}$$

with

$$\Gamma(x) = \prod_\mu \gamma_\mu^{(x_\mu/a)}. \tag{56}$$

In terms of $\bar{\chi}$ and χ, Eq. (43) can be written as

$$\bar{\chi}(\eta_\mu D_\mu + m)\chi, \qquad \eta_\mu(x) = (-1)^{\sum_{\nu>\mu} x_\nu}, \tag{57}$$

where $\eta_\mu(x)$ is a pure phase factor making explicit the decoupling of the four spin components of χ. Defining χ on a single component only, we have reduced the fermion content of the theory by a factor of 4, from 16 four-component spinors to 16 single component modes that are still symmetrically distributed over the Brillouin zone at the momenta Π given in Eq. (47).

The staggered fermion operator

$$M = \eta_\mu D_\mu + m \tag{58}$$

is anti-Hermitian in the massless case, i.e., its eigenvalues are restricted to the imaginary axis for $m = 0$. Therefore any finite mass $m > 0$ provides an IR cutoff and the operator is invertible. In addition, the massless staggered fermion operator preserves a remnant of the chiral symmetry of the naive fermion operator (48):

$$\begin{aligned}\chi(x) &\to \chi'(x) = e^{i\phi\epsilon}\chi(x),\\ \bar{\chi}(x) &\to \bar{\chi}'(x) = \bar{\chi}(x)e^{i\phi\epsilon},\end{aligned} \tag{59}$$

where $\epsilon = (-1)^{\sum_\mu x_\mu}$. For the staggered fermion operator (58) this implies that

$$\epsilon M = M^\dagger \epsilon \tag{60}$$

is Hermitian. Therefore, the eigenvalues of M come in complex conjugate pairs and det$M$ is real and positive. Furthermore, we see that

$$M^\dagger M = \eta_\mu D_\mu^\dagger \eta_\nu D_\nu + |m|^2 \tag{61}$$

does not couple odd and even sites so that the pseudofermion representation (33) may be used for the fermion determinant.

As demonstrated by Sharatchandra, Thun, and Weisz (1981), Gliozzi (1982), Kluberg-Stern *et al.* (1983), van den Doel and Smit (1983), Golterman and Smit (1984b), and Daniel and Kieu (1986), these 16 spinor components may again be interpreted as four fermion flavors (also referred to as tastes in the literature), each one described by a four-component spinor. Following Golterman (1986), we split the lattice coordinate $x = y + h$ into a piece y that describes the origin of the elementary 2^4 hypercube that x is located in and an offset h that describes the location of x within this hypercube. We construct

$$X(y) = \frac{1}{4}\sum_h \Gamma(h) U(y+h, y)\chi(y+h), \tag{62}$$

where $h_\mu \in \{0, a\}$ and $U(y+h, y)$ is any parallel transport from $y+h$ to y. Interpreting $X(y)$ as a 16 component vector, we can define an arbitrary fermion bilinear with spin structure γ_s and flavor structure γ_f as

$$\bar{X}(\gamma_s \otimes \xi_f)X = \mathrm{Tr}(\bar{X}\gamma_s X \gamma_f^\dagger) \tag{63}$$

and the staggered fermion action (57) can be written as

$$\bar{X}[(\mathbb{1}\otimes\mathbb{1})m + (\gamma_\mu \otimes \mathbb{1})\hat{D}_\mu + (\gamma_5 \otimes \xi_\mu \xi_5)\hat{C}_\mu]X, \tag{64}$$

with the first and second derivative operators on the coarse lattice

$$\hat{D}_\mu = \tfrac{1}{4}(\hat{V}_\mu - \hat{V}_\mu^\dagger), \qquad \hat{C}_\mu = \tfrac{1}{4}(\hat{V}_\mu - 2\mathbb{1} + \hat{V}_\mu^\dagger), \tag{65}$$

where

$$(\hat{V}_\mu)_{xy} = U_\mu(x+\hat{\mu})U_\mu(x)\delta_{x+2\hat{\mu},y}. \tag{66}$$

Note that the third term in Eq. (64) that implies a mixing of the four remaining flavors (tastes) is an artifact of the taste assignment (62) which does not respect the full set of symmetries of the staggered action. In fact, for the noninteracting case, Adams (2005) found a taste assignment that is diagonal in the tastes and local.

A massless four-flavor continuum theory has a classical U(4) chiral symmetry that gets reduced to SU(4) by the anomaly. This implies a 15-plet of massless pseudoscalar Goldstone particles (pions) and an additional massive one (η'). As seen in Eq. (59), staggered fermions retain a U(1) subgroup of this symmetry. In the spin-flavor basis, the remnant staggered chiral symmetry reads

$$\begin{aligned} X(y) &\to X'(y) = e^{i\phi(\gamma_5\otimes\xi_5)}X(y), \\ \bar{X}(y) &\to \bar{X}'(y) = \bar{X}(y)e^{i\phi(\gamma_5\otimes\xi_5)}. \end{aligned} \tag{67}$$

This symmetry is spontaneously broken implying a single Goldstone particle, the pseudoscalar in taste space, that is exactly massless.

In order to obtain one, respectively, two flavors in the functional integral (24), it is customary to take the quartic, respectively, square root of the four-flavor staggered functional determinant det$M$. This procedure, commonly referred to as rooting, was introduced by Marinari, Parisi, and Rebbi (1981b) in the context of the Schwinger model. On a technical level this is realized in a pseudofermion based algorithm by a fractional power $\alpha = 1/4$, respectively, $\alpha = 1/2$ in Eq. (33).

On a more fundamental level, the validity of rooted staggered fermions relies upon the assumption that there exists a local lattice fermion operator that squared or to the fourth power has the same functional determinant det$M$ as the four-flavor staggered operator. In fact, Adams (2005) demonstrated that in the massive free case such an operator can be found. In the interacting case, however, the situation is more complex. As Durr and Hoelbling (2005b) demonstrated, rooted staggered fermions are in the wrong universality class in the strictly massless case $m = 0$ implying that the chiral $m \to 0$ limit does not commute with removing the cutoff $a \to 0$, a result already anticipated by Smit and Vink (1987). This observation reflects the fact that the staggered chiral symmetry (63) and (72) is not anomalously broken. In fact, the staggered chiral symmetry is retained even in the single flavor rooted theory implying an exactly massless η' for $m = 0$ and as demonstrated by Bernard (2006), Prelovsek (2006), Bernard, DeTar *et al.* (2007), and Bernard, Golterman *et al.* (2007), nonunitarity of the rooted theory at finite cutoff. On the other hand, there is some numerical indication that out of the chiral limit rooted staggered fermions do indeed have correct continuum behavior for many observables (Aubin *et al.*, 2004; Davies *et al.*, 2004, 2005; Durr and Hoelbling, 2004; Durr, Hoelbling, and Wenger, 2004; Durr and Hoelbling, 2005b; Follana *et al.*, 2008; Bazavov *et al.*, 2010a, 2010b). More formally, Bernard, Golterman, and Shamir (2006) showed by a symmetry argument that rooted staggered fermions cannot be described by a local operator. However, analytical calculations (Bernard, Golterman, and Shamir, 2006, 2008; Giedt, 2007; Shamir, 2007) indicated that the nonlocal terms vanish in the continuum limit and consequently that rooted staggered fermions have the correct continuum limit as long as the proper order of limits is observed. Implications of the delicate nature of the staggered fermion continuum limit were also extensively discussed (Bernard, 2005; Durr and Hoelbling, 2006; Hasenfratz and Hoffmann, 2006; Bernard, Golterman *et al.*, 2007; Creutz, 2007a, 2007b). For recent reviews see, e.g., Durr (2006) and Sharpe (2006).

The representation of the spin-taste structure by different points within an elementary hypercube (56) and (62) and the taste breaking term in the action (64) imply some additional complications for extracting hadron masses with staggered fermions that will be discussed further in Sec. III.

2. Wilson fermions

We now turn our attention to lattice fermion formulations that fully lift the naive flavor degeneracy and are able to naturally describe a single flavor theory in the continuum limit. It was first realized by Wilson (1975) that the fermion doubling problem can be solved by adding a Laplacian term to the naive fermion operator (43)

$$S_W = \bar{\Psi}\left(\gamma_\mu D_\mu + m + \frac{r}{2}\Box\right)\Psi, \tag{68}$$

where

$$\Box = \sum_\mu C_\mu, \qquad C_\mu = V_\mu - 2 + V_\mu^\dagger, \tag{69}$$

with the parallel transport V_μ defined in Eq. (15) and the Wilson parameter r that is usually set to 1. The additional term in the action, the so-called Wilson term, may be interpreted as a momentum dependent mass term. Note that in contrast to naive and staggered fermions, the Wilson fermion operator is generally not normal due to the additional Laplacian term, although it still is in the free case. The free Wilson operator

$$M_W = \gamma_\mu D_\mu + m + \frac{r}{2}\Box \tag{70}$$

in momentum space reads

$$M_W(p) = \frac{i}{a}\sum_\mu \gamma_\mu \sin(a p_\mu) + m - \frac{r}{a}\sum_\mu [\cos(a p_\mu) - 1]. \tag{71}$$

Comparing Eq. (71) to the naive operator (45) we see that the additional term $(r/a)\sum_\mu[\cos(ap_\mu) - 1]$ vanishes as $O(a)$ for any fixed *physical* momentum p. On the other hand, for a fixed *lattice* momentum ap the additional term gives a contribution that is divergent as $O(1/a)$ except for $p = 0$. In particular, all doubler modes with n momentum components π/a receive an additional mass of $2rn/a$ thus effectively removing them from the spectrum in the continuum limit.

Since the additional Laplacian term in Eq. (68) does not anticommute with γ_5, the exact chiral symmetry of naive fermions (48) is broken as required by the Nielsen-Ninomiya theorem (Nielsen and Ninomiya, 1981a, 1981b, 1981c). In fact, the Laplacian term commutes with γ_5 due to its trivial spin structure. Consequently, the Wilson operator obeys the relation

$$M_W^\dagger = \gamma_5 M_W \gamma_5, \tag{72}$$

which is known as γ_5 Hermiticity. It implies that the operator

$$\gamma_5 M_W = (\gamma_5 M_W)^\dagger \tag{73}$$

is Hermitian and the eigenvalues of M_W are either real or come in complex conjugate pairs. Consequently, $\det(M_W)$ is real. In order for the pseudofermion representation (31) to be well defined, $\det(M_W)$ needs to be positive definite in addition, which is guaranteed if $m > 0$. However, due to the breaking of chiral symmetry the fermion mass is not protected against additive renormalization. The bare fermion mass receives corrections that are divergent in the continuum limit and needs to be renormalized. Because of this additive renormalization, the bare fermion mass corresponding to a physically interesting renormalized mass often turns out to be negative. While pairs of complex conjugate eigenvalues still give a positive contribution to $\det(M_W)$ in this case, the real eigenmodes only do so if the number of negative ones is even. Furthermore, even eigenmodes that are positive but very small pose serious problems for matrix inverters. In the case of an exact zero eigenmode, it is not possible to define the fermion determinant in terms of the pseudofermion fields according to Eq. (31). Hitting such a configuration within numerical precision will result in a failure of the matrix inversion to properly converge (Bardeen *et al.*, 1998). These configurations are known as "exceptional" and the appearance of even a single exceptional configuration in a Markov chain indicates that one is not able to properly sample a relevant region in configuration space. Ensembles exhibiting an exceptional configuration therefore have to be discarded.

In practice, exceptional configurations therefore set a lower limit to the masses one can reach with Wilson-type fermions. One has to make sure that all eigenmodes of the fermion matrix are sufficiently separated from zero. While these restrictions were initially very severe, they do not present a substantial obstacle for current state of the art lattice calculations. The use of large physical volumes, small lattice spacings, improved gauge actions (see Sec. II.E.1), and smeared link fermion actions (see Sec. II.E.2) all reduce the probability of exceptional configurations appearing in a simulation.

Because of the strong correlation between the condition number of the fermion matrix and the iteration count of the inverter and because the relative fluctuations of the largest eigenvalue are small, one can use the distribution of the inverse iteration count instead of the distribution of the lowest eigenmode. A tail of this distribution that extends toward the origin is a clear and direct indication of problems with exceptional configurations while a clear separation from 0 demonstrates the absence of exceptional configurations and positivity of the fermion determinant. Such a distribution is plotted in Fig. 3 for a recent study with light Wilson-type fermions (Durr *et al.*, 2011c).

The dominance of low modes in the computational cost of inverting a Wilson-type Dirac operator has led to efforts of preconditioning the inversion by removing or effectively projecting out a relatively small number of low modes. These techniques are generally known as deflation methods

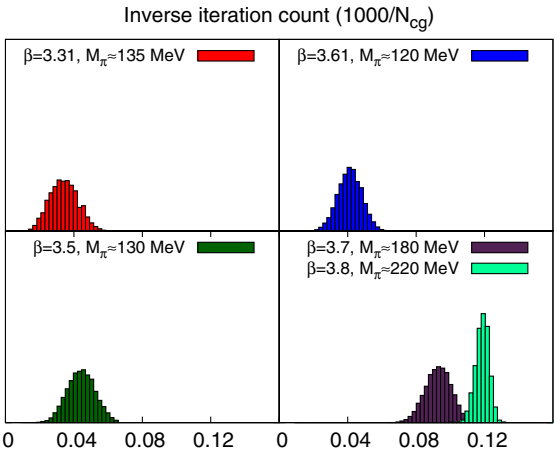

FIG. 3 (color online). Inverse iteration count of the fermion matrix inverter for Wilson-type fermions and a number of different ensembles with bare couplings β and approximate pion masses M_π. The lower tail of the distributions shows a clear separation from 0 indicating the absence of exceptional configurations in the ensembles. From Durr *et al.*, 2011c.

(de Forcrand, 1996; Neff *et al.*, 2001; Giusti *et al.*, 2003, 2004; DeGrand and Schaefer, 2004; Luscher, 2007; Stathopoulos and Orginos, 2007; Darnell, Morgan, and Wilcox, 2008). They can lead to a large decrease in the cost of computing propagators on gauge configurations, especially in circumstances where one needs to compute many propagators on the same gauge configuration. In this case, one can perform a rather expensive eigenmode projection step since it has to be performed only once for each gauge configuration. For a further discussion see also Sec. III.B.

On a more fundamental level, real modes of the Wilson operator are related to the topological charge of the gauge configuration by the index theorem (Atiyah and Singer, 1968). In the continuum limit, real modes become exactly degenerate zero modes that are tied to the gauge field topology (Smit and Vink, 1987; Setoodeh, Davies, and Barbour, 1988; Vink, 1988; Bardeen *et al.*, 1998; Gattringer and Hip, 1998; Hasenfratz, Laliena, and Niedermayer, 1998).

Recently it was proposed to construct a Wilson-like operator that instead of lifting the flavor degeneracy of the naive operator (44) lifts the taste degeneracy of the staggered operator (58) (de Forcrand, Kurkela, and Panero, 2010; Adams, 2011; Hoelbling, 2011) [for earlier work in this direction see also Becher and Joos (1982), Mitra (1983), Mitra and Weisz (1983), Gockeler (1984), Golterman and Smit (1984a, 1984b), and Golterman (1986)]. Conceptual aspects of this formulation are still being studied and no application to hadron spectroscopy or other phenomenologically relevant computations are available in the literature yet.

3. Twisted mass fermions

Twisted mass fermions (Frezzotti *et al.*, 2001) are a variant of the Wilson fermion formulation that has recently gained attention. The basic idea is to perform a chiral rotation, that is not affected by an anomaly, on the mass term. Because the transformation has to be anomaly free, the number of flavors to be chirally rotated has to be even. In the simplest case of two flavors the mass term reads

$$\bar{m}e^{i\alpha\gamma_5\tau_3} = m + i\mu\gamma_5\tau_3, \tag{74}$$

where

$$\tan(\alpha) = \frac{\mu}{m}, \qquad \bar{m} = m^2 + \mu^2, \tag{75}$$

and τ_3 is the diagonal Pauli matrix in flavor space. Because of the opposite twist angles between the two flavors, the anomaly cancels and the chiral rotation of the mass term (74) may be absorbed into a chiral rotation of the fermion fields

$$\bar{\Psi} \to \bar{\Psi}e^{i\alpha/2\gamma_5\tau_3}, \qquad \Psi \to e^{i\alpha/2\gamma_5\tau_3}\Psi, \tag{76}$$

provided that the massless part of the fermion operator is invariant under the chiral transformation (76). For Wilson fermions, however, chiral symmetry is explicitly broken. Replacing the standard mass term in Eq. (70) with a twisted mass term of the form (74) therefore results in a different theory where the two-flavor fermion matrix is given by

$$M_{tm} = \gamma_\mu D_\mu + \frac{r}{2}\Box + m + i\mu\gamma_5\tau_3. \tag{77}$$

This represents the twisted mass fermion matrix in the so-called twisted basis. The basis is called twisted because Eq. (77) describes the physically uninteresting case of a complex mass term. In order to obtain physically interesting predictions for a theory with a real mass term from Eq. (77), the chiral rotation in the mass term has to be supplemented by an equivalent transformation of the fermion fields (76). In the new basis, Eq. (77) describes the physically interesting case of real mass fermions. This rotated basis of the fermion fields is therefore usually referred to as the physical basis.

Wilson fermions with a twisted mass term do not obey standard time reversal and parity transformation symmetries but modified versions thereof. However, standard *CPT* symmetry is fulfilled and the behavior with regard to chiral and flavor symmetry is the same as for standard Wilson fermions, i.e., chiral symmetry is broken while flavor symmetry is exactly conserved in the twisted basis. In the physical basis (76), however, a subset of the flavor and axial symmetries gets transformed into each other. Consequently, flavor symmetry is broken while part of the chiral symmetry is restored at maximal twist $\alpha = \pi/2$. This implies that at maximal twist, on the one hand, there are isospin breaking cutoff effects (Scorzato, 2004; Bar, 2010), while, on the other hand, the cutoff terms are generally of $O(a^2)$ (Aoki and Bar, 2004; Frezzotti and Rossi, 2004a). Note that the bare mass is not protected against additive renormalization and therefore the mixing angle α gets renormalized. In order to achieve maximal renormalized twist, the bare mass needs to be tuned. This tuning is routinely done as part of any twisted mass calculation [see, e.g., Baron *et al.* (2010a)].

Introducing a pair of nondegenerate quarks is usually done with the help of an additional mass term that carries a nondiagonal flavor structure τ_1 resulting in a nondegenerate two-flavor fermion operator of the form

$$\hat{M}_{tm} = \gamma_\mu D_\mu + \frac{r}{2}\Box + m + i\mu\gamma_5\tau_3 + \epsilon\tau_1 \tag{78}$$

(Frezzotti and Rossi, 2004b; Chiarappa *et al.*, 2007). An alternative suggestion was proposed by Pena, Sint, and Vladikas (2004).

From Eq. (77) it follows that the two-flavor operator has a determinant which is bounded from below by μ^2 (Frezzotti *et al.*, 2001) and a spectral gap of size μ around the real axis (Gattringer and Solbrig, 2005). Furthermore, the twisted mass fermion matrix fulfills a generalized form of the γ_5-Hermiticity condition of the Wilson operator (72)

$$M_{tm}^\dagger = \gamma_5\tau_1 M_{tm}\tau_1\gamma_5 \tag{79}$$

that similarly implies the appearance of eigenmodes in complex conjugate pairs. In contrast to Wilson fermions however there are no real eigenmodes due to the spectral gap (Gattringer and Solbrig, 2005) and therefore no exceptional configurations. Note that Eq. (79) also holds for the nondegenerate $\hat{M}_{tm}$ from Eq. (78).

Numerical evidence was found with twisted mass fermions for a line of first order phase transition in the bare quark mass that extends into the twisted mass direction (Farchioni *et al.*, 2005a, 2005b). This observation can be understood in terms of the phase structure of lattice QCD with Wilson fermions as proposed by Sharpe and Singleton (1998) from analysis of the

effective chiral potential. It represents one of two possibilities of finding a minimum, the other one being the appearance of an unphysical phase where parity and flavor are spontaneously broken (Aoki, 1984; Aoki, Kaneda, and Ukawa, 1997). Evidence for the Aoki phase was found at coarser lattice spacings (Ilgenfritz *et al.*, 2004; Sternbeck *et al.*, 2004).

In general, it is mandatory for all simulations with Wilson-type fermions to avoid being too close to the line of first order phase transition. The situation is particularly challenging to twisted mass fermions at maximal twist, however, since the line of first order phase transition opens up in the twisted mass direction at the critical bare mass. The minimum pion mass one can reach with twisted mass fermions at a given lattice spacing is estimated by Shindler (2008) to be $\sim$300 MeV at $a \sim 0.07$–0.1 fm which is roughly consistent with recent numerical results (Baron *et al.*, 2010).

For further details about twisted mass fermions we refer the interested reader to a recent review (Shindler, 2008).

4. Chirally symmetric fermions

Although the Nielsen-Ninomiya theorem does not allow one to retain the continuum form of chiral symmetry for local, doubler free fermions, an exact symmetry may be found at finite lattice spacing that goes over into the continuum chiral symmetry upon removal of the cutoff (Ginsparg and Wilson, 1982; Narayanan and Neuberger, 1995; Hasenfratz, Laliena, and Niedermayer, 1998; Luscher, 1998). The continuum form of chiral symmetry implies that the massless fermion operator M anticommutes with γ_5. One can generalize that relation by introducing a modified

$$\hat{\gamma}_5 = \gamma_5(1 - 2aRM) \tag{80}$$

and demanding that

$$\gamma_5 M + M\hat{\gamma}_5 = 0. \tag{81}$$

The condition (81) is known as the Ginsparg-Wilson relation (Ginsparg and Wilson, 1982) and the operator R in Eq. (81) has to be local and is known as the Ginsparg-Wilson kernel. From Eq. (80) one can see that the action

$$S_{\mathrm{GW}} = \bar{\Psi} M \Psi \tag{82}$$

is invariant under the chiral symmetry

$$\bar{\Psi} \to \bar{\Psi}(1 + i\gamma_5), \qquad \Psi \to (1 + i\hat{\gamma}_5)\Psi. \tag{83}$$

The continuum form of chiral symmetry can be regained in observables by constructing them with the chirally rotated fermion field

$$\hat{\Psi} = \tilde{1}\Psi, \qquad \tilde{1} = 1 - aRM, \tag{84}$$

instead of the bare Ψ. As the full chiral symmetry is preserved by Ginsparg-Wilson fermions, all consequences of this symmetry such as the appearance of exact zero modes, an exactly conserved axial current (Kikukawa and Yamada, 1999), and the anomalous breaking of the flavor singlet part of the symmetry are also retained. It was proven by Horvath (1998) and Bietenholz (1999) that chirally symmetric lattice fermion operators cannot be ultralocal, i.e., they cannot be realized by couplings to a finite number of nearest neighbors. It is therefore necessary to prove the locality of chiral fermion actions in the sense that the coupling decreases exponentially with distance with an exponent that is on the order of the cutoff and not a physical mass.

Different fermion operators fulfilling the Ginsparg-Wilson relation have been suggested. The overlap operator (Narayanan and Neuberger, 1993a, 1993b, 1994, 1995; Neuberger, 1998b, 1998c) is an explicit construction that corresponds to the unitary part of a Wilson operator at negative bare mass $-\rho$. In the massless case, the fermion matrix is given by

$$M_o = \rho 1 + \left(\frac{M_W(-\rho)}{\sqrt{M_W^\dagger(-\rho) M_W(-\rho)}} \right), \tag{85}$$

and a real mass term may be added as

$$M_o(m) = M_o + \tilde{1}m. \tag{86}$$

The overlap operator (85) obeys the Ginsparg-Wilson relation with an ultralocal $R = 1/2\rho$. Locality of the overlap operator was established numerically (Hernandez, Jansen, and Luscher, 1999) [see also Golterman and Shamir (2003)]. Note that by construction the overlap operator is normal.

Overlap fermions are numerically extremely demanding. In contrast to all previously discussed fermion discretizations, the fermion operator M_o is not sparse. The multiplication of M_o on a vector has to proceed via approximating the inverse matrix square root in Eq. (85). While it is possible to do this with polynomial (Giusti *et al.*, 2003) or rational (Neuberger, 1998a; Edwards, Heller, and Narayanan, 1999; van den Eshof *et al.*, 2002) approximations, it typically requires at least $O(100)$ applications of the kernel Wilson operator to perform one matrix-vector multiplication with M_o.

Because of the exact chiral symmetry, overlap fermions are free of exceptional configurations at finite mass. This leads, however, to a nontrivial technical problem for dynamical overlap fermions that was first observed by Fodor, Katz, and Szabo (2004). The nonanalyticity of Eq. (85) implies a divergence of the fermionic force term (39) at certain points in configuration space. Specifically, such a divergence occurs at topological sector boundaries where the number of zero modes changes. These points have to be treated separately in the HMC integration (Fodor, Katz, and Szabo, 2004; Egri, 2006; Cundy *et al.*, 2009), specifically at fine lattices, as the simulation can get stuck in one topological sector.[6] Alternatively, one can artificially constrain the simulation to a single topological sector via the addition of extra Wilson fermions with large negative mass (Izubuchi and Dawson, 2002; Fukaya *et al.*, 2006; Vranas, 2006) and treat this constraint as an additional finite-volume effect.

Historically, overlap fermions were first formulated in five dimensions based on the realization that one may have chiral domain wall defects in a $(2n + 1)$-dimensional vectorlike gauge theory (Callan, Curtis, and Harvey, 1985; Kaplan, 1992; Frolov and Slavnov, 1993). This five-dimensional

[6]Note that while the nonanalyticity problem is particularly apparent for overlap quarks, its origin is physical. Upon removing the cutoff, every fermion formulation ultimately develops nonanalyticities at the topological sector boundaries.

form of chiral fermions was further developed by Shamir (1993) and is known as domain wall fermions. Domain wall fermions have an exact chiral symmetry only in the limit that the fifth dimension is large. Of course, on the lattice this cannot be realized and there is a remnant breaking of chiral symmetry (Blum and Soni, 1997) [for a recent update on the size of this effect see, e.g., Aoki *et al.* (2011)].

On a technical level, domain wall fermions are realized by five-dimensional Wilson fermions at a negative bare mass M. The gauge field is four dimensional only and identical for each slice in the fifth dimension. Along the fifth dimension s, gauge links are set to $U_5(x, s) = \mathbb{1}$ for $s \neq 0$ except at the defect location $s = 0$, where they are set to $U_5(x, 0) = \mathbb{1}m$. According to Shamir (1993), a left-, respectively, a right-handed chiral mode will form at the positive, respectively, negative side of the defect in the limit of an infinite fifth dimension and these modes couple with the mass term m. A remnant coupling of the chiral modes through the bulk will appear for a finite fifth dimension that will be suppressed exponentially in the size of the fifth dimension N_5.

Because of the residual chiral symmetry breaking, domain wall fermions suffer a small additive mass renormalization known as residual mass m_{res}. As in the case of Wilson fermions it is therefore necessary in principle to take negative bare mass values for reaching arbitrarily small but positive renormalized quark masses. One could therefore encounter exceptional configurations, but due to the smallness of m_{res} this is not a problem in current simulations. The extent of the fifth dimension is typically around $N_5 = 16$ in present day calculations rendering domain wall fermions numerically more expensive than Wilson fermions by about an order of magnitude.

Another variant of chirally symmetric lattice fermion operators is known as perfect action or fixed point fermions (Hasenfratz and Niedermayer, 1994; DeGrand *et al.*, 1995; Bietenholz and Wiese, 1996). Perfect actions are obtained by following the renormalization group flow of a blocking transformation to the renormalized trajectory that ends in a fixed point. Therefore, their form is not explicitly given but needs to be determined by following the renormalization group flow. Up to truncation errors, the action so obtained is classically perfect in the sense that it has no remaining cutoff effects in the classical theory (see Sec. II.E.2 for a more detailed discussion).

From a numerical perspective, fixed point actions are expensive to simulate. In principle, fixed point fermion operators are not sparse matrices and neither can they be explicitly constructed out of a sparse matrix as is the case for overlap fermions. Consequently, one needs to truncate the operator to a finite range and the chiral symmetry is only approximate. The resulting additive mass renormalization is small, however, and no problems with exceptional configurations have been seen (Gattringer *et al.*, 2004). The same paper also reports that the numerical cost is increased between 1 and 2 orders of magnitude compared to Wilson fermions. For a review of truncated perfect action fermions, see Bietenholz (2008).

Yet another variant of approximately chiral lattice fermions is obtained by inserting a truncated expansion of a general fermion operator into the Ginsparg-Wilson relation (81) and explicitly solving for the expansion coefficients (Gattringer, 2001). Numerical properties and cost of this variant of approximately chiral fermions are roughly comparable to those of the truncated perfect action as demonstrated by Gattringer *et al.* (2004).

E. Constructing efficient regularizations

As mentioned in Sec. II.B, lattice discretizations of continuum actions are not unique. The essential step in discretizing a continuum action is the replacement of derivative terms by lattice finite difference operators. Disregarding quantum effects, it is easy to see how the discretization of derivative operators can be systematically improved by adding finite difference operators with increasing distances. For the simple case of one-dimensional symmetric difference operators

$$\begin{aligned}\Delta_1 f(x) &= \frac{f(x+a) - f(x-a)}{2a} \\ &= f'(x) + \frac{a^2}{6} f'''(x) + O(a^4), \\ \Delta_2 f(x) &= \frac{f(x+2a) - f(x-2a)}{4a} \\ &= f'(x) + \frac{4a^2}{6} f'''(x) + O(a^4),\end{aligned} \tag{87}$$

we find discretization errors of $O(a^2)$. In the linear combination

$$\Delta^i = \frac{4\Delta_1 - \Delta_2}{3}, \tag{88}$$

however the $O(a^2)$ terms cancel and therefore

$$\Delta^i f(x) = f'(x) + O(a^4). \tag{89}$$

Generally speaking, one can systematically improve discretized continuum operators by taking liner combinations of lattice operators and imposing conditions on the coefficients such that the continuum limit is correct and leading order discretization effects are canceled.

Finding the proper coefficients in the linear combination is of course not always as trivial as in the example above. Specifically, one needs to keep in mind that when computing observables in a quantum theory, the classically computed coefficients can receive radiative corrections. One can then look at a certain set of observables and try to cancel higher order effects in them on a quantum level. Such a strategy was first suggested by Symanzik (1983a, 1983b) who realized that a lattice Lagrangian in general is equivalent order by order in a and g^2 to a continuum local effective Lagrangian.

Other strategies of finding improved discretizations are based on the mean field approximation or the renormalization group as detailed below. One common feature that all of the methods share is that they use the freedom in defining a lattice regularization of a continuum operator in order to suppress unphysical UV fluctuations in the lattice action. There is no *a priori* guide for determining which specific improvement out of the rather large number of possibilities is optimal. It is therefore essential to consider the potential benefits of a specific improvement in relation to its computational cost. In the end, the optimal action will be the one that provides the

smallest error (including all systematics) on the physical observables (i.e., the hadron masses) for a given amount of available computer time. To find a good improvement strategy one therefore needs to find the right balance of different improvements such that the overall error is minimized.

1. Gauge field improvement

The simple Wilson gauge action (20) contains only the elementary plaquette and has discretization errors of $O(a^2)$. As demonstrated by Weisz (1983) and Luscher and Weisz (1985b, 1985c), one can improve the scaling by taking proper linear combinations of the elementary Wilson plaquette and more extended gauge loops. The coefficients must of course be chosen such that in the continuum limit one still obtains the correct continuum gauge action (21). In addition, however, one can demand that all corrections that are of $O(a^2)$ vanish classically. The desired continuum action has the form

$$\mathcal{O}_0 = \mathrm{Tr}(F_{\mu\nu}F_{\mu\nu}). \tag{90}$$

All together, there are three different terms that represent possible $O(a^2)$ corrections to this form

$$\begin{aligned}\mathcal{O}_1 &= \mathrm{Tr}(D_\mu F_{\mu\nu} D_\mu F_{\mu\nu}),\\ \mathcal{O}_2 &= \mathrm{Tr}(D_\sigma F_{\mu\nu} D_\sigma F_{\mu\nu}),\\ \mathcal{O}_3 &= \mathrm{Tr}(D_\mu F_{\mu\nu} D_\sigma F_{\sigma\nu}),\end{aligned} \tag{91}$$

where the covariant derivative D_μ is given by Eq. (5). In order to reach classical improvement, we have to demand that these additional terms vanish.

On the lattice, a gauge action can generically be written as a sum of terms of the form

$$S_i = \beta \sum_{\mathcal{P}\in\mathcal{C}_i} \left\{1 - \frac{1}{3}\,\mathrm{Re}\,\mathrm{Tr}[U(\mathcal{P})]\right\}, \tag{92}$$

where the $U(\mathcal{P})$ are path ordered products of gauge links along a closed path $\mathcal{P}$. For the simple Wilson gauge action (20), which we refer to as S_0 in this context, the set of closed gauge loops $\mathcal{C}_0$ consists of all elementary plaquettes. Going 1 order higher, we see that there are also three possible forms of six-link loops that are the minimal extensions of the elementary plaquette. The first one of them is the planar 2×1 loop while the other ones extend into the elementary hypercube (see Fig. 4). Not distinguishing between loops that differ only by rotation, we label the sets of loops of these different forms $\mathcal{C}_1$, $\mathcal{C}_2$, and $\mathcal{C}_3$. The expansion of the corresponding gauge actions (92) in terms of continuum operators (91) up to next-to-leading order (NLO) reads (Luscher and Weisz, 1985b, 1985c)

$$\begin{aligned}S_0 &= -\tfrac{1}{4}\mathcal{O}_0 + \tfrac{1}{24}\mathcal{O}_1 + \cdots,\\ S_1 &= -2\mathcal{O}_0 + \tfrac{5}{6}\mathcal{O}_1 + \cdots,\\ S_2 &= -2\mathcal{O}_0 - \tfrac{1}{6}\mathcal{O}_1 + \tfrac{1}{6}\mathcal{O}_2 + \tfrac{1}{6}\mathcal{O}_3 + \cdots,\\ S_3 &= -4\mathcal{O}_0 + \tfrac{1}{6}\mathcal{O}_1 + \tfrac{1}{2}\mathcal{O}_3 + \cdots,\end{aligned} \tag{93}$$

where volume sums are implied. For a general linear combination

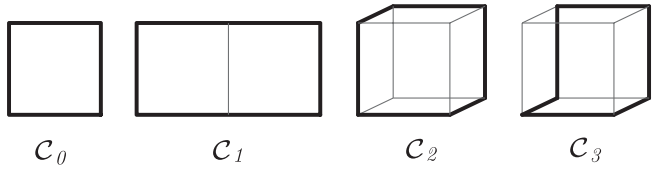

FIG. 4. The four possible forms of closed gauge loops on a hypercubic lattice with six or less gauge links corresponding to the members of the sets $\mathcal{C}_0, \ldots, \mathcal{C}_3$ as described in the text.

$$S = \sum_{i=0}^{4} c_i S_i, \tag{94}$$

the correct continuum limit is therefore imposed by the condition

$$c_0 + 8c_1 + 8c_2 + 16c_3 = 1. \tag{95}$$

The cancellation of all the higher order operators (91) may be achieved by imposing

$$c_0 + 20c_1 = 0, \qquad c_2 = c_3 = 0, \tag{96}$$

which leads to a choice of coefficients $c_0 = 5/3$ and $c_1 = -1/12$. The resulting action is known as the tree level Lüscher-Weisz action. It realizes the tree level (i.e., classical) $O(a^2)$ improvement of the Wilson plaquette gauge action (20). Even before the work of Lüscher and Weisz these coefficients were found by Curci, Menotti, and Paffuti (1983) with a different matching procedure.

As mentioned, in a quantum theory radiative corrections can in general reintroduce $O(a^2)$ terms into observables. Generically, these corrections are proportional to g^2 such that the tree level Lüscher-Weisz action is correct up to $O(g^2a^2)$ terms as opposed to $O(a^4)$ in the classical theory. In order to correct for these radiative effects, one may look at different on-shell observables. Looking at the scattering amplitudes of massive gluons one can construct an action with $O(g^4a^2)$ scaling by modifying c_0, c_1, and c_2 with $O(g^2)$ terms (Luscher and Weisz, 1985a). The resulting coefficients read $c_0 = 5/3 + 0.237g^2$, $c_1 = -1/12 - 0.025\,21g^2$, and $c_2 = -0.004\,41g^2$. Note that the one-loop coefficients are explicitly scale dependent via g^2.

It is of course possible to go beyond perturbative Symanzik improvement and concentrate on specific discretization terms that are found to be important in nonperturbative calculations. One case of particular relevance was found by Parisi (1980) and Lepage and Mackenzie (1993). As the gauge field is represented on the lattice in exponentiated form

$$\begin{aligned}U_\mu(x) &= e^{igaA_\mu(x)}\\ &= 1 + igaA_\mu(x) - \frac{g^2a^2}{2}A_\mu^2(x) + \cdots,\end{aligned} \tag{97}$$

the theory contains vertices with an arbitrary number of gluons that give rise to tadpole diagrams. Although these are formally suppressed by powers of a, UV divergences in the tadpole loops appear and these terms are in fact scaling as powers of g^2 instead.

This problem may be addressed in mean field theory by redefining the relation between the lattice U_μ and the

continuum A_μ. Formally writing the gauge field U_μ as a product of an IR and an UV part

$$U_\mu = U_\mu^{(\mathrm{UV})} U_\mu^{(\mathrm{IR})}, \tag{98}$$

and replacing the UV part by its mean field value u_0, one can now identify the physically relevant IR part $U_\mu^{(\mathrm{IR})}$ of the lattice gauge field with the continuum field obtaining a relation

$$U_\mu = u_0 e^{igaA_\mu(x)} \tag{99}$$

between the lattice gauge field U_μ and the continuum A_μ. One can therefore implement tadpole improvement by replacing all gauge links U_μ in lattice operators by U_μ/u_0. Because UV fluctuations are dominant, one can obtain a good estimate of u_0 by simply taking the expectation value of the trace of a gauge link in a fixed gauge or, alternatively, defining

$$u_0 = \langle \tfrac{1}{3} \mathrm{Re}\,\mathrm{Tr}(U_{\mu\nu}) \rangle^{1/4}. \tag{100}$$

In both cases u_0 can be determined either in perturbation theory or by measuring it directly as part of a nonperturbative calculation. In the latter case, care has to be taken to determine u_0 self-consistently because it is both a parameter in the action and an observable.

There is a third, independent strategy of improving the gauge action that is based on the renormalization group. As mentioned in Sec. II.D.4, one may try to follow the renormalization group flow of a blocking transformation in the space of all possible actions toward the renormalized trajectory. The renormalized trajectory is the trajectory of the renormalization group flow that starts from a fixed point at the critical surface where the correlation length diverges. Any point along the renormalized trajectory therefore corresponds to the action at a certain finite correlation length that has vanishing irrelevant operator contributions and therefore reproduces continuum physics without cutoff effects. Actions along the renormalized trajectory are thus called perfect actions.

The exact position of the renormalized trajectory is elusive since the renormalization flow is not known analytically. Strategies of finding approximations are based on the fact that the renormalized trajectory is attractive under blocking transformations as they reduce irrelevant operators. One should also keep in mind that a perfect action generally lives in an infinite dimensional space of couplings that has to be truncated for practical purposes and that a thus truncated perfect action is not guaranteed to exhibit the smallest scaling violations possible among actions living in that subspace.

Studying the repeated application of a blocking transformation in a truncated subspace of gauge loops, Iwasaki (1983) suggested an action of the Lüscher-Weisz form (94) but with a set of coefficients $c_0 = 3.648$, $c_1 = -0.331$, and $c_2 = c_3 = 0$. Also within the same truncation scheme, the doubly blocked Wilson (DBW2) action (Takaishi, 1996; de Forcrand *et al.*, 2000) was obtained by double blocking from Wilson configurations. It has the coefficients $c_0 = 12.2704$, $c_1 = -1.4088$, and $c_2 = c_3 = 0$. Note that these coefficients do not have an explicit scale dependence and therefore can cancel quantum effects only at the scale where they are computed.

A different strategy was followed by Hasenfratz and Niedermayer (1994) and DeGrand *et al.* (1995) who obtained a classically perfect action by a saddle point integration around $g = 0$ followed by a truncation to a rather large set of couplings.

2. Fermion field improvement

In the case of lattice gauge actions, the Wilson plaquette action (20) provided a unique starting point for all improvement efforts. In the case of fermion actions the range of unimproved actions is quite diverse and so are their major discretization effects. There are some common improvements that positively affect all fermion actions, but the improvement strategies are sufficiently distinct for different discretizations so we will discuss them separately. We start by first discussing the improvement of Wilson fermions.

The Wilson fermion action (68) has leading discretization effects of $O(a)$. These can be canceled classically by adding a two-hop term to the action (Hamber and Wu, 1983)

$$S_{\mathrm{HW}} = \bar{\Psi}\Big(\gamma_\mu(2D_\mu - \hat{D}_\mu) + \frac{r}{2}(2\Box - \hat{\Box}) + m\Big)\Psi, \tag{101}$$

with $\hat{\Box} = \sum_\mu \hat{C}_\mu$ and the covariant two-hop operators from Eq. (65). One could in principle compute the coefficients of the one-hop and two-hop terms in perturbation theory or nonperturbatively to achieve further improvement. This was not further pursued in practice, however, since Sheikholeslami and Wohlert (1985) discovered that one can remove $O(a)$ discretization terms with a more local operator. This additional term is the discretized magnetic moment operator and the corresponding action reads

$$S_{\mathrm{SW}} = S_W - \frac{r c_{\mathrm{SW}}}{2} \sum_{\mu<\nu} \bar{\Psi}\, \sigma_{\mu\nu} F_{\mu\nu} \Psi, \tag{102}$$

where the field strength $F_{\mu\nu}(x)$ is usually obtained by taking an average of the imaginary parts of all the plaquettes around the point x. Because of the arrangement of the four plaquettes involved in the average, the additional term and the resulting action are commonly referred to as the clover term and the clover action. Tree level improvement is achieved by setting the coefficient $c_{\mathrm{SW}} = 1$. The resulting action has discretization effects of $O(g^2 a)$ and $O(a^2)$. Numerically, the $O(g^2 a)$ and $O(a^2)$ corrections are competing and it is not possible to say *a priori* which of these effects are dominant for a specific observable at a specific lattice spacing. Further improvement is possible by perturbation theory (Wohlert, 1987; Luscher and Weisz, 1996), mean field tadpole improvement, or nonperturbative methods (Luscher *et al.*, 1997). It turns out that the clover action (102) is equivalent to the Hamber-Wu action (101) up to $O(a^2)$ terms in terms of rotated fermion fields (Heatlie *et al.*, 1991; Martinelli, Sachrajda, and Vladikas, 1991).

Although suggestions exist for further improving the Wilson operator by adding more extended terms (Alford, Klassen, and Lepage, 1997; DeGrand, 1998; Durr and Koutsou, 2011), they are not often pursued due to the computational overhead.

In contrast to Wilson fermions the staggered action has leading discretization effects of $O(a^2)$. These can be eliminated on a classical level by replacing the one-hop derivative of the staggered action (57) with a suitable combination of one-hop and three-hop derivative operators such that $O(a^2)$ terms cancel (Naik, 1989). The three-hop term is used rather than the two-hop term in order not to interfere with the staggered flavor structure.

The main concern for staggered fermions, however, is not the Symanzik improvement but rather the minimization of taste breaking effects. Since the different fermion components sit at the edges of the Brillouin zone, they interact via the exchange of hard gluons with momenta on the order of the cutoff scale. Suppressing these interactions, i.e., reducing the unphysical UV fluctuations, is therefore especially important for staggered fermions.

The primary method in use today for reducing unphysical UV noise is link smearing (also known as UV filtering or fattening). Since link smearing is used for Wilson-type and chirally symmetric fermion actions as well, we discuss it in a more general context. Although on a technical level it can be implemented by modifying the gauge fields only, it is important to remember that it strictly is a modification of the fermion action only. The original suggestion, put forward by the APE Collaboration (Albanese *et al.*, 1987), is commonly known as APE smearing. The basic idea is that one can use the freedom in defining the parallel transport in the covariant one-hop term (15) of any fermion operator to suppress UV fluctuations. It is not necessary that one takes the same gauge link as used in the gauge action but instead a linear combination of various paths that have the correct starting and end points. In the case of APE smearing these paths are, in addition to the original gauge link, all three-link connections of the same two points (see Fig. 5) usually referred to as staples.[7]

One can define an APE smeared gauge link $U_\mu^{(\mathrm{APE})}(x)$ from the original gauge links $U_\mu(x)$ in d dimensions via

$$U_\mu^{(\mathrm{APE})}(x) = (1-\alpha)U_\mu(x) + \frac{\alpha}{2(d-1)}\Omega_\mu(x), \tag{103}$$

where we used the staple sum

$$\Omega_\mu(x) = \sum_{\pm\nu\neq\mu} U_\nu(x)U_\mu(x+\hat{\nu})U_\nu^\dagger(x+\hat{\mu}) \tag{104}$$

with the identity $U_{-\mu}(x) = U_\mu^\dagger(x-\hat{\mu})$. The smearing parameter α determines the relative weight of the staple versus the original link and is typically set to a value $\alpha \sim 0.6$. The resulting gauge links $U_\mu^{(\mathrm{APE})}(x)$ are no more an element of the gauge group and it is therefore customary to backproject them onto the gauge group via

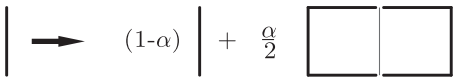

FIG. 5. The principle of APE smearing displayed in the two-dimensional case. The "thin" gauge link is replaced by a weighted average over the gauge link and the staples, which is then usually backprojected onto the gauge group.

$$U' = \frac{U^{(\mathrm{APE})}}{\sqrt{U^{(\mathrm{APE})\dagger}U^{(\mathrm{APE})}}}, \qquad \hat{U} = \frac{U'}{(\det U')^{1/3}}, \tag{105}$$

where U' is unitary and $\hat{U}$ also has unit determinant.[8]

As the backprojection (105) is not analytic, the fermionic force term (39) in the pseudofermion field integration may exhibit singularities. Although there are suggestions to remedy this situation by leaving out the second step of the backprojection (105) and use U' only (Hasenfratz, Hoffmann, and Schaefer, 2007), it is customary in dynamical simulations to use the analytic link smearing suggested by Morningstar and Peardon (2004). They define the so-called stout link as[9]

$$V_\mu(x) = e^{\rho S_\mu(x)}U_\mu(x), \tag{106}$$

where

$$S_\mu(x) = \frac{1}{2}\left(A_\mu(x) - \frac{1}{N}\,\mathrm{Tr}A_\mu(x)\right), \tag{107}$$

with

$$A_\mu(x) = \Omega_\mu(x)U_\mu^\dagger(x) - U_\mu(x)\Omega_\mu^\dagger(x). \tag{108}$$

The parameter ρ is a smearing parameter that, similar to α in the case of APE smearing, determines the relative weights of the original link and the staple. For small smearing parameters, APE and stout link smearing are equivalent if one sets $\alpha = 2(d-1)\rho$ (Capitani, Durr, and Hoelbling, 2006). With a proper matching of the smearing parameters one can find a close correspondence even if their values are large (Hasenfratz, Hoffmann, and Schaefer, 2007).

Both APE and stout smearing, as in general all link smearing techniques, generate a smeared gauge field from the original one, which is usually called a thin link. It is therefore straightforward to apply the smearing prescription repeatedly on the already smeared links and use this multiply smeared gauge link field for constructing the fermionic operator. As long as the smearing parameter and the number of smearing steps is held constant, it amounts to an ultralocal redefinition of the fermion operator and does not affect the continuum limit. In fact, the locality range of an ultralocal fermion operator itself is not at all affected by smearing the gauge links. Gauge link smearing does not introduce any new couplings into the fermion operator. What is affected by gauge link smearing is the fermion to gauge field coupling which becomes more extended. For smeared gauge links the

[7]Note that in the literature the sum over all three-link connections is also sometimes referred to as the staple.

[8]For an alternative suggestion on doing the backprojection see Durr and Koutsou (2011).

[9]We use the term stout link as is commonly done in the literature. Note, however, that in the original paper the term stout link was used in a slightly different way.

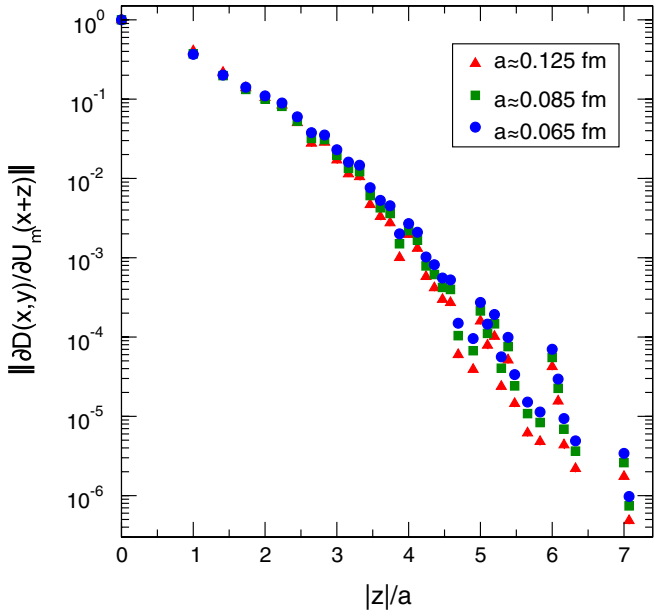

FIG. 6 (color online). Locality of a fermion operator coupling to a 6-times stout smeared gauge field. The stout smearing parameter is set to $\rho = 0.11$. At small distances the coupling decreases exponentially with an effective mass of $\sim 2.2a^{-1}$ that is proportional to the lattice cutoff. At Euclidean distances larger than $\sqrt{50}a$ couplings are zero due to the ultralocality of the smearing procedure. From Durr *et al.*, 2008.

fermion matrix elements are affected by changes of the original gauge field at further distances. If one keeps the number of smearing steps constant when going to the continuum limit, however, this redefinition is still ultralocal. In addition, if the smearing parameter is not excessive, one expects an exponential decrease of the gauge field to fermion coupling within the ultralocality range with an exponent that is proportional to the cutoff. This has been numerically demonstrated for a 6-times stout link smeared tree level improved Wilson operator in Durr *et al.* (2008) (see Fig. 6).

A variant of APE link smearing where one tries to maximize the smearing while only taking into account links that have a distance of at most one single lattice unit to the original link is known as hypercubic (HYP) smearing (Hasenfratz and Knechtli, 2001). One step of HYP smearing combines three steps of APE smearing where in the first two APE steps all dimensions that would give distance two contributions in any one direction are disregarded in forming the staple sum. The analytic version of HYP smearing along the lines of Morningstar and Peardon (2004) is known as hypercubic exponential (HEX) smearing (Capitani, Durr, and Hoelbling, 2006).

In the context of Wilson-type fermions smearing has been found to drastically reduce the additive mass renormalization, especially in combination with $O(a)$ improvement (Capitani, Durr, and Hoelbling, 2006). Furthermore, renormalization constants and the value of the improvement coefficient c_{SW} from Eq. (102) are much closer to their tree level values and the normality of the operator is improved (Durr, Hoelbling, and Wenger, 2005; Hoffmann, Hasenfratz, and Schaefer, 2007; Horsley *et al.*, 2008; Durr *et al.*, 2009). Most importantly, gauge link smearing reduces the fluctuations in the real modes that lead to exceptional configurations (DeGrand, Hasenfratz, and Kovacs, 1999; Stephenson *et al.*, 2000). Thus it is possible with smeared link Wilson-type fermions to reach physical quark masses (Durr *et al.*, 2011c), which has proven to be difficult without link smearing. These are clear indications that gauge link smearing efficiently suppresses UV fluctuations and ameliorates the chiral symmetry breaking that is inherent in Wilson-type fermions.

One can combine nonperturbative improvement of the Wilson action with smearing as is done, e.g., in the stout link improved nonperturbative clover (SLINC) action (Horsley *et al.*, 2008).

It is also possible to use different gauge link definitions for different parts of the fermion operator. An operator of this form, the so-called fat link irrelevant clover (FLIC) fermions suggested by Zanotti *et al.* (2002), uses an $O(a)$ improved Wilson operator with smeared links in the continuum irrelevant terms and original thin links for the rest.

The improvements of Wilson-type fermions carry over to their use as kernel operators for the overlap construction. Overlap operators with smeared Wilson kernels are generally cheaper computationally, have renormalization constants closer to their tree level values, and require less fine-tuning of the negative mass parameter ρ (DeGrand, Hasenfratz, and Kovacs, 2003; Kovacs, 2003; Durr, Hoelbling, and Wenger, 2005; Durr and Hoelbling, 2005a).

In the context of staggered fermions the main advantage of smeared links is the suppression of taste violation (Blum *et al.*, 1997; Lepage, 1998, 1999; Lagae and Sinclair, 1998; Orginos and Toussaint, 1998; Orginos, Toussaint, and Sugar, 1999).[10] In the context of staggered fermions, the staples used in APE smearing are referred to as fat3 staples. Adding to these staples ones that extend in a second lattice direction and consist of five links one arrives at the so-called fat5 links. Adding staples that extend in all three other lattice directions and consist of seven links each one obtains smeared gauge links referred to as fat7. Finally, staples that consist of five links and extend two lattice spacings in one direction are referred to as the Lepage term (Lepage, 1999). Adding a Naik term to the staggered action, replacing the gauge links with fat7 gauge links plus a Lepage term and tadpole improving the action one obtains the so-called "asqtad" action that is frequently used in current staggered fermion calculations and has scaling corrections of $O(g^2a^2)$. More recently, two steps of fat7 link smearing, the first one without the second one with the Lepage term, with a gauge group projection after the first smearing step were suggested by Follana *et al.* (2007). Staggered fermions with this variant of link smearing are known as "highly improved staggered quarks" or HISQ.

Besides these smearing terms that were specifically designed to reduce taste splitting, simple stout link smearing has also been applied to the staggered fermion operator. Depending on the quark mass, the level of taste splitting was found to be generally comparable to that of the HISQ action or slightly less than for the specially designed asqtad action (Aoki *et al.*, 2009; Borsanyi *et al.*, 2010).

[10]For a study of reduced taste violation with an improved, unsmeared action see Bernard *et al.* (1998b).

F. Anisotropic discretizations

As we will discuss in Sec. III, information about excited states can be extracted from correlation functions at short Euclidean distances. It is therefore desirable for excited hadron spectroscopy to have a fine resolution in the time direction while keeping the resolution in the space direction coarser in order to keep the overall computational effort small.

Choosing an anisotropic discretization explicitly breaks the hypercubic lattice remnant of the Lorentz symmetry down to the subgroup of spatial cubic rotations. Consequently spatial and temporal lattice extents receive different normalization and the renormalized anisotropy generally differs from the input bare one.

Generalizing the simple case of the Wilson plaquette action (20) to include an anisotropy one obtains

$$S_{\mathrm{AW}} = \beta\xi_0 \sum_{x,i>j}\left\{1 - \frac{1}{3}\,\mathrm{Re}\,\mathrm{Tr}[U_{ij}(x)]\right\} + \frac{\beta}{\xi_0}\sum_{x,i}\left\{1 - \frac{1}{3}\,\mathrm{Re}\,\mathrm{Tr}[U_{i0}(x)]\right\}, \tag{109}$$

where $\xi_0 = a_0^s/a_0^t$ is the bare anisotropy factor for the gauge action, i.e., the ratio of bare spatial to temporal lattice spacings. Similarly one can define an anisotropic Wilson fermion operator as a generalization of the isotropic case (70)

$$M_{\mathrm{aniso}} = m + \nu_s\left(\gamma_i D_i + \frac{r}{2}\sum_i C_i\right) + \nu_t\left(\gamma_0 D_0 + \frac{r}{2}C_0\right), \tag{110}$$

with C_μ defined in Eq. (69) and $\nu_{s/t}$ the speed of light in the spatial or temporal direction. In order to obtain the same renormalized aspect ratio for both fermion and gauge actions one needs to tune ν_s and ν_t. An additional tuning of the gauge action anisotropy is required only if one wants to tune to a specific renormalized aspect ratio.

The improvement program for gauge and fermion fields as outlined in Sec. II.E can be carried over to anisotropic lattices if one keeps in mind the separation between spatial and temporal split and ultimate tuning of both gauge and fermion field anisotropies. Since spatial and temporal directions are in any case treated differently for anisotropic lattices, one may even use different improvements on spatial and temporal field components that are specifically suited for either coarse or fine lattices. For further details on implementation and parameter tuning of anisotropic scalar, gauge, and fermion actions, see, e.g., Burgers *et al.* (1988), Karsch and Stamatescu (1989), Csikor, Fodor, and Heitger (1998), Klassen (1998), Engels, Karsch, and Scheideler (2000), Alford *et al.* (2001), Chen (2001), Harada *et al.* (2001), Umeda *et al.* (2003), Morrin *et al.* (2006), and Edwards, Joo, and Lin (2008).

III. EXTRACTION OF HADRON MASSES

In Sec. II we set up the framework for regularizing QCD on a discrete spacetime lattice. In this section we discuss how to extract the observables of interest, the hadron masses and energy levels, from lattice QCD. The emphasis in this section is on the technical details of extracting hadron masses in a nonperturbative lattice QCD calculation. The question of how these measured hadron masses can be turned into physical predictions is discussed in Sec. IV.

We start by discussing the basic concept of extracting energy levels in lattice QCD in Sec. III.A with an emphasis on the extraction of the ground state. The efficiency of this extraction of energy levels depends on the choice of source and sink operators, which is reviewed in Sec. III.B. Finally, we discuss the particular challenges involved in extracting excited states in Sec. III.C.

A. Extraction of energy levels in lattice QCD

The principle of extracting energy levels of hadrons from lattice QCD is relatively straightforward. Given a specific fermion matrix $M(U)$ on a gauge field background U, the Feynman propagator $S_U(x, y)$ of the fermion field on this given gauge field background is

$$S_U(y, x) = (M_U^{-1})_{y,x}, \tag{111}$$

where we suppressed additional color and spinor indices that both M and S carry. These quark propagators on a fixed gauge field background are the basic building blocks from which hadronic observables may be built. Note that for every action that fulfills the γ_5-Hermiticity condition (72) one can write

$$S_U(x, y) = \gamma_5 S_U^\dagger(y, x)\gamma_5 \tag{112}$$

to exchange source and sink points of the propagator. For staggered fermions an equivalent relation is provided by the ϵ-Hermiticity (60) that implies

$$S_U(x, y) = \epsilon S_U^\dagger(y, x)\epsilon. \tag{113}$$

Having constructed a hadronic observable, one can simply average it over the configurations that were produced using an importance sampling technique (see Sec. II.C) to obtain the path integral expectation value (24) up to a statistical precision which is limited by the size of the ensemble of configurations.

We assume that we are interested in the mass of a certain hadronic state $|h\rangle$ that we do not know how to construct explicitly. We choose two (not necessarily different) interpolating operators $\mathcal{O}_{i/f}$ that have a nonvanishing overlap with $|h\rangle$:

$$\langle 0|\mathcal{O}_{i/f}|h\rangle \neq 0 \tag{114}$$

and compute the expectation value of the correlation function

$$G(t, 0) = \langle 0|\mathcal{O}_f(t)\mathcal{O}_i^\dagger(0)|0\rangle = \langle 0|e^{\mathcal{H}t}\mathcal{O}_f(0)e^{-\mathcal{H}t}\mathcal{O}_i^\dagger(0)|0\rangle \tag{115}$$

between times 0 and t. Inserting a complete set of eigenstates of the Hamiltonian $\mathcal{H}$ in the standard fashion we find

$$G(t, 0) = \sum_n \frac{\langle 0|\mathcal{O}_f|n\rangle\langle n|\mathcal{O}_i^\dagger|0\rangle}{2E_n} e^{-E_n t}, \tag{116}$$

where E_n is the energy of the nth eigenstate of $\mathcal{H}$ above the vacuum energy. If the state $|h\rangle$ we are interested in happens to be the lowest energy state with the quantum numbers of $\mathcal{O}_{i/f}$,

one simply needs to go to asymptotic times for all other states to die out in the correlation function (114)

$$G(t,0)\overset{t\to\infty}{\longrightarrow}\frac{\langle 0|\mathcal{O}_f|h\rangle\langle h|\mathcal{O}_i^\dagger|0\rangle}{2M_h}e^{-M_h t} \tag{117}$$

and to extract the mass M_h and the product of matrix elements $\langle 0|\mathcal{O}_f|h\rangle\langle h|\mathcal{O}_i^\dagger|0\rangle$ from it.

It is of course not possible to go to asymptotic times on a finite lattice. However, since the higher energy states are dying off exponentially in Euclidean time with an exponent that is their energy difference to the ground state, it is often possible to reach a distance that is effectively asymptotic for limited lattice time extents. The time interval that starts from where one cannot see the effect of higher energy states and ends at a possible loss of signal is called the plateau region. For ground state spectroscopy it is desirable to extend this plateau region in order to get a statistically clean signal. This is often achieved by choosing the operators $\mathcal{O}_{i/f}$ in such a way that they have a large overlap with the ground state and small overlap with all other states. This will be detailed further in Sec. III.B.

Another common strategy to extend the plateau range is to take either $\mathcal{O}_i$ or $\mathcal{O}_f$ to be a sum of local operators $\mathcal{O}_l$ over an entire time slice

$$\mathcal{O}_{i/f}(t)=\sum_{\vec{x}}\mathcal{O}_l(t,\vec{x}). \tag{118}$$

With this choice either the initial or the final state is projected to zero spatial momentum and consequently all higher momentum excitations that may appear in the sum over states (116) are canceled.

Since our lattices have a torus topology with a period T in time direction, there is a backward contribution that is dominant for $T-t>t$. It has a similar form than Eq. (117) with the difference that the complete set of states has now been inserted on the other side

$$G(t,0)\overset{T-t\to\infty}{\longrightarrow}b\frac{\langle 0|\mathcal{O}_i^\dagger|\bar{h}\rangle\langle\bar{h}|\mathcal{O}_f|0\rangle}{2M_{\bar{h}}}e^{-M_{\bar{h}}(T-t)}. \tag{119}$$

Note the appearance of the ground state $\bar{h}$. It coincides with h except for cases where the lowest state that couples to both $\mathcal{O}_i$ and $\mathcal{O}_f$ is different from the lowest state that couples to both $\mathcal{O}_i^\dagger$ and $\mathcal{O}_f^\dagger$. The factor $b=\pm 1$ has been inserted to account for a sign flip that occurs for interpolating operators with an odd number of quark fields when the time slice is crossed that incorporates antiperiodic boundary conditions in the time direction. Without loss of generality, we assume here that this time slice is traversed in the backward contribution.

In addition one also has in principle contributions from propagators that wrap 1 or more times around the lattice in the time direction. These contributions are small, however; each additional wrapping gives a suppression factor e^{-TM_h} or $e^{-TM_{\bar{h}}}$, and the resulting geometric series can be summed up. Putting all this together, we find that in the plateau range the correlation function (115) is given by

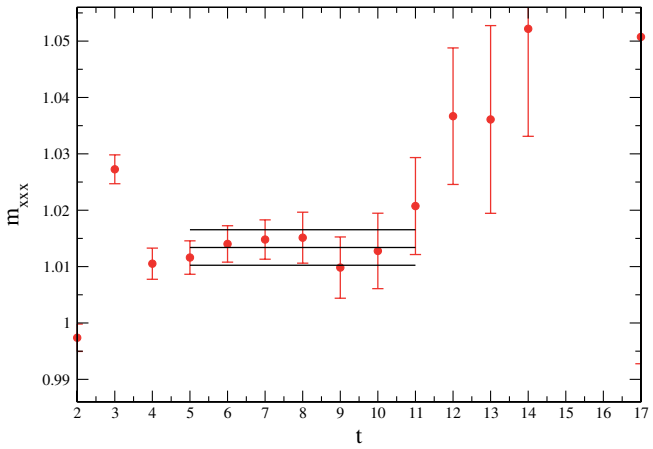

FIG. 7 (color online). The effective mass $M_{\rm eff}(t+a/2)$ vs t/a Eq. (142) of a decuplet baryon from a recent lattice calculation (Aoki *et al.*, 2011). One can see clearly the onset of the plateau and the eventual loss of signal. The plateau region is indicated together with the value of the mass obtained from a fit to the correlation function. Figure courtesy of the RBC-UKQCD Collaboration.

$$G(t,0)=\mathcal{A}_f\frac{e^{-M_h t}}{2M_h(1-be^{-TM_h})}+\mathcal{A}_b\frac{e^{-M_{\bar{h}}(T-t)}}{2M_{\bar{h}}(1-be^{-TM_{\bar{h}}})} \tag{120}$$

with the matrix elements

$$\begin{aligned}\mathcal{A}_f&=\langle 0|\mathcal{O}_f|h\rangle\langle h|\mathcal{O}_i^\dagger|0\rangle,\\ \mathcal{A}_b&=b\langle 0|\mathcal{O}_i^\dagger|\bar{h}\rangle\langle\bar{h}|\mathcal{O}_f|0\rangle.\end{aligned} \tag{121}$$

One undesirable feature of Eq. (120) is the exponential decay of the signal with Euclidean time. For large time separations t or $T-t$, the signal exponentially vanishes.

In order to check for the existence and extent of the plateau region, one can define an effective mass

$$M_{\rm eff}(t+a/2)=\ln\frac{G(t+a,0)}{G(t,0)}, \tag{122}$$

which will be M_h or $-M_{h'}$ in the region where either the first or the second exponential dominates in Eq. (120).[11] As one can see in Fig. 7, the effective mass plot is very useful for identifying the plateau region of a correlation function. One should, however, keep in mind that the time t for which the asymptotic regime (117) is reached may vary widely. It is possible that the coupling of an operator to the lowest energy state of the same quantum numbers is nonzero but so small that the ground state is not reachable.

We now turn to the explicit form of the interpolating operators $\mathcal{O}_{i/f}$. For Wilson fermions the simplest form they can assume is that of a local operator with the correct quantum number. For pseudoscalar mesons composed of two different quark flavors one can, e.g., take

[11] In the case where $G(t,0)$ is either symmetric or antisymmetric, one can modify Eq. (122) such that it gives $M_{\rm eff}=M_h$ throughout the entire plateau region. See Fleming *et al.* (2009) for a more thorough discussion of effective masses.

$$\mathcal{P}_l(x) = \bar{\Psi}_1(x)\gamma_5\Psi_2(x) \tag{123}$$

or

$$\mathcal{A}_{0l}(x) = \bar{\Psi}_1(x)\gamma_0\gamma_5\Psi_2(x). \tag{124}$$

In order to demonstrate how to construct a proper lattice observable, we take as an example $\mathcal{O}_f(t) = \mathcal{P}_l(t, \vec{x})$ and $\mathcal{O}_i(0) = \mathcal{P}_l(0, \vec{0})$ and plug these operators into Eq. (115). Using $x = (t, \vec{x})$, the resulting Green's function is

$$\begin{aligned} G_{PP}(x,0) &= \langle 0|\mathcal{P}_l(x)\mathcal{P}_l^\dagger(0)|0\rangle \\ &= \langle 0|\bar{\Psi}_1(x)\gamma_5\Psi_2(x)\bar{\Psi}_2(0)\gamma_5\Psi_1(0)|0\rangle \\ &= \langle \bar{\Psi}_1(x)\gamma_5\Psi_2(x)\bar{\Psi}_2(0)\gamma_5\Psi_1(0)\rangle \\ &= -\langle \mathrm{Tr}(S_1(0,x)\gamma_5 S_2(x,0)\gamma_5)\rangle, \end{aligned} \tag{125}$$

where in the last line the expectation value $\langle\cdots\rangle$ denotes the (properly weighted) average over all gauge configurations and S_i denote the Feynman propagator of the quark flavor i on a given gauge field background. A graphical representation of this Green's function in terms of quark propagators is displayed in Fig. 8(a). Using the γ_5-Hermiticity relation (112), Eq. (125) can be cast in the form

$$G_{PP}(x,0) = -\langle \mathrm{Tr}[S_1^\dagger(x,0)S_2(x,0)]\rangle, \tag{126}$$

which can be obtained in practice by computing the inverse of the fermion matrix on just one source point 0. Note that this is true for an arbitrary sink point x so that, in particular, one does not need to perform more inversions when either summing over all sink points $\vec{x}$ in a given time slice or computing the Green's function from 0 to a different sink point in an arbitrary time slice.

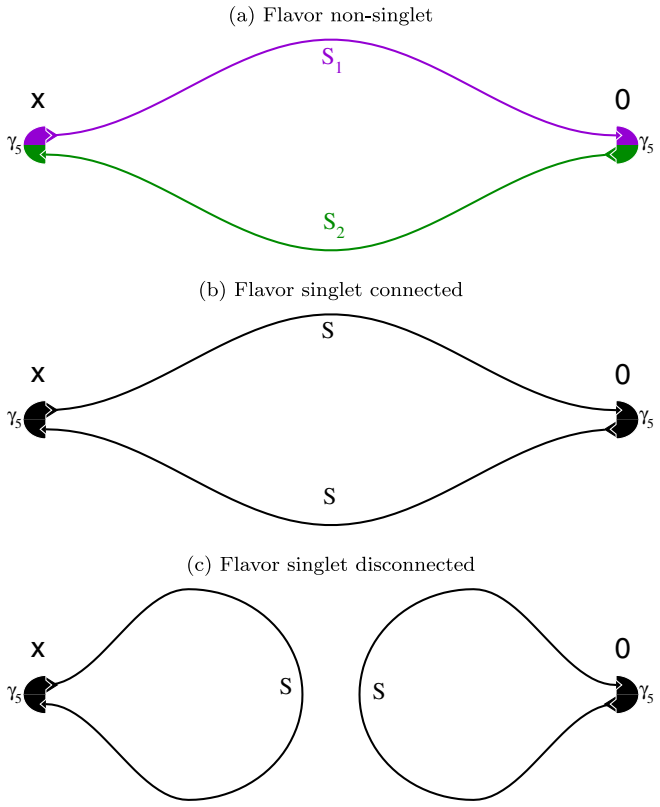

FIG. 8 (color online). Graphical representation of the contraction for a flavor nonsinglet (a) Green's function (125) and (126) and of the (b) connected and (c) disconnected contributions to a flavor singlet mesonic Green's function (128).

In the case of flavor singlet interpolating operators

$$\mathcal{P}(x) = \bar{\Psi}(x)\gamma_5\Psi(x), \tag{127}$$

the Green's function contains one more Wick contraction

$$\begin{aligned} G_{PP}^{(s)}(x,0) &= \langle 0|\mathcal{P}(x)\mathcal{P}^\dagger(0)|0\rangle \\ &= \langle 0|\bar{\Psi}(x)\gamma_5\Psi(x)\bar{\Psi}(0)\gamma_5\Psi(0)|0\rangle \\ &= \langle \bar{\Psi}(x)\gamma_5\Psi(x)\bar{\Psi}(0)\gamma_5\Psi(0)\rangle \\ &\quad + \langle \bar{\Psi}(x)\gamma_5\Psi(x)\bar{\Psi}(0)\gamma_5\Psi(0)\rangle \\ &= -\langle \mathrm{Tr}(S^\dagger(x,0)S(x,0))\rangle \\ &\quad + \langle \mathrm{Tr}(S(0,0)\gamma_5)\,\mathrm{Tr}(S(x,x)\gamma_5)\rangle \end{aligned} \tag{128}$$

that leads to a quark line disconnected contribution to the Green's function that is displayed in Fig. 8(c) in addition to the connected piece [Fig. 8(b)] that is also present in the flavor nonsinglet case (126). Since the source and sink points coincide in the disconnected piece, the γ_5-Hermiticity relation (112) does not provide any further simplification as in the case of the connected piece.

For twisted mass, chiral, and clover fermions the construction of operators has to be done in the properly transformed basis [see Eqs. (76) and (84) for the case of twisted mass and chiral fermions, respectively], but it is identical to the Wilson case otherwise.

For staggered fermions the construction of interpolating operators is complicated by the presence of four interacting tastes for each fermion flavor. Roughly speaking, when using the spin-flavor basis introduced in Sec. II.D.1 as a guide, one can construct mesonic interpolating operators along the same lines as for Wilson-type fermions [the rigorous construction can be found in Kluberg-Stern *et al.* (1983), Golterman and Smit (1984b), and Kilcup and Sharpe (1987)]. One should note however that due to the distribution of spin degrees of freedom within an elementary hypercube all operators that have a taste structure different from their spin structure are not necessarily localized to a single lattice point. One relevant example of an operator that is local and also leads to a correlation function that is positive on every gauge configuration is

$$\mathcal{P}_l^5(y) = \bar{X}_1(y)(\gamma_5 \otimes \xi_5)X_2(y) \tag{129}$$

for which the Goldstone pion is the ground state.

The simplest baryon operators for Wilson quarks that have the nucleon as a ground state are the local

$$\mathcal{N}_l^{(1)} = \epsilon_{abc}(u_a^T C\gamma_5 d_b)u_c \tag{130}$$

and

$$\mathcal{N}_l^{(2)} = \epsilon_{abc}(u_a^T C d_b)\gamma_5 u_c, \tag{131}$$

where a, b, and c are color indices and the charge conjugation operator $C = \gamma_0\gamma_2$ s. We suppressed explicit spin indices and coordinates. The difference between Eqs. (130) and

(131) is that in the first case one starts off with a pseudoscalar "diquark" (the bracketed expression), whereas in the second case the diquark is scalar and the γ_5 enters only when combining the diquark with the remaining u. This difference in spin structure leads to a very different nonrelativistic limit of the two operators, $O(1)$ for $\mathcal{N}^{(1)}$ vs $O(p^2/E^2)$ for $\mathcal{N}^{(2)}$, which in turn implies that the relative overlap of $\mathcal{N}^{(1)}$ with the ground state as compared to the excited states is much larger than that of $\mathcal{N}^{(2)}$ (Bowler *et al.*, 1984; Leinweber, 1995). For decuplet baryons, one can construct an interpolating operator by replacing the pseudoscalar diquark in Eq. (130) with a vector one (Chung *et al.*, 1982; Leinweber, Draper, and Woloshyn, 1992). An interpolating operator coupling to the Δ^{++} can, for example, be obtained by

$$\mathcal{D}_\mu = \epsilon_{abc}(u_a^T C\gamma_\mu u_b)u_c. \tag{132}$$

Green's functions $G_{\mu\nu}$ that arise from using Eq. (132) for both source and sink are, however, not pure spin $\frac{3}{2}$ (Leinweber, Draper, and Woloshyn, 1992). A spin projection to a pure spin $\frac{3}{2}$ state may be performed using the projection operator (Van Nieuwenhuizen, 1981; Benmerrouche, Davidson, and Mukhopadhyay, 1989)

$$P^{3/2}_{\mu\nu} = \delta_{\mu\nu} - \frac{1}{3}\gamma_\mu\gamma_\nu - \frac{1}{3p^2}(\gamma_\tau p_\tau \gamma_\mu p_\mu + p_\mu\gamma_\nu\gamma_\tau p_\tau). \tag{133}$$

Numerical evidence suggests that even the unprojected correlator couples almost exclusively to the spin $\frac{3}{2}$ state (Leinweber, Draper, and Woloshyn, 1992).

For staggered fermions, zero momentum baryon operators were constructed by Golterman and Smit (1985). This construction does not rely on the spin-flavor interpretation of baryons but instead is based on analyzing the discrete spacetime symmetry group of staggered fermions. One interesting feature of this construction is that there exists an operator that couples to the Δ but does not couple to the nucleon, while, on the other hand, every operator that couples to the nucleon also couples to the Δ. Since the mass difference δM of these two states is rather small, the Δ dies off slowly in Euclidean time t as $\propto e^{-\delta M t}$ and it is challenging to find a plateau region. Effects of different quark flavors have recently been added to this formulation by Bailey (2007).

An alternative approach to extracting hadron masses via measuring the free energy of a system with a finite baryon density has been suggested by Fodor, Szabo, and Toth (2007). This method however requires the introduction of a chemical potential and its practical use is severely limited due to the sign problem.

B. The role of operators

As seen in Sec. III.A, the choice of operators determines the relative strength of the coupling to different states with the same quantum numbers and therefore potentially has a large influence on the quality of signal. We first consider the case of the simple method of improving a local operator by summing it over either a source or a sink time slice to obtain a projection to zero spatial momentum.

When writing the hadron correlation function (115) in terms of Wick contractions of the quark fields, it is often possible to use the Eqs. (112) or (113) in order to obtain an expression where the quark field sources are restricted to time slice 0 [an explicit example for the flavor nonsinglet pseudoscalar propagator was given in Eq. (126)]. In these cases, if one needs only to do the momentum projection at the sink time slice t, it is a trivial summation. Performing the momentum zero projection on the source side in principle requires computing the inverse of the fermion matrix for every point in the source time slice $t = 0$. Since this would involve a prohibitively large number of fermion matrix inversions, a range of methods has been developed to deal with this problem and related ones where one needs information of the fermion propagator from every source point to every sink point on the lattice (Bitar *et al.*, 1989; Bernardson, McCarty, and Thron, 1994; Kuramashi *et al.*, 1993; Dong and Liu, 1994; Eicker *et al.*, 1996; de Divitiis *et al.*, 1996; Michael and Peisa, 1998; Wilcox, 1999; McNeile and Michael, 2001; Neff *et al.*, 2001; DeGrand and Heller, 2002; Duncan and Eichten, 2002; Bali *et al.*, 2005; Foley *et al.*, 2005; Boucaud *et al.*, 2008; Bali, Collins, and Schafer, 2010). These methods, commonly known as all-to-all techniques, are based on either stochastic estimates or eigenmode approximations of the full propagator or a combination of both.

The basic idea behind a stochastic estimate of the all-to-all propagator is to compute the inverse of the fermion matrix on a number of source vectors $\xi^{(i)}$:

$$\sigma_U^{(i)} = M_U^{-1}\xi^{(i)}. \tag{134}$$

Provided that the $\xi^{(i)}$ fulfill the condition

$$\sum_i \xi^{(i)\dagger}(y)\xi^{(i)}(x) = \delta_{x,y}\mathbb{1}, \tag{135}$$

one can obtain the propagator between any two lattice points on a fixed gauge background U as

$$S_U(y,x) = \sum_i \xi^{(i)\dagger}(y)\sigma_U^{(i)}(x). \tag{136}$$

It is often useful to restrict the vectors $\xi^{(i)}$ to a subspace of the lattice, i.e., to modify the Eq. (135) so that it is zero outside a certain subspace. If one wants to obtain full all-to-all propagators it is then of course necessary to have more than one set of source vectors $\xi^{(i)}$ so that all sets together cover the entire space desired. This method is sometimes referred to as partitioning or dilution and commonly used subspaces include individual spin components and individual time slices.

We are interested in the case where the source vectors $\xi^{(i)}$ are random vectors and the Eq. (135) is fulfilled stochastically. Examples of sets of stochastic source vectors that fulfill Eq. (135) are Z_2 noise where every component of $\xi^{(i)}$ is randomly chosen to be either of ± 1, or $U(1)$ noise where every element is a complex random number with unit modulus. The question of how many source vectors are necessary to get an optimal signal for a specific observable at minimum computational cost has to be answered numerically. It is important to note, however, that since one is usually not interested in the propagator on a specific gauge configuration U and the path integral sum commutes with the sum over all

source vectors $\xi^{(i)}$, the optimal number of sources per configuration might even turn out to be 1.

Eigenmode approximations generally assume that the inverse of the fermion operator is well approximated by restricting it to a subspace that is spanned by a number of its lowest eigenmodes. These eigenmodes are then computed and an approximation of the full matrix inverse can be found. This truncation represents an uncontrolled approximation, but it may easily be supplemented with a stochastic estimate of the effect of the higher eigenmodes. One needs only to project out the components of the original source vector that lie in the space of low eigenmodes, treat them exactly, and use stochastic estimators on the orthogonal compliment.

Until now we have discussed only (sums of) local operators, i.e., operators where all the quarks originate from a single lattice point. Hadrons, however, are extended objects with quark distributions that have finite widths and different shapes. One strategy to improve the overlap between an interpolating field operator and a specific hadronic state therefore consists of trying to model its quark distribution. One possibility that is often used is to replace the quark point sources $\Psi(t,\vec{x})$ by a sum over quark sources at neighboring sites. In its simplest form, one can take

$$\Psi'(t,\vec{y}) = \sum_{\vec{x}} G(\vec{y},\vec{x})\Psi(t,\vec{x}), \tag{137}$$

where $G(\vec{y},\vec{x})$ is the smearing kernel that determines the relative weight of the source points. A computationally convenient restriction of the smearing kernel is the factorization ansatz (Bacilieri *et al.*, 1988; DeGrand and Loft, 1991)

$$G(\vec{y},\vec{x}) = g(\vec{x})g(\vec{y}), \tag{138}$$

where effectively the quark fields are independently smeared. Typical choices for the form of $g(\vec{x})$ include a wall (Bitar *et al.*, 1990a), a hard sphere or box (Bacilieri *et al.*, 1988), a Gaussian (DeGrand, 1998; DeGrand, Hasenfratz, and Kovacs, 1998), or a radial exponential (Ali Khan *et al.*, 2002) of different size. Note that in general $\Psi'(t,\vec{y})$ in Eq. (137) is not gauge invariant and one therefore needs to work in a fixed gauge on the source time slice. A more sophisticated method of smearing the quark source that is gauge invariant is known as Wuppertal smearing (or gauge invariant Gaussian smearing) (Gusken, 1990), where a covariant Laplacian is added to the unit operator and repeatedly applied N times

$$G = \left(1 + \sum_{i=1}^{3} \alpha(V_i + V_i^\dagger)\right)^N. \tag{139}$$

The one-hop term V_i is given by Eq. (15) and the smearing parameters α and N determine the form and width of the source that is approximately Gaussian for large N on a trivial gauge field.[12] In order to suppress gauge noise, one can use smeared links (see Sec. II.E.2) for the gauge field in Eq. (139). A variant of this method is the Laplace-Heaviside (LapH) smearing (Peardon *et al.*, 2009), where the smearing kernel is defined as a Heaviside step function on the lowest eigenmodes of the covariant Laplacian. This method requires the explicit inversion of the fermion matrix on a number of lowest eigenmodes of the covariant Laplacian that grows with the volume of the system. This growth with the volume of the number of required fermion matrix inversions can be countered by not computing propagators on all eigenmodes exactly but instead using stochastic techniques, similar to the ones described above, in the eigenspace of low modes to estimate them (Morningstar *et al.*, 2010, 2011).

Replacing the original quark sources in local hadron operators such as Eqs. (123), (124), (130), and (131) with smeared ones usually improves the overlap with the desired state. Especially in the case of excited states, it is often useful to go further. When trying to find an operator that has maximal overlap with a certain state, one can use its quantum numbers and expected wave function to model a lattice operator. The two quantum numbers of interest are spin and parity. Parity is not broken by the lattice regularization and therefore one can construct operators that couple only to states of a given parity exclusively. Note however that the backward contribution in Eq. (120) will be of opposite parity from the forward one. For interpolating operators with an odd number of quark fields, it is possible to use the relative sign flip in the backward amplitude $\mathcal{A}_b$ Eq. (121) between periodic and antiperiodic boundary conditions to eliminate these (Sasaki, Blum, and Ohta, 2002; Csikor *et al.*, 2003; Leinweber *et al.*, 2005; Sasaki and Sasaki, 2005).

Spin, on the other hand, is the quantum number corresponding to the continuum rotational symmetry group SU(2) that is broken down to the symmetry group of cubic lattice rotations. This group, the octahedral group $\mathcal{O}$, has been studied by Johnson (1982) and it was found that there are five irreducible representations corresponding to integer spin and three corresponding to half-integer spin, all of them containing a whole tower of partially overlapping continuum spin representations. One can construct lattice operators that transform irreducibly under the octahedral group $\mathcal{O}$ (Basak *et al.*, 2005a, 2005b, 2007) and are especially beneficial for the extraction of highly excited baryon resonances. In addition to the quark source smearing, these operators generally involve quark sources that can each be covariantly displaced from a reference point by one lattice unit in any direction. The general form of such a baryon operator is an appropriate linear combination of terms of the form

$$\mathcal{B} = \epsilon_{abc}(D_i'\Psi)^a(D_j'\Psi)^b(D_k'\Psi)^c, \tag{140}$$

where abc is color and we have suppressed spin and flavor indices. The operators D_i' are gauge covariant displacement operators by one step in direction i (or the unit operator if $i = 0$). For more detailed reviews on the construction of operators for excited state baryon spectroscopy see, e.g., Leinweber *et al.* (2005), Basak *et al.* (2006), and Lang (2008).

A different approach of finding an operator that has optimal overlap with the ground state was developed[13] by Babich *et al.* (2006, 2007). They considered at the sink side a general meson operator of the form

[12] See Allton *et al.* (1993), Lacock *et al.* (1995), and Burch *et al.* (2004) for different constructions of nonlocal gauge invariant operators.

[13] See Draper and McNeile (1994) for a similar approach for heavy-light systems.

$$\mathcal{M}(t,r) = \bar{\Psi}_1(t,\vec{x})\Gamma\Psi_2(t,\vec{y})\delta(|\vec{y}-\vec{x}|-r) \tag{141}$$

and studied the profile in r of the resulting correlation function as a function of t. Once a plateau is reached, the profile was found to settle into an asymptotic form $\phi(r)$ which can then be used to construct an optimal sink operator

$$\mathcal{O}(t) = \sum_r \phi(r)\mathcal{M}(t,r). \tag{142}$$

A special problem occurs when one tries to extract the energy level of a scattering state or a bound state of hadrons with a nonminimal number of valence quarks. As repeatedly noted in the literature [see, e.g., Bulava *et al.* (2010) and Engel *et al.* (2010)], the coupling of single hadron operators to multihadron states is extremely small. A prominent example is the ρ resonance which has a $\pi-\pi$ scattering state as a ground state in infinite volume. A closely related phenomenon occurs in heavy quark physics where string breaking between static quarks can be observed only when one explicitly introduces a "broken string" operator that consists of two separated static-light mesons (Knechtli and Sommer, 1998; Bali *et al.*, 2005).

Both phenomena suggest that it is difficult to produce a pair of appropriate sea quarks from the vacuum that allows for the propagation of an intermediate multihadron state. Intuitively this is understandable as the occurrence of large sea quark loops is suppressed in the path integral (24).

For spectroscopy in channels where there is a scattering state below the relevant resonance or for the spectroscopy of exotic objects that consist of a nonminimal number of valence quarks, such as tetraquarks or pentaquarks, one therefore needs to use appropriate interpolating operators that correctly reflect the valence quark structure of the desired object.

When constructing interpolating operators one usually tries to avoid situations where a quark line may start and terminate at the same time slice, since these operators are known to be much noisier than operators where all the quark lines run from the source to the sink time slice. In some cases, however, e.g., for isoscalar mesons or generally for the multihadron operators mentioned above, quark propagators that attach to one time slice with both ends are unavoidable. As an example of how a combination of the above mentioned techniques can lead to a decent signal in these notoriously difficult channels, Fig. 9 displays one current determination of the correlation function and mass plateau in the η channel that was obtained using the stochastic LapH technique described above. [For similar results with a different mix of techniques, see also Alexandrou *et al.* (2010)].

Finally, there are also suggestions to completely avoid the problem of computing disconnected diagrams by finding relations between them and disconnected diagrams in partially quenched chiral perturbation theory (Della Morte and Juttner, 2010).

C. Extracting multiple energy levels

In Sec. III.A we saw how to extract the ground state of a channel by going to asymptotic Euclidean time. In order to extract excited state masses, one can in principle fit the correlation function to a multiexponential form

$$G(t,0) = \sum_n \mathcal{A}_n e^{-M_n t}, \tag{143}$$

where we ignored backward contributions. A fit of the form (143) with free parameters $\mathcal{A}_n$ and M_n cannot typically be stabilized numerically for more than two states and even extracting reliable first excited state masses with this technique is challenging.

One can overcome these problem by using a variational method (Michael, 1985; Luscher and Wolff, 1990; Blossier *et al.*, 2009). The basic idea is to expand the basis to include N initial and final state operators $\mathcal{O}_{i_k}$ and $\mathcal{O}_{f_k}$ with the same quantum numbers that ideally couple to different energy states preferentially and then construct the complete cross-correlator matrix

$$G_{lm}(t,0) = \langle 0|\mathcal{O}_{f_l}(t)\mathcal{O}^\dagger_{i_m}(0)|0\rangle. \tag{144}$$

One can then define a matrix $M(t,t_0)$ from

$$G(t,0) = M(t,t_0)G(t_0,0) \tag{145}$$

and analyze its eigenvalues $\lambda_n(t,t_0)$ and eigenvectors $v_n(t,t_0)$. At large Euclidean times t and t_0 the eigenbasis of the matrix M will then align with the eigenbasis of the Hamiltonian and the eigenvectors will behave as

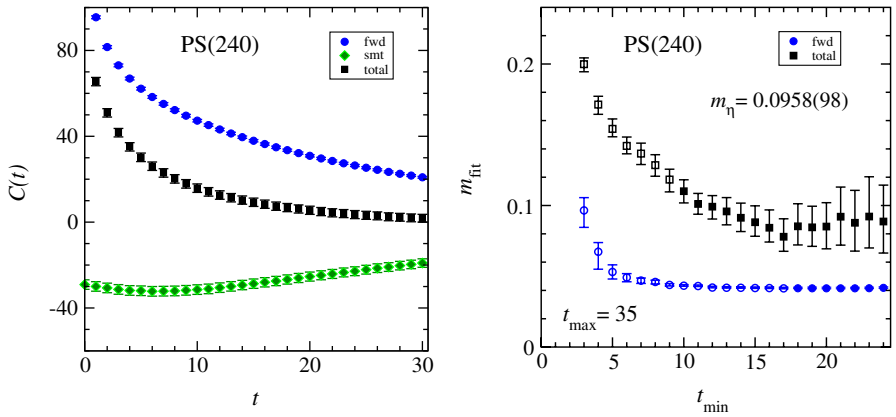

FIG. 9 (color online). Correlation function (left panel) and effective mass (right panel) in the η channel using a stochastic LapH source. Connected (fwd) and in the left panel disconnected (smt) contributions are plotted additionally. From Morningstar *et al.*, 2011, with permission of K. J. Juge.

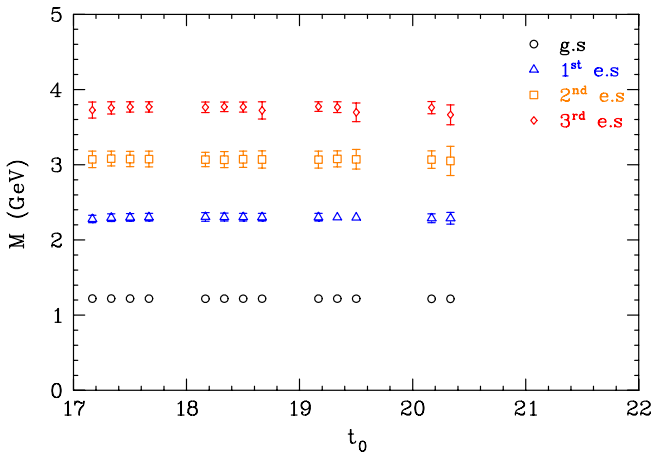

FIG. 10 (color online). Plot of the masses of the ground and excited states in the nucleon channel. The extraction has been performed by fitting single state correlators that were obtained by projection of a 4×4 matrix correlator onto the elements of the eigenbasis of the transfer matrix $M(t, t_0)$ for different t and t_0. From Mahbub *et al.*, 2010b, with permission of D. Leinweber.

$$\lambda_n = e^{-E_n(t-t_0)} \tag{146}$$

from which one can extract an effective mass for each of the energy levels similar to Eq. (122). The energies of a number of lowest lying states in a given channel can thus be determined provided that the operator basis chosen has sufficient overlap with all of these states and the quality of the data is good enough to determine all the elements of the transfer matrix with sufficient accuracy.

A robust variant of the variational method was suggested by Mahbub *et al.* (2009a).[14] Instead of extracting the energies from the eigenvalues directly one can use the elements of the eigenbasis to project out effective single state components from the matrix valued propagator and analyze them with standard single channel methods.

Figure 10 displays masses of the ground state and the first three excited states of the nucleon channel extracted with the variational projection method.

IV. PHYSICAL PREDICTIONS

Having extracted hadron masses from nonperturbative lattice QCD calculations, we now need to turn them into physical predictions. QCD, and also lattice QCD, is a theory without any intrinsic scale; it is formulated in terms of dimensionless quantities entirely. In order to extract dimensionful quantities such as hadron masses from it, we need to supply it with a scale. We can do this in general by picking a scale setting observable, a quantity that is dimensionful in the continuum theory. In the lattice theory we can then measure the appropriate dimensionless combination of any target observable we wish to extract with the scale setting observable and get a dimensionful prediction for the target observable by fixing the scale setting observable to its dimensionful input value. One such target observable would be the lattice spacing a itself.

The scale setting procedure outlined above is not entirely sufficient for making physical predictions. Once we have supplied lattice QCD with a scale we still need to fix its remaining parameters, the bare quark masses. For N_f nondegenerate quark flavors we can generally do so by fixing N_f linearly independent dimensionless observables in the lattice theory to their desired input value. What one would ideally like to do then is to fix the $N_f + 1$ dimensionless bare parameters of the lattice theory, the bare quark masses and the gauge coupling, such that the N_f dimensionless observables on the lattice assume their physical values exactly and the lattice spacing a is of the desired size. One could then measure any observable on the lattice for a range of lattice spacings a and, with the appropriate functional form that is given by the discretization effects of the specific action used, extrapolate them into the continuum $a = 0$.

There are a few obstacles toward implementing this ideal procedure in nonperturbative lattice calculations. The first one is that one cannot simply go to the physical point by setting the bare coupling and input quark masses in a lattice calculation to their physically observed values since these physical values cannot directly be measured in experiment. Quantities that are accessible experimentally, such as hadron masses or decay widths, have relations to the bare parameters that need to be determined on the lattice themselves. One is therefore left with the choice of either tuning the bare parameters or computing both target observables and those used for scale setting and parameter fixing at various unphysical points followed by an interpolation to the physical point.

When trying to implement either of the two procedures, tuning or interpolating to the physical point, one faces the more technical problem that it is difficult to reach the physical point for light quarks. As discussed in Sec. II.D there is a variety of different fermion discretizations but each one has a specific problem when making the quark mass light. In the case of Wilson fermions one is faced with exceptional configurations: staggered and twisted mass fermions have the problem of flavor and taste splitting and chiral fermions are simply expensive in terms of computer time needed. None of these problems is insurmountable but they turn out to be sufficiently severe so that an extrapolation in the light quark mass to the physical point is still the rule rather than the exception in hadron spectroscopy calculations.

A third problem that is less severe in practice but still has to be considered is that nature is not QCD alone, even for the light hadron spectrum. Quarks are electrically charged and there are QED corrections to hadron masses. Similarly, isospin symmetry is usually assumed in lattice calculations but broken in nature. Both of these effects are relatively small as can be seen from the isospin splitting of the experimentally observed hadron spectrum, but they still need to be considered.

We start in Sec. IV.A by reviewing the problem of reaching the physical point. In Sec. IV.B we discuss how to remove the cutoff, i.e., how to reach the continuum limit for the various lattice discretizations. Finally, in Sec. IV.C, we consider finite-volume corrections that are especially relevant for

[14] See Draper, McNeile, and Nenkov (1995) for a similar method for heavy-light systems.

resonant states and we conclude with the discussion of subleading effects from QED and isospin breaking in Sec. IV.D.

A. Reaching the physical point

Having extracted hadron masses from simulations we now need to turn them into physical predictions. As discussed in the beginning of Sec. IV, we need to go or extrapolate to the physical point and we need to set the scale.

On a technical level tuning to the physical or any other target point is achieved through tuning the bare parameters of the lattice theory, the coupling β and the bare quark masses in the lattice Lagrangian. Defining the physical or any other target point, on the other hand, is generally done by comparing dimensionless combinations of continuum observables with the corresponding lattice observables and the scale can be set by comparing any one dimensionful continuum observable. Provided that all effects beyond QCD with the given number of flavors are correctly accounted for and provided also that the chosen lattice discretization of QCD has the correct continuum limit, all possible choices of finding the physical point are equivalent in the continuum limit. If any of the above assumptions is violated, such as is the case, e.g., in quenched QCD, continuum predictions are not unique and depend on the specific choice of defining the physical point.

It is usual to treat the two light quark flavors u and d as degenerate and to include isospin breaking as well as electromagnetic effects as corrections. One can then define a light quark mass $\hat{m} = (m_u + m_d)/2$. In order to tune to the correct light quark mass one combination that is often used is the ratio of the pion mass, the square of which is proportional to the light quark mass at leading order, to an observable that depends less on the light quark mass. In early quenched work on lattice hadron spectroscopy the QCD string tension was often used for this purpose (Creutz, 1980a; Hamber and Parisi, 1981; Marinari, Parisi, and Rebbi, 1981a; Pietarinen, 1981; Weingarten, 1982; Bernard, Draper, and Olynyk, 1983; Creutz, Jacobs, and Rebbi, 1983) as was M_ρ later on (Fucito *et al.*, 1982) or M_Φ (Lipps *et al.*, 1983). In full QCD these choices are not optimal. The vector meson ρ is a broad resonance and not the ground state in its channel, the singlet ϕ contains disconnected diagrams, and the string tension is ill defined with dynamical quarks. Even in the quenched approximation any resonant state mass is not an ideal choice for a scale setting observable as the connection of the measured ground state mass to the experimentally measured mass above decay threshold is not obvious. Quantities that are frequently used today are either baryon masses that are stable in QCD (M_N, M_Ξ, and M_Ω) (Durr *et al.*, 2008; Alexandrou *et al.*, 2009; Aoki *et al.*, 2009, 2010; Lin *et al.*, 2009; Brandt *et al.*, 2010; Bulava *et al.*, 2010; Engel *et al.*, 2010), average masses of baryon multiplets (Bietenholz *et al.*, 2010b), or distance measures (r_0, r_1) in the heavy quark potential (Sommer, 1994) that are in turn determined from Υ spectroscopy (Bernard *et al.*, 2001; Bazavov *et al.*, 2010a; Davies *et al.*, 2010). The use of matrix elements, such as the pseudoscalar decay constants, although common in other areas (Giusti, Hoelbling, and Rebbi, 2001; Blossier *et al.*, 2009; Noaki *et al.*, 2009; Borsanyi *et al.*, 2010) is less often seen in lattice hadron spectroscopy.

At the physical point the scale can then be set by comparing a dimensionful continuum observable with the corresponding lattice observable. At any other nonphysical point the scale setting is conceptually ill defined. It is nonetheless usual either to use the scale defined at the physical point for all theories with the same coupling β and arbitrary quark masses (mass independent scale setting) or to obtain the scale by comparing a dimensionful continuum observable with its lattice counterpart at any nonphysical point (mass dependent scale setting).

In computations with a dynamical strange quark its mass also has to be set. In analogy to the light quark case, this is usually done via the kaon mass, the combination $M_K^2 - M_\pi^2/2$, which is proportional to the strange quark mass to leading order, or the mass of the fictitious η_s, the pseudoscalar meson that is composed of two strange valence quarks.

As for the specific functional form of an extrapolation or interpolation to the physical point the most straightforward form is one that is linear in the quark mass. Since $M_\pi^2 \propto \hat{m}$ and $\bar{M}_K^2 = M_K^2 - M_\pi^2/2 \propto m_s$ to leading order (Gell-Mann, Oakes, and Renner, 1968), one can fit any other hadron mass M_X to a form

$$M_X = a + bM_\pi^2 + c\bar{M}_K^2. \tag{147}$$

Going beyond this leading order one can perform systematic expansions around either a point with two or three massless quark flavors or a general, massive point. For the first case, chiral perturbation theory (χPT), an effective field theory based upon the chiral symmetry pattern of QCD has been developed (Weinberg, 1979; Gasser and Leutwyler, 1984, 1985). It provides an asymptotic expansion around either the two- or three-flavor massless point. As it is built around the assumption of spontaneous chiral symmetry breaking in the massless theory, it is particularly suited for treating properties of the pseudo-Goldstone bosons of this symmetry, i.e., the pions and, to a somewhat lesser extent, the kaons.

For masses other than the pseudoscalars, χPT generically predicts a leading nonanalytic term of the form M_π^3 (Langacker and Pagels, 1974). More formally, one can include baryons in χPT (Gasser, Sainio, and Svarc, 1988), but the resulting series is only slowly converging. An alternative formulation with better convergence properties is heavy baryon χPT (Jenkins and Manohar, 1991; Bernard *et al.*, 1992) which treats baryons as nonrelativistic particles and currently is most commonly used to fit lattice baryon data. An extension of heavy baryon χPT for staggered fermions was developed by Bailey (2008). Recently, the covariant approach (Becher and Leutwyler, 1999) that promises better convergence behavior for heavier pion masses was revived (Dorati, Gail, and Hemmert, 2008; Durr *et al.*, 2010, 2012) and used for chiral fits of the baryon octet.

Partially quenched heavy baryon χPT is an extension of heavy baryon χPT, where the sea and valence quark masses may have different values (Labrenz and Sharpe, 1996; Beane and Savage, 2002; Chen and Savage, 2002; Savage, 2002). It is useful to describe lattice data with multiple valence quark masses for each sea quark mass and for describing ''hybrid'' calculations where the sea quarks are regularized differently than the valence quarks. This technique is sometimes

employed to keep the computational costs of dynamical ensembles small by using a fast fermion discretization such as the staggered one while having the advantages of a more computationally demanding regularization, such as domain wall fermions or overlap fermions, in the valence sector.

An alternative to the chiral expansion for describing the pion mass dependence of any hadronic observable is a Taylor expansion around a finite pion mass. In contrast to the chiral expansion, the Taylor expansion is performed around a nonsingular point and has a finite radius of convergence. Typically this convergence radius is given by the distance of the expansion point $M_{\pi 0}$ to the chiral limit. Usually, the expansion is performed in powers of the pseudoscalar mass square $M_\pi^2 - M_{\pi_0}^2$ resulting in

$$M_X = a + b(M_\pi^2 - M_{\pi_0}^2) + c\bar{M}_K^2 + d(M_\pi^2 - M_{\pi_0}^2)^2, \tag{148}$$

but the chiral behavior of baryon masses has also been fairly successfully described, at least within the statistical accuracy of current data sets, by a linear expansion in M_π (Walker-Loud *et al.*, 2009). Optimal convergence is achieved in principle by placing the expansion point at the middle of the interval spanned by all simulation points and the physical point (Durr *et al.*, 2008; Lellouch, 2009). Note, however, that from a practical perspective the choice of the expansion point $M_{\pi_0}^2$ does not play a role in the fit itself as a redefinition of $M_{\pi_0}^2$ may be absorbed by redefining the lower order fit coefficients a and b of Eq. (148).

One may also try to fit ratios (Durr *et al.*, 2008) or differences (Bietenholz *et al.*, 2010b) of baryon masses in order to cancel common contributions and obtain a more regular chiral behavior. Further it is possible to study SU(3) breaking effects in baryon multiplets in the $1/N_c$ expansion (Jenkins *et al.*, 2010), which offers an alternative way of describing the chiral behavior of baryon mass multiplets.

An alternative to extrapolating or interpolating results to the physical point is tuning the bare parameters of the lattice theory such that the physical point is directly reached, i.e., that the dimensionless combinations of continuum variables mentioned above assume their physical value on the lattice. While recent advances in lattice discretizations, algorithms, and computer technology have made such an approach possible in principle, the computational overhead that is associated with the parameter tuning is still large and the physical point is generally only reached within the precision of the tuning procedure.

In order to avoid these problems, reweighting techniques were recently applied to this problem. In Aoki *et al.* (2010), the PACS-CS Collaboration reweighted one ensemble to the physical point directly while the RBC-UKQCD Collaboration (Aoki *et al.*, 2011) followed a mixed strategy where the ensembles were first reweighted to the physical strange quark mass and a subsequent extrapolation to the physical pion mass was performed.

The general idea behind reweighting (Ferrenberg and Swendsen, 1988) is to reuse an ensemble produced with a certain set of parameters $p_0 = \{\beta_0, m_{i0}\}$ to obtain predictions with a different set $p = \{\beta, m_i\}$. As discussed in Sec. II.C, gauge configurations $U \in \mathcal{U}$ with the original set of parameters p_0 in the action are produced according to the weight

$$w(p_0; U) \propto \prod_i \det M(m_{i0}; U) e^{-S_G(\beta_0; U)}, \tag{149}$$

such that expectation values of observables (24) may be formed by just summing them over gauge configurations

$$\langle O \rangle_{p_0} = \frac{\sum_{U \in \mathcal{U}} O(U)}{\sum_{U \in \mathcal{U}} 1}. \tag{150}$$

For a new set of parameters p, one may in principle circumvent the generation of a new ensemble with the weight

$$w(p; U) \propto \prod_i \det M(m_i; U) e^{-S_G(\beta; U)} \tag{151}$$

by reusing the old ensemble generated with the weight $w(p_0; U)$ from Eq. (149) and putting the ratio of weights into the observable

$$\langle O \rangle_p = \frac{\sum_{U \in \mathcal{U}} O(U) w(p; U)/w(p_0; U)}{\sum_{U \in \mathcal{U}} w(p; U)/w(p_0; U)}. \tag{152}$$

Although Eq. (152) would in principle allow for a combined reweighting in both the coupling and the masses, a reweighting was carried out in the quark masses only by Aoki *et al.* (2010, 2011). For this purpose it is necessary to compute ratios of fermion determinants at different quark masses. As it is prohibitively expensive to compute them exactly, stochastic methods were applied.

Of course the reweighting method has its limitations. As one can see from Eq. (152), reweighting exponentially enhances or suppresses the weight of individual configurations in an ensemble with an exponent that is extrinsic, i.e., contains an explicit volume factor. As it is crucial for any observable to be computed on the relevant subset of configurations for the specific parameters used, these exponential factors should not be so large as to allow for one configuration to dominate the expectation value entirely. This in turn limits the allowed range in parameter space that one may reach safely with reweighting depending on the original set of parameters p_0 and the volume. Within this safe range, the relative suppression of some configurations is that of effectively decreasing the statistics. As the relative weight factors are explicitly computed (Csikor *et al.*, 2004), one has a good handle on these effects. Note also that one could in principle bypass some of the negative effects with a multihistogram technique (Ferrenberg and Swendsen, 1989).

Figure 11 provides an overview of currently used lattice QCD ensembles with respect to their position in the $\sqrt{2M_K^2 - M_\pi^2}$ vs M_π plane. Note that in leading order of the chiral expansion the axes are proportional to $\sqrt{\hat{m}}$ and $\sqrt{m_s}$. The location of the physical point is also indicated. As Fig. 11 indicates, the physical point has already been reached.

B. Continuum extrapolation

The removal of the cutoff, also known as continuum extrapolation, is an unavoidable part of any lattice calculation that wants to make a statement about the underlying fundamental continuum theory. The severity of the continuum extrapolation, however, depends strongly on both the action

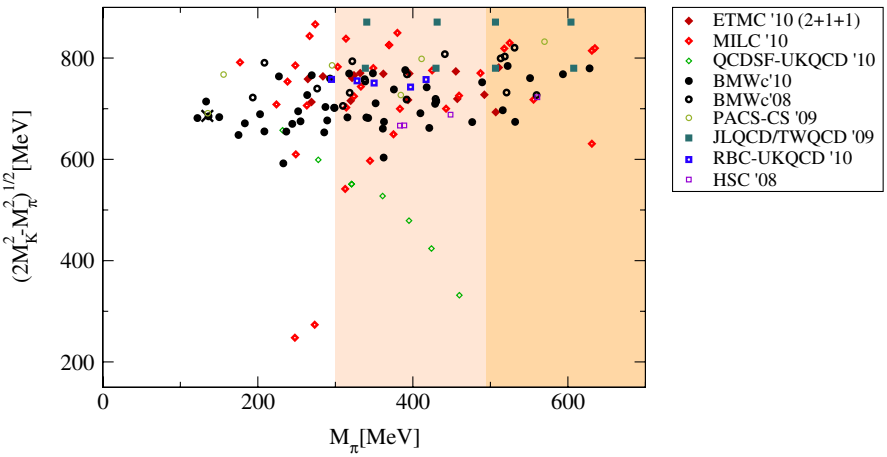

FIG. 11 (color online). The landscape of recent dynamical fermion simulations projected to the $\sqrt{2M_K^2 - M_\pi^2}$ vs M_π plane. The cross marks the physical point while shaded areas with increasingly light shade indicate physically more desirable regions of parameter space. Data points are taken from the following references: ETMC'10(2 + 1 + 1) (Baron *et al.*, 2010a); MILC'10 (Bazavov *et al.*, 2010a); QCDSF-UKQCD'10 (Bietenholz *et al.*, 2010a); BMWc'08 (Durr *et al.*, 2008); BMWc'10 (Durr *et al.*, 2011c); PACS-CS'09 (Aoki *et al.*, 2009, 2010); RBC-UKQCD'10 (Mawhinney, 2010; Aoki *et al.*, 2011); JLQCD/TWQCD'09 (Noaki *et al.*, 2009); and HSC'10 (Lin *et al.*, 2009). All ensembles are from $N_f = 2 + 1$ simulations except explicitly noted otherwise. For staggered, respectively, twisted mass ensembles, the Goldstone, respectively, charged pion masses are plotted.

used and the combination of scale setting observable and measured observable.

As discussed in Sec. II.E, the simplest gluonic action already has cutoff effects of $O(a^2)$ that can be improved to at least $O(g^2a^2)$ through various techniques. In contrast, the scaling behavior of the various fermion actions is typically not as good. Formally, staggered fermions and twisted mass fermions at maximal twist as well as exactly chiral fermions show $O(a^2)$ continuum scaling while Wilson-type fermions generically start with $O(a)$ scaling. Only improved staggered fermions such as asqtad have a leading scaling behavior of $O(g^2a^2)$. There are several caveats to this statement however.

For twisted mass fermions, $O(a^2)$ scaling is realized at maximal renormalized twist (Aoki and Bar, 2004; Frezzotti and Rossi, 2004a), which requires the tuning of one additional parameter. This tuning is routinely done as part of any twisted mass calculation [see, e.g., Baron *et al.* (2010a)]. Since this tuning has a typical accuracy on the few percent level, it is expected that the $O(a^2)$ terms are numerically dominant. In addition, twisted mass calculations often employ a doublet of valence fermions with an opposite Wilson parameter to cancel remnant $O(a)$ effects.

Similarly $O(a^2)$ scaling is only strictly realized for chirally symmetric fermions if the chiral symmetry is exact. Fermion formulations that incorporate an inexact chiral symmetry, such as domain wall fermions at a finite fifth dimension, formally have a remaining $O(g^{2n}a)$ scaling behavior. The smallness of the residual mass and other numerical evidence (Aoki *et al.*, 2011), however, suggests that, similar to the twisted mass case, the $O(a^2)$ term is dominant although it is formally subleading.

Wilson-type fermions, on the other hand, are typically Symanzik improved by the addition of a Sheikholeslami-Wohlert (clover) term (102). At tree level ($c_{SW} = 1$), this results in an $O(g^2a)$ scaling of on-shell observables while with a suitable nonperturbative tuning one can in principle obtain $O(a^2)$ scaling. In addition, there is numerical evidence (Hoffmann, Hasenfratz, and Schaefer, 2007; Durr *et al.*, 2009, 2011c; Kurth *et al.*, 2010) that the scaling behavior of clover fermions is substantially improved by gauge link smearing, which is commonly used today.

Apart from the action used, the continuum scaling is also largely dependent on the observables considered. As discussed in Sec. IV.A, all observables in lattice QCD are dimensionless quantities and in order to extract dimensionful quantities such as baryon masses a scale setting observable is needed. The scaling is of course affected by the choice of scale setting variable. For baryons and vector mesons good scaling is observed when choosing a stable light baryon mass as the scale setting observable (Durr *et al.*, 2008; Alexandrou *et al.*, 2009).

Some care has to be taken about the size of the scaling window. While generally scaling is not expected to set in for lattice spacings coarser than $a \sim 0.1$–0.15 fm, it has been observed (Del Debbio, Panagopoulos, and Vicari, 2002; Antonio *et al.*, 2008; Bazavov *et al.*, 2010c; Luscher, 2010; Schaefer, Sommer, and Virotta, 2011) that for fine lattices the autocorrelation time of the topological charge is rapidly growing. It therefore seems to be prohibitively expensive with current algorithms to obtain a sufficiently large and statistically independent ensemble of configurations for lattice spacings finer than $a \sim 0.05$ fm.

Generally, for the observables considered in this review continuum scaling is rather mild and not a leading source of systematic error. Figure 12 gives an overview of the lattice spacing a vs M_π for currently used lattice ensembles.

C. Finite-volume effects

Besides reaching the physical point and removing the cutoff, the third step that generically has to be taken in order to make physical predictions is the extrapolation to infinite volume. As is the case for the continuum limit, the infinite volume limit can never be reached and an extrapolation in the volume is in principle unavoidable. For most observables,

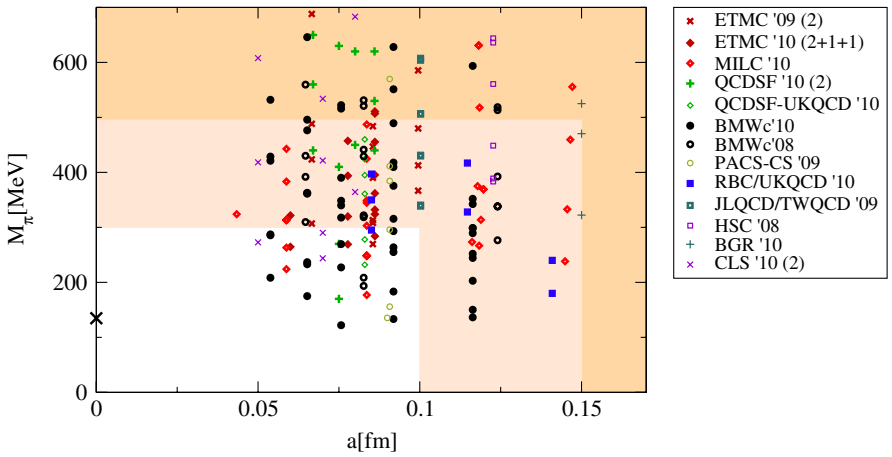

FIG. 12 (color online). The landscape of recent dynamical fermion simulations projected to the M_π vs a plane. The cross marks the physical point while shaded areas with increasingly light shade indicate physically more desirable regions of parameter space. Data points are taken from the following references: ETMC'09(2) (Blossier *et al.*, 2009); ETMC'10(2 + 1 + 1) (Baron *et al.*, 2010a); MILC'10 (Bazavov *et al.*, 2010a); QCDSF'10(2) (Schierholz, 2010); QCDSF-UKQCD'10 (Bietenholz *et al.*, 2010a); BMWc'08 (Durr *et al.*, 2008); BMWc'10 (Durr *et al.*, 2011c); PACS-CS'09 (Aoki *et al.*, 2009, 2010); RBC-UKQCD'10 (Mawhinney, 2010; Aoki *et al.*, 2011); JLQCD/TWQCD'09 (Noaki *et al.*, 2009); HSC'10 (Lin *et al.*, 2009); BGR'10(2) (Engel *et al.*, 2010); and CLS'10(2) (Brandt *et al.*, 2010). All ensembles are from $N_f = 2 + 1$ simulations except explicitly noted otherwise. For staggered, respectively, twisted mass ensembles, the Goldstone, respectively, charged pion masses are plotted.

however, the leading finite-volume corrections are exponentially small in the box size and not polynomially and can therefore be made sufficiently small in practice by increasing the volume (Luscher, 1986a). These finite-volume effects are discussed in Sec. IV.C.1. Resonant states, on the other hand, are embedded into a continuum of scattering states at infinite volume. In finite volume these levels become discrete and carry a strong volume dependence. Consequently the leading finite-volume effects on resonant states are of a different origin and are discussed separately in Sec. IV.C.2.

Finally we mention that fixing the global topological charge in QCD is a restriction that becomes irrelevant in the infinite volume limit, too. For this reason lattice QCD calculations in a fixed topological sector may be viewed as introducing an additional third type of finite-volume corrections (Brower *et al.*, 2003; Aoki *et al.*, 2007). Since currently this technique has not been used in any work on light hadron spectroscopy, we will not discuss it any further.

1. Finite-volume effects for stable particles

In an interacting field theory, the properties of a particle in a finite box are affected by mirror charge effects. For hadron spectroscopy this entails that all hadron masses in a finite box deviate from their infinite volume value with a leading contribution originating from the pion warping around one spatial lattice dimension.[15] A generic expectation for the finite-volume correction to any hadron mass M in an $L^3 \times T$ box is therefore[16]

$$1 - \frac{M_L}{M_\infty} \propto e^{-M_\pi L}. \tag{153}$$

As Luscher (1986a) demonstrated, there is a relation between the Euclidean finite-volume mass correction of a hadron P and the forward πP scattering amplitude in Minkowski space. Concentrating on the case where a single propagator receives finite-volume corrections, he obtained an explicit expression for the leading term in an expansion for asymptotically large L. Using an alternative approach, Gasser and Leutwyler (1987a, 1987b, 1988) incorporated finite-volume effects into chiral perturbation theory. They demonstrated that the finite volume affects only the propagators and that it can be accounted for by simply replacing the momentum integration by a summation over the allowed discrete momenta $p_i = 2\pi n_i/L$.

Expanding the relation of Luscher (1986a) to include subleading terms in asymptotic L and using χPT input for the scattering amplitudes, Colangelo and Durr (2004) and Colangelo, Durr, and Haefeli (2005) combined the two approaches mentioned above for the case of pseudoscalar mesons. A similar expansion for baryons was also pioneered (Colangelo, Fuhrer, and Lanz, 2010).

From a practical point of view these results imply that there is a safe asymptotic region of relatively large lattice volumes where these finite size effects are exponentially small and in addition can be systematically corrected for. As a rule of thumb for lattice computations with pion masses above $\sim$300 MeV, lattices with $M_\pi L > 4$ are considered safe while those with $m_\pi L < 3$ are widely affected by finite-volume corrections. For a more quantitative statement, Fig. 13 shows a plot of box size L vs pion mass M_π where regions are identified that according to Colangelo, Durr, and Haefeli (2005) imply the finite-volume effect on the pion mass to be $<1\%$, $<0.3\%$, and $<0.1\%$, respectively. On top of these regions parameters of current or recent lattice computations

[15]Alternatively in the momentum space view these effects may be considered as consequences of the discreteness of the momenta in a finite box.

[16]For the case of smaller volumes, see also Fukugita *et al.* (1992). They argue that the dominant (polynomial) finite size effect is due to the truncation of a hadrons wave function.

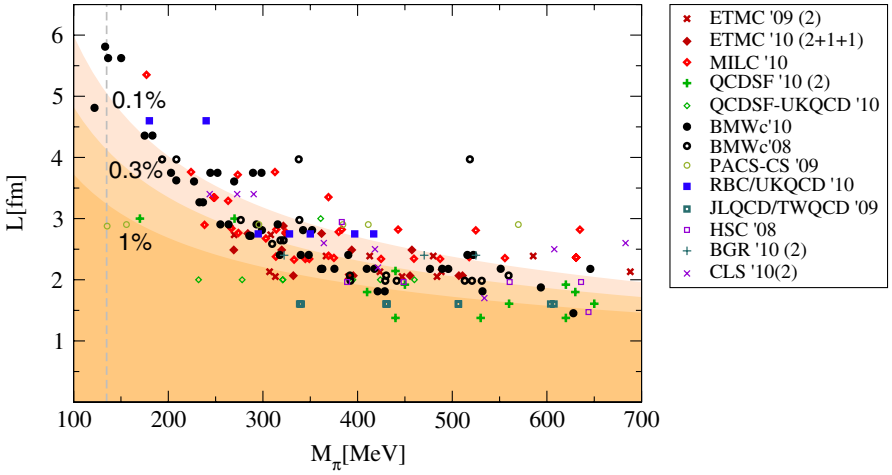

FIG. 13 (color online). The landscape of recent dynamical fermion simulations projected to the L vs M_π plane as given by Hoelbling (2010). The borders of the shaded regions are placed where the expected relative error of the pion mass is 1%, 0.3%, and 0.1% according to Colangelo, Durr, and Haefeli (2005). The vertical dashed line indicates the physical pion mass. Data points are taken from the following references: ETMC'09(2) (Blossier *et al.*, 2009); ETMC'10(2 + 1 + 1) (Baron *et al.*, 2010a); MILC'10 (Bazavov *et al.*, 2010a); QCDSF'10(2) (Schierholz, 2010); QCDSF-UKQCD'10 (Bietenholz *et al.*, 2010a); BMWc'08 (Durr *et al.*, 2008); BMWc'10 (Durr *et al.*, 2011c); PACS-CS'09 (Aoki *et al.*, 2009, 2010); RBC-UKQCD'10 (Mawhinney, 2010; Aoki *et al.*, 2011); JLQCD/TWQCD'09 (Noaki *et al.*, 2009); HSC'10 (Lin *et al.*, 2009); BGR'10(2) (Engel *et al.*, 2010); and CLS'10(2) (Brandt *et al.*, 2010). All ensembles are from $N_f = 2 + 1$ simulations except explicitly noted otherwise. For staggered, respectively, twisted mass ensembles, the Goldstone, respectively, charged pion masses are plotted.

are superimposed. As one can see current lattices are typically large enough to have percent level or smaller finite-volume corrections on the pion mass. Note, however, that corrections to baryon masses can be substantially larger (Colangelo, Fuhrer, and Lanz, 2010).

2. Finite-volume effects for unstable particles

Finite-volume corrections are not always just exponentially small at large L as discussed in Sec. IV.C.1. In the case where one is interested in extracting the mass of a resonant state that in infinite volume is embedded into a continuous spectrum of scattering states finite-volume effects are more complicated. For illustration we start by considering the hypothetical case where there is no coupling between the resonance (which we refer to as a "heavy state" in this paragraph) and the scattering states. In a finite box of size L, the spectrum in the center of mass frame consists of two particle states with energy

$$\sqrt{M_1^2 + \vec{k}^2} + \sqrt{M_2^2 + \vec{k}^2}, \tag{154}$$

where $k_i = 2n_i\pi/L$ and M_1, M_2 are the finite-volume masses of the lighter particles (cf. Sec. IV.C.1) and, in addition, of the state of the heavy particle with finite-volume mass M_X. As we increase L, the energy of any one of the two particle states decreases and eventually becomes smaller than the energy M_X of X. An analogous phenomenon can occur when we fix L but reduce the quark mass since the energy of the two light particles changes more than M_X. In the presence of interactions, this level crossing disappears and, due to the mixing of the heavy state and the scattering state, an avoided level crossing phenomenon is observed. Such mass shifts due to avoided level crossing can distort the chiral extrapolation of hadron masses to the physical pion mass.

The literature (Luscher, 1986b, 1991a, 1991b; Rummukainen and Gottlieb, 1995; Durr *et al.*, 2008) provides a conceptually satisfactory basis to study resonances in lattice QCD: each measured energy corresponds to a momentum $|\mathbf{k}|$ which is a solution of a complicated nonlinear equation. We follow Luscher (1991a), where the ρ resonance was taken as an example and it was pointed out that other resonances can be treated in the same way without additional difficulties. The ρ resonance decays almost exclusively into two pions. The absolute value of the pion momentum is denoted by $k = |\mathbf{k}|$. The total energy of the scattered particles is

$$W = 2\sqrt{M_\pi^2 + k^2} \tag{155}$$

in the center of mass frame. The $\pi\pi$ scattering phase $\delta_{11}(k)$ in the isospin $I = 1$, spin $J = 1$ channel passes through $\pi/2$ at the resonance energy, which corresponds to a pion momentum k equal to

$$k_\rho = \sqrt{\frac{M_\rho^2}{4} - M_\pi^2}. \tag{156}$$

In the effective range formula

$$(k^3/W)\cot\delta_{11} = a + bk^2, \tag{157}$$

this behavior implies

$$a = -bk_\rho^2 = \frac{4k_\rho^5}{M_\rho^2\Gamma_\rho}, \tag{158}$$

where Γ_ρ is the decay width of the resonance (which can be parametrized by an effective coupling between the pions and the ρ). The basic result of Luscher (1991b) is that the finite-volume energy spectrum is still given by Eq. (155) but with k being a solution of a complicated nonlinear equation, which

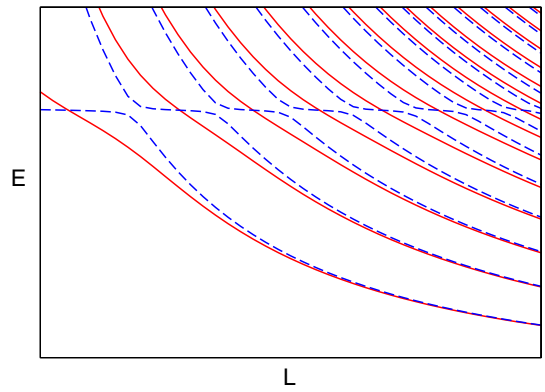

FIG. 14 (color online). The finite-volume energy levels vs box size L according to Luscher (1991b). The solid lines roughly correspond to the $\rho - \pi\pi$ system, while the dashed lines show the behavior in the case of a much smaller coupling g_ρ.

involves the $\pi\pi$ scattering phase $\delta_{11}(k)$ in the isospin $I = 1$, spin $J = 1$ channel and reads

$$n\pi - \delta_{11}(k) = \phi(q). \tag{159}$$

Here k is in the range $0 < k < \sqrt{3}M_\pi$, n is an integer, $q = kL/(2\pi)$, and $\phi(q)$ is a known kinematical function which can be evaluated numerically. In the limit of small q, $\phi(q) \propto q^3$, and $\phi(q) \approx \pi q^2$ for $q \geq 0.1$ to a good approximation. Solving the above equation leads to energy levels for different volumes and pion masses. Figure 14 illustrates these solutions as a function of the box size.

Thus, the spectrum is determined by the box length L, the infinite volume masses of the resonance M_X, and the two decay products M_1 and M_2 and one parameter, g_X, which describes the effective coupling of the resonance to the two decay products and is thus directly related to the width of the resonance.

In infinite volume the resonance manifests itself as an increased state density in a continuous spectrum. Identifying the infinite volume resonance on a lattice at a given finite volume is therefore not straightforward; generically it is not possible to identify the resonance with a single energy level. Scanning over different system lengths it is, however, possible to identify energies with an increased probability of finding a state[17] as seen in Fig. 14. This property may in principle be used to identify a resonance in a lattice calculation (Bernard *et al.*, 2008, 2011; Giudice, McManus, and Peardon, 2010). An alternative method based on finite time correlators was also recently suggested by Meissner, Polejaeva, and Rusetsky (2011).

Although conceptually clear, the treatment of resonant states in a region where they are not the ground state faces the large challenge of reliably extracting the ground state as well as a number of excited states. One therefore often uses the assumption that an operator which does not mirror the valence quark structure of a scattering state will almost exclusively couple to the resonance for directly extracting the desired resonance level. Recent studies (Lin *et al.*, 2009; Engel *et al.*, 2010) provide some evidence for the validity of this assumption.

[17]Note that depending on the specific volume this might be either the ground state or any of the excited states (cf. Fig. 14).

D. Electromagnetic effects and isospin breaking

Including dynamical fermions into a lattice QCD calculation is numerically expensive due to the occurrence of the fermion determinant in Eq. (24). For this reason, early lattice calculations were performed ignoring the effect of dynamical fermions all together (quenched approximation). With improved algorithmic understanding and the increase in available computer power the inclusion of some dynamical fermion effects has become possible. The first step is usually the inclusion of a degenerate pair of light quarks followed by the inclusion of a single strange quark.

Although the physical u and d quarks are far from degenerate $m_u/m_d \sim 0.56$ (Nakamura *et al.*, 2010), both masses are much smaller than the QCD scale $\Lambda_{\rm QCD}$ and therefore can be treated as a pair of degenerate light quarks with mass $\hat{m} = (m_u + m_d)/2$ to a very good approximation. In addition, quarks are electrically charged and a full understanding of the experimentally observed hadron spectrum therefore necessarily includes QED effects, too. For most observables related to hadron spectroscopy, these are, however, subdominant as can be readily seen by the smallness of the coupling constant $\alpha_{\rm EM}$ relative to the QCD coupling constant α. Effects of other interactions or of heavier quarks are negligible for light hadron spectroscopy within the currently attainable precision.

The relatively largest electromagnetic and isospin breaking effects can be observed in the pions, and also for kaons the effect is still at the percent level. Since both pion and kaon masses are often used to define the physical point, it is necessary to define a properly isospin averaged pion and kaon mass as an input to lattice QCD calculations with a degenerate pair of light quarks. We denote the physical mass splittings in the pion and kaon sectors as $\Delta_\pi = M^2_{\pi^\pm} - M^2_{\pi^0}$ and $\Delta_K = M^2_{K^\pm} - M^2_{K^0}$. Calling the pion and kaon masses in pure, isospin averaged QCD M_π and M_K, respectively, we can write the pion and kaon masses in full QCD + QED as

$$M^2_\pi + \begin{cases} I_{\pi^+} + \Gamma_{\pi^+} = M^2_{\pi^+}, \\ I_{\pi^0} + \Gamma_{\pi^0} = M^2_{\pi^0}, \end{cases} \tag{160}$$

and

$$M^2_K + \begin{cases} I_{K^+} + \Gamma_{K^+} = M^2_{K^+}, \\ I_{K^0} + \Gamma_{K^0} = M^2_{K^0}, \end{cases} \tag{161}$$

where the I_x are the isospin and the Γ_x are the QED corrections to the squared mass of the particle x. In order to obtain these, we start by noting that upon interchanging u and d in the pion sector π^+ and π^- are interchanged while for kaons a K^+ goes over into a K^0 and vice versa. Disregarding QED effects, we therefore see that both $M^2_{\pi^+}$ and $(M^2_{K^+} + M^2_{K^0})/2$ may contain only even powers when expanding in the isospin breaking parameter $(m_u - m_d)$ and are therefore $I_{\pi^+} \propto (m_u - m_d)^2$ and $I_{K^0} + I_{K^+} \propto (m_u - m_d)^2$ are free of leading (linear) isospin breaking effects. Moreover, as Gasser and Leutwyler (1984) demonstrated, $I_{\pi^+} \propto (m_u - m_d)^2(m_u + m_d)$

leading to an even stronger suppression. Within currently attainable precision, isospin breaking corrections to both $M_{\pi^+}^2$ and $(M_{K^+}^2 + M_{K^0}^2)/2$ are therefore negligible and we can assume $I_{\pi^+} = I_{K^0} + I_{K^+} = 0$.

Regarding the isospin correction to the charged pion, $I_{\pi^0} - I_{\pi^+} \propto (m_u - m_d)^2$ itself and Gasser and Leutwyler (1985) found a parameter-free expression at NLO in terms of physical meson masses that yields

$$\epsilon_m \equiv \frac{I_{\pi^+} - I_{\pi^0}}{\Delta_\pi} \simeq 0.04 \tag{162}$$

indicating that the bulk of the pion mass splitting is due to electromagnetic effects.

Regarding electromagnetic effects, according to Dashen (1969) the picture in the leading order of the SU(3) chiral expansion is that while neutral pseudo-Goldstone masses stay unaffected by electromagnetic corrections, i.e., $\Gamma_{\pi^0} = \Gamma_{K^0} = 0$, the difference of the square of the charged masses receives the same correction $\Gamma_{\pi^+} = \Gamma_{K^+}$. The absence of electromagnetic corrections in the π^0 and to a lesser extent the K^0 mass is further justified by Das *et al.* (1967) who demonstrated that these corrections vanish in the massless limit $m_u = m_d = 0$, respectively, $m_u = m_d = m_s = 0$. On the other hand, a range of model calculations (Bijnens and Prades, 1997; Donoghue and Perez, 1997) that are partly based on the inclusion of QED effects into chiral perturbation theory (Urech, 1995) and dispersive calculations based on the $\eta \to 3\pi$ decay (Anisovich and Leutwyler, 1996; Kambor, Wiesendanger, and Wyler, 1996; Leutwyler, 1996; Bijnens and Ghorbani, 2007; Colangelo, Lanz, and Passemar, 2009; Ditsche, Kubis, and Meissner, 2009) suggest that there are noticeable corrections to the other parts of Dashen's theorem. A recent world average of these corrections was given by Colangelo *et al.* (2011) as

$$\epsilon \equiv \frac{\Gamma_{\pi^0} - \Gamma_{\pi^+} - (\Gamma_{K^0} - \Gamma_{K^+})}{\Delta_\pi} = 0.7(5). \tag{163}$$

Assuming Dashen's theorem holds, we would thus get for the QED corrected, isospin averaged pion and kaon masses $M_\pi \simeq 134.8$ MeV and $M_K \simeq 495$ MeV. Including the correction (163) while keeping the reasonable assumption $\Gamma_{\pi^0} = \Gamma_{K^0} = 0$, the kaon mass is shifted by less than 1% to $M_K \simeq 494.6$ MeV while the pion mass is unaffected.

In order to go beyond these results, we need to treat QED and isospin breaking effects on the lattice. Since it has been difficult to reach the physical point even in the isospin limit with two degenerate light quarks and since at least for the pion QED effects are substantially larger, it is these QED effects that have received the most attention in the literature to date.

Regularizing QED on the lattice poses a very different set of problems than regularizing QCD. There is a straightforward way of including the leading QED corrections into QCD calculations that was first employed by Duncan, Eichten, and Thacker (1996) to obtain an estimate for the pion mass splitting. Since QED is an Abelian gauge theory, the electromagnetic gauge field is trivial when ignoring the electrical charge of the sea quarks. In this partially quenched approximation one can therefore sample free QED U(1) fields independently of the QCD SU(3) fields. This is most conveniently achieved by not sampling the parallel transports $U_\mu(x) = e^{ieA_\mu(x)a}$ directly but by instead fixing the gauge and sampling the underlying gauge fields $A_\mu(x)$ in which the Maxwell equations are linear. The corresponding action

$$S_{\mathrm{QED}} = \frac{1}{4e^2}\sum_x [\partial_\mu A_\nu(x) - \partial_\nu A_\mu(x)]^2 \tag{164}$$

with the forward difference operator ∂_μ decouples in Fourier space and gauge field configuration with the proper weight $e^{-S_{\mathrm{QED}}}$ may thus be produced by simply producing each Fourier component with a proper random weight. The only further restriction is the vanishing of the $p = 0$ component due to the compact space provided by the finite lattice.

In a calculation with dynamical sea quarks, the electromagnetic correction to the light quark masses that is introduced in the valence sector leads to a mismatch of sea and valence quark masses. In order to minimize these unitarity violating effects, one can retune the valence light quark masses such that after the inclusion of quenched QED effects both m_u and m_d have the same value as they had in pure QCD (Portelli *et al.*, 2010).

In the quenched approximation calculation of Duncan, Eichten, and Thacker (1996), a large violation of Dashen's theorem was found corresponding to $\epsilon \sim 0.5$. In later work with $N_f = 2$ dynamical flavors of domain wall fermions, Blum *et al.* (2007) reported a somewhat larger value while in the most recent update $N_f = 2 + 1$, Blum *et al.* (2010) found a value compatible with the original estimate of Duncan, Eichten, and Thacker (1996). Preliminary results are also available from the MILC Collaboration using $N_f = 2 + 1$ flavors of staggered fermions (Basak *et al.*, 2008) and the Budapest-Marseille-Wuppertal Collaboration with $N_f = 2 + 1$ Wilson fermions (Portelli *et al.*, 2010).

The general picture that emerges is that the corrections to Dashen's theorem that are parametrized in ϵ are in agreement with the phenomenological determinations. Taking lattice determinations into account, Colangelo *et al.* (2011) combined recent results on QED and isospin splitting effects into a world average of the QED corrected, isospin averaged pion and kaon masses. For the individual symmetry breaking parameters they found

$$\begin{aligned} &\epsilon = 0.7(5), \qquad \epsilon_m = 0.04(2), \\ &\Gamma_{\pi^0} = 0.07(7)\Delta_\pi, \qquad \Gamma_{K^0} = 0.3(3)\Delta_\pi, \end{aligned} \tag{165}$$

and consequently $M_\pi = 134.8(3)$ MeV and $M_K = 494.2(5)$ MeV, which agree within error with the values quoted above that were obtained under the assumption that Dashen's theorem holds.

Isospin splitting effects in the baryon spectrum are less dramatic than for the pseudoscalar mesons. As an example, the mass splitting in the nucleon system is $M_n - M_p = 1.293\,332\,1(4)$ MeV (Nakamura *et al.*, 2010) and an effective theory estimate of the electromagnetic contribution turns out to be negative $(M_n - M_p)_{\mathrm{QED}} = -0.76(30)$ MeV (Gasser and Leutwyler, 1982). If one is interested in isospin averaged baryon masses only, a straight isospin average is therefore sufficient for the accuracies that are presently obtainable in lattice calculations.

The first dedicated lattice study of the nucleon mass splitting was carried out by Beane, Orginos, and Savage (2007). They used a hybrid setup with domain wall valence on $N_f = 2 + 1$ staggered sea quarks with pion masses in the range of ~290–350 MeV. A single lattice spacing $a \sim 0.125$ fm was used and an extrapolation to the physical point was carried out in the framework of NLO partially quenched heavy baryon χPT. Using the experimental value of $M_\Delta - M_N$ as an input they obtain for the isospin part of the mass splitting $(M_n - M_p)_{\mathrm{QCD}} = 2.26(57)(43)$ MeV.

In addition to the isospin part of the nucleon mass diference, Blum *et al.* (2010) also calculated the QED part. They used $N_f = 2 + 1$ partially quenched domain wall fermions with pion masses in the range of ~250–400 MeV at a single lattice spacing $a \sim 0.11$ fm. Two volumes were used to estimate finite size effects in the final result and an extrapolation to the physical point was performed using NLO partially quenched heavy baryon χPT. They quoted the final results $(M_n - M_p)_{\mathrm{QCD}} = 2.24(12)$ MeV, $(M_n - M_p)_{\mathrm{QED}} = -0.383(68)$ MeV, and $M_n - M_p = 1.86(14)(47)$ MeV, where the first error is statistical and the second is part of the systematic error.

V. LATTICE RESULTS

In this section we discuss lattice results on the light hadron spectrum. Historically, the first results were from the quenched approximation that is discussed in Sec. V.A. The inclusion of dynamical fermions was pioneered with heavy, degenerate quarks (see Sec. V.B) before it developed into the study of theories with nondegenerate light and strange quarks that we review in Sec. V.C. While Secs. V.A and V.B are now of mainly historical interest, the three-flavor (and coming four-flavor) dynamical calculations are the definitive modern calculations.

Our review of lattice results does not include glueballs. For recent reviews on this topic see, e.g., Teper (1998), Klempt and Zaitsev (2007), Mathieu, Kochelev, and Vento (2009), and McNeile (2009).

A. Results in the quenched approximation

Although the quantitative understanding of the light hadron spectrum is an obvious and essential check for any candidate theory of the strong interaction, it took several years from the original proposal of Wilson (1974) that contained the lattice discretization of gauge theories and the strong coupling picture of quark confinement to the first numerical studies of the hadron spectrum (Hamber and Parisi, 1981, 1983; Marinari, Parisi, and Rebbi, 1981a; Fucito *et al.*, 1982; Hasenfratz *et al.*, 1982; Martinelli *et al.*, 1982; Weingarten, 1983; Fukugita, Kaneko, and Ukawa, 1984). Because of the lack of viable dynamical fermion algorithms and computer power, these pioneering studies were carried out in the quenched approximation sometimes with an SU(2) gauge group and even further discrete truncations. Lattices had a typical size of $6^3 \times 12$ and O(10) gauge configurations were generated with the Wilson gauge action. Naive or plain Wilson fermion actions were typically used to extract hadron masses and physical point predictions were obtained by linear extrapolation of either squares of meson masses or baryon masses. A first world average of these pioneering results was given by Creutz, Jacobs, and Rebbi (1983)

$$\begin{aligned} m_\rho &= 800(100)\ \mathrm{MeV}, & m_{a_0} &= 950(150)\ \mathrm{MeV}, \\ m_{a_1} &= 1100(150)\ \mathrm{MeV}, & m_p &= 1000(150)\ \mathrm{MeV}, \\ m_\Delta &= 1300(150)\ \mathrm{MeV}. \end{aligned} \tag{166}$$

From a modern perspective, these results should be viewed with some caution as these calculations were clearly exploratory and pioneering. The computer power of the times was not sufficient to properly clarify many systematic effects. As an example, the inverse lattice spacing of SU(3) gauge theory with the Wilson gauge action at $\beta = 6.0$ used by Marinari, Parisi, and Rebbi (1981a) was $a^{-1} = 1.12$ GeV, whereas modern determinations from various observables agree that it is $a^{-1} \simeq 2.1$–2.3 GeV (Gutbrod *et al.*, 1983; Lipps *et al.*, 1983; Otto and Stack, 1984; Aoki *et al.*, 2000; Giusti, Hoelbling, and Rebbi, 2001; Necco and Sommer, 2002; Durr *et al.*, 2007).

It was quickly realized (Bernard, Draper, and Olynyk, 1983; Bowler *et al.*, 1983; Gupta and Patel, 1983; Hasenfratz and Montvay, 1983; Politzer, 1984) that physical volumes were not big enough and that one should use larger time extents in order to safely extract a ground state signal. In the following years, quenched calculations with unimproved Wilson and staggered fermions on Wilson gauge action were pushed to larger lattice volumes and higher statistics (Lipps *et al.*, 1983; Billoire *et al.*, 1984; Bowler *et al.*, 1984, 1985; Gilchrist *et al.*, 1984; Konig, Mutter, and Schilling, 1984; Kunszt and Montvay, 1984; Billoire, Marinari, and Petronzio, 1985; Itoh *et al.*, 1986; Itoh, Iwasaki, and Yoshie, 1986), where lattices were often doubled in the time direction in order to obtain a clean signal. With gauge couplings typically $\beta \sim 5.7$–6 and spatial lattice extents typically 10–16 lattice units and time extents typically twice as much, a qualitatively consistent picture of the hadron masses started to emerge, although large systematic effects were present that could not clearly be identified yet. [For reviews of this generation of results, see Hasenfratz and Hasenfratz (1985) and Montvay (1987)]. In particular, the ratio of the nucleon mass to the ρ mass, which experimentally is $M_N/M_\rho \simeq 1.21$, turned out to be consistently too high $M_N/M_\rho > 1.6$, which is even larger than the static quark limit $M_N/M_\rho = 1.5$. Another stumbling block for these early calculations was the absence of sufficient splitting between the masses of the nucleon and the Δ.

During the following years, the focus shifted slightly toward inclusion of sea quark effects with steady progress in quenched spectroscopy (Gupta *et al.*, 1987; Bacilieri *et al.*, 1988, 1989; Fukugita, Oyanagi, and Ukawa, 1988) until the first precision calculations of the quenched light hadron spectrum emerged in the early 1990s (Bacilieri *et al.*, 1990; Cabasino *et al.*, 1991a, 1991b; Gupta *et al.*, 1991; Allton *et al.*, 1992, 1994; Bitar *et al.*, 1992; Daniel *et al.*, 1992; Guagnelli *et al.*, 1992; Butler *et al.*, 1993, 1994; Kim and Sinclair, 1993).

Among these, the first landmark precision calculation of the quenched light hadron spectrum was carried out by the GF11 Collaboration (Butler *et al.*, 1993, 1994). Wilson

fermions were used on a Wilson gauge action at three different values of the lattice spacing in the range $a \sim 0.07$–0.14 fm. Propagators were extracted using point and Gaussian smeared sources at different quark masses corresponding to $M_\pi/M_\rho > 0.5$, i.e., with pion masses $M_\pi \gtrsim 400$ MeV. Lattice volumes in the range $16^3 \times 32$ to $30^2 \times 32 \times 40$ were used corresponding to a spatial lattice extent of ~ 2.3 fm at all three lattice spacings. At the coarsest lattice spacing, dedicated runs at larger and smaller volumes were performed in order to extract the finite-volume dependence of the result. They were used in the end to correct the physical predictions to infinite volume.[18] Considering degenerate quarks only, a linear relation was established between the degenerate quark masses m_q and M_π^2, while for all other hadrons a fit of the form $M = a + bm_q$ described the data. Assuming that these linear relations extend to the nondegenerate case with two quarks of mass m_1 and m_2, i.e., $M_\pi^2 \propto (m_1 + m_2)^2$ and $M = a + b_1 m_1 + b_2 m_2$, the physical point was found using M_π, M_K, and M_ρ input with the latter used as a scale setting observable. A continuum extrapolation linear in a was performed that turned out to be rather mild.

Table I shows the resulting spectrum obtained by Butler *et al.* (1993, 1994). Despite the many approximations used, the overall agreement with experiment is rather remarkable and at the $<10\%$ level.

Similarly sophisticated quenched analyses were soon after performed for the $\eta - \eta'$ system (Kuramashi *et al.*, 1994) and for excited state mesons (Lacock and Michael, 1995; Lacock *et al.*, 1996). These calculations and detailed studies of systematic effects such as finite size (Aoki *et al.*, 1994), excited state contaminations (Iwasaki *et al.*, 1996), or quenched chiral logarithms and SU(3) splittings (Kim and Sinclair, 1995; Bhattacharya *et al.*, 1996) revealed potential inconsistencies of the quenched approximation of up to 20%. On the other hand, results with improved Wilson actions (Collins *et al.*, 1997; Gockeler *et al.*, 1997, 1998b; Edwards, Heller, and Klassen, 1998) and for staggered fermions that reached finer lattice spacings and smaller quark masses (Bernard *et al.*, 1998a; Kim and Ohta, 2000) indicated quenching effects that were less dramatic at $O(5\%)$. In the case of the latter two results it was especially noted that a simple linear extrapolation in the light quark mass was no more sufficient. Several χPT motivated fit forms were found to describe the chiral behavior of the ρ and nucleon masses but the coefficients were not found to be in agreement with quenched χPT expectations at all.

The accuracy of the quenched approximation was addressed in the large scale calculation by the CP-PACS Collaboration (Aoki *et al.*, 2000, 2003a). They used lattices of ~ 3 fm spatial extent at four values of the lattice spacing in the range $a \sim 0.05$–0.1 fm with quark masses corresponding to $M_\pi/M_\rho \sim 0.4$–0.75. Both fermion and gauge action used were plain Wilson, and nondegenerate quark masses were used to investigate splittings in the SU(3) multiplets. While pseudoscalar meson masses were found to have a chiral behavior compatible with the quenched χPT expectations,

TABLE I. Quenched lattice QCD prediction of the light hadron spectrum according to Butler *et al.* (1993, 1994). The ratio of various hadron masses and the QCD scale $\Lambda_{\overline{\mathrm{MS}}}^{(0)}$ to the mass of the ρ that was used to set the scale are given. The label Δm refers to the combination $\Delta m = m_\Xi + m_\Sigma - m_N$. Observed values are experimental results from Hikasa *et al.* (1992) except for the case of the QCD scale $\Lambda_{\overline{\mathrm{MS}}}^{(0)}$, where they refer to two previous results from the literature (El-Khadra *et al.*, 1992; Bali and Schilling, 1993a, 1993b). Note that some experimental values, notably the mass of the ρ, have been updated since (Nakamura *et al.*, 2010).

Ratio	Finite volume	Infinite volume	Observed
m_{K^*}/m_ρ	1.149 ± 0.010	1.167 ± 0.016	1.164
m_Φ/m_ρ	1.297 ± 0.019	1.333 ± 0.032	1.327
m_N/m_ρ	1.285 ± 0.070	1.219 ± 0.105	1.222
$\Delta m/m_\rho$	1.867 ± 0.046	1.930 ± 0.073	2.047
m_Δ/m_ρ	1.628 ± 0.075	1.595 ± 0.111	1.604
m_{Σ^*}/m_ρ	1.813 ± 0.051	1.821 ± 0.075	1.803
m_{Ξ^*}/m_ρ	2.013 ± 0.052	2.063 ± 0.067	1.996
m_Ω/m_ρ	2.206 ± 0.058	2.298 ± 0.098	2.177
$\Lambda_{\overline{\mathrm{MS}}}^{(0)}/m_\rho$	0.305 ± 0.008	0.319 ± 0.012	0.305 ± 0.018 0.320 ± 0.007

the discrepancy in the vector meson and baryon sector found in the staggered results of Bernard *et al.* (1998a) and Kim and Ohta (2000) was confirmed. For these masses, χPT motivated fits were used to extrapolate to the physical point. The physical point in the light quark mass was defined using M_π and M_ρ and either M_K or M_ϕ were used to define the physical strange mass.[19] The final result that has a precision of $\sim$1–3% is displayed in Fig. 15.

A statistically significant deviation from the experimentally observed spectrum was noted with discrepancies up to $\sim 10\%$. These discrepancies, however, are particularly pronounced due to the choice of M_ρ as a scale setting observable. Since the ρ does not decay in the quenched approximation and therefore represents the ground state in the vector channel, it is in principle a viable scale setting variable from a pure lattice perspective. Nonetheless, the identification of the stable quenched ground state energy with the mass of a resonance with ~ 150 MeV experimental width is not optimal. On top of that, an accurate determination of ρ meson properties is a challenging experimental task. This is highlighted by the fact that the experimental value of M_ρ itself has moved by $\sim 1\%$ or more than 10 standard deviations over the last two decades (Hikasa *et al.*, 1992; Nakamura *et al.*, 2010).

As Garden *et al.* (2000) noted, one can derive from the CP-PACS results predictions for hadron masses with the scale set by the nucleon mass instead of M_ρ. In this case, the maximum deviation from experiment turns out to be significantly lower at $\sim 4\%$ indicating that indeed the quenched approximation is substantially worse for resonance masses than for masses of hadrons that are stable within QCD. A confirmation of these results with somewhat lower statistical accuracy was reported by Bowler *et al.* (2000).

The CP-PACS calculation was one of the last large scale calculations aimed at a precision determination of the

[18] See Gottlieb (1997) for a detailed discussion of the finite-volume effects.

[19] Note that although the ϕ is a singlet meson, its disconnected part is usually disregarded in lattice studies.

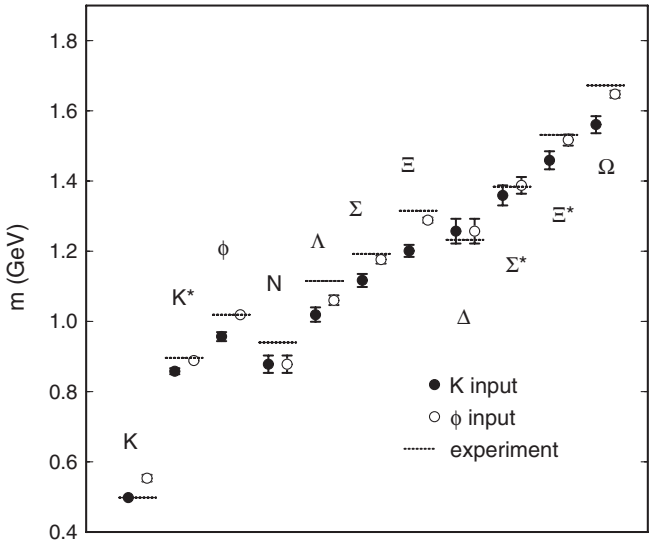

FIG. 15. Quenched lattice QCD prediction of the light hadron spectrum according to Aoki *et al.* (2000, 2003a). For both data sets plotted M_ρ and M_π were used to set the scale and the light quark mass. In order to set the strange mass, either M_K (filled circles) or M_ϕ (open circles) are used. Figure courtesy of the CP-PACS Collaboration.

quenched ground state light hadron spectrum. As quenching effects became statistically significant, the focus of efforts to get a quantitative confirmation of QCD reproducing the experimentally observed ground state light hadron spectrum moved toward inclusion of dynamical fermion effects. Nonetheless, due to its relatively low numerical cost, the quenched approximation continues to be used to this day as a test bed for new numerical approaches and as a first step in studying computationally demanding observables. In the following years, the quenched ground state hadron spectrum was used to check various variants of chirally symmetric fermion actions (Gattringer *et al.*, 2004; Babich *et al.*, 2006; Galletly *et al.*, 2007) or to develop improved (Melnitchouk *et al.*, 2003) or anisotropic (Nemoto *et al.*, 2003) actions that were intended for studying excited hadrons.

Following the CP-PACS determination of the ground state quenched hadron spectrum the attention in quenched hadron spectroscopy turned toward resonant and singlet states (Lee and Weingarten, 1999; McNeile and Michael, 2001; Gockeler *et al.*, 2002; Sasaki, Blum, and Ohta, 2002; Melnitchouk *et al.*, 2003; Nemoto *et al.*, 2003; Brommel *et al.*, 2004; Gattringer *et al.*, 2004; Mathur *et al.*, 2005, 2007; Sasaki, Sasaki, and Hatsuda, 2005; Burch *et al.*, 2006a, 2006b; Basak *et al.*, 2007; Lasscock *et al.*, 2007; Wada *et al.*, 2007; Fleming *et al.*, 2009; Engel *et al.*, 2010). In particular, many groups reported on the splitting between the nucleon and its lightest negative parity partner, the $N^*(1535)$. In all cases, a clear signal of the mass splitting between the nucleon ground state and the $N^*(1535)$ could be seen on the lattice. The splitting is increasing as one lowers the light quark masses toward the physical point and in all cases is roughly consistent with the experimentally observed mass splitting. It is an interesting peculiarity, however, that the lightest experimentally observed nucleon excited state is not the nucleon parity partner $N^*(1535)$ but, in fact, the $N^*(1440)$, the so-called Roper resonance which carries positive parity and $J = 1/2$ as the nucleon. With the exception of Mathur *et al.* (2005) and Sasaki, Sasaki, and Hatsuda (2005), who employed Bayesian techniques to extract excited state information from a single channel,[20] however, the first positive parity excitation of the nucleon turned out to lie above the first negative nucleon state in all lattice calculations. A possible solution to this discrepancy was recently proposed by Mahbub *et al.* (2009b) and Mahbub, Cais *et al.* (2010) who demonstrated that a mix of excited states enters typical interpolating operators. By using a large operator basis they could explicitly disentangle up to eight states and demonstrate a level crossing between the negative parity ground state and the first positive parity excitation for light quark masses that is consistent with the finding of Mathur *et al.* (2005) and Sasaki, Sasaki, and Hatsuda (2005) and the experimentally observed level ordering between the $N^*(1535)$ and $N^*(1440)$ states.

Another interesting case in excited state baryon spectroscopy is the $\Lambda(1405)$. In the quark model picture, it is the lightest negative parity partner of the Λ with a valence quark structure uds. It is, however, the lightest negative octet baryon, more than 100 MeV lighter than the lightest negative parity nucleon, the $N^*(1520)$, even though it contains a strange quark. This is the most striking of many peculiar features that have given rise to a number of suggestions for a nontrivial structure of the $\Lambda(1405)$ such as that of a $N\bar{K}$ hadronic molecule or a pentaquark state [for a recent review, see Klempt and Richard (2010)]. Melnitchouk *et al.* (2003) and Nemoto *et al.* (2003) studied the negative parity Λ states in the quenched approximation with standard interpolating operators and found it impossible to reproduce the $\Lambda(1405)$ which they interpret as an indication for a nontrivial structure of the $\Lambda(1405)$ that might not be properly reflected in the quenched approximation. In contrast, Burch *et al.* (2006a) found the $\Lambda(1405)$ to be consistent with the negative parity octet state.

With the exception of the $N^*(1440)$ and the $\Lambda(1405)$ that were discussed above, no qualitative tension between experiment and the above-mentioned quenched excited baryon studies was found. For a more detailed review, see Leinweber *et al.* (2005).

B. Results with degenerate dynamical quarks

The spectrum calculation of the CP-PACS Collaboration (Aoki *et al.*, 2000, 2003a) reached a numerical precision such that quenching effects could clearly be seen. In order to obtain a quantitative understanding of the ground state light hadron spectrum on the few percent level it is therefore necessary to include dynamical fermion effects into the lattice calculation. From the six fermion flavors in nature, the charm, bottom, and top each have masses much larger than the QCD scale $\Lambda_{\rm QCD}$. Their contribution to light hadron masses through quark loop effects is therefore believed to be negligible. Among the remaining three flavors $m_{u/d} \ll \Lambda_{\rm QCD}$, while $m_s \sim \Lambda_{\rm QCD}$. Consequently, and because an even

[20]See Sasaki and Sasaki (2005) for a discussion of possibly large finite size effects for this technique.

number of quark flavors is usually easier to implement (cf. Sec. II.C), the first attempts at unquenching lattice QCD calculations were performed with two degenerate quark flavors. In the case of staggered fermions, calculations with four dynamical quark flavors are even easier due to the remnant doubling (cf. Sec. II.D.1). In this section we review results obtained with (a usually even number of) degenerate[21] dynamical fermions. While this still represents an approximation that is necessitated by the lack of proper computational resources, it is still a very significant step forward from the quenched approximation.

Pioneering work on lattice hadron spectroscopy with dynamical fermions was done by Langguth and Montvay (1984) where dynamical fermions were implemented using a strong coupling expansion of the determinant ratio. During the following years unquenching via the inclusion of $N_f = 2$ and 4 dynamical Wilson fermions and $N_f = 2$, 3, and 4 staggered fermions was investigated by several groups (Fucito *et al.*, 1986; Fukugita, Oyanagi, and Ukawa, 1986, 1987; Billoire and Marinari, 1987; Campostrini *et al.*, 1987; Detar and Kogut, 1987a, 1987b; Fukugita *et al.*, 1987; Gottlieb *et al.*, 1987a; Hamber, 1987; Grady, Sinclair, and Kogut, 1988). These early works demonstrated that the main effect of including dynamical fermions was a change in dependence of the lattice spacing on bare coupling constant β. Apart from this effect, no clear sign of unquenching could be observed. In particular, the M_ρ/M_N ratio tended to stay constant or even increase. In studies with staggered fermions, the taste breaking effects were also observed to be rather severe. For a comprehensive review of these early studies, see Fukugita (1988).

During the following years it became clear that with staggered fermions one could go to substantially lighter quark masses than with Wilson fermions (Patel *et al.*, 1989; Bitar *et al.*, 1990a, 1990b, 1992; Brown *et al.*, 1991; Gupta *et al.*, 1991; Altmeyer *et al.*, 1993; Fukugita *et al.*, 1993) in the sense that the M_π/M_ρ ratio attainable with Wilson fermions was limited to $M_\pi/M_\rho \gtrsim 0.7$, while if taking the lightest pion one could go down to about half this number in the staggered case. Since reducing the mass of the valence quarks only was substantially easier, some of these studies started exploring partially quenched setups, where the valence quark masses are varied independently of the sea quark masses and even hybrid calculations with valence Wilson quarks on a dynamical staggered sea. None of these calculations, however, gave a clear signal for a M_ρ/M_N ratio that was substantially better than the ones obtained in contemporary quenched calculations. Although there was steady progress over the following few years (Bitar *et al.*, 1994; Allton *et al.*, 1999; Eicker *et al.*, 1998), the focus of large scale calculations shifted more toward precision computations in the quenched approximation. This was in large part due to the tremendous computational effort that was needed for dynamical fermion computations which exceeded the computer capabilities of that time. A first unquenched study of the $\eta - \eta'$ mixing was performed by McNeile and Michael (2000) which found a mixing angle of $\theta \sim -10°$ albeit without continuum and chiral extrapolation.[22]

These efforts culminated in the first large scale project to compute the light hadron spectrum in $N_f = 2$ QCD by the CP-PACS Collaboration (Ali Khan *et al.*, 2002). They used two degenerate flavors of mean field improved clover fermions on an Iwasaki gauge action. The strange valence quark was included in a quenched setup. Three relatively coarse lattice spacings in the range $a \sim 0.11$–0.22 fm were used with an approximately constant physical volume $L \sim 2.5$ fm and $T = 2L$. Four sea and valence quark masses in a range corresponding to $M_\rho/M_N \sim 0.6$–0.8 and an additional valence quark mass at $M_\rho/M_N \sim 0.5$ were investigated. Point sources and exponentially smeared quark sources on a gauge fixed background were chosen for optimal plateau onset. Chiral extrapolation was performed by a combined fit to all partially quenched masses for each channel on a given sea quark mass. Vector meson and baryon masses were extrapolated to the physical point using quadratic functions in the valence and sea M_π^2 with certain restrictions on the quadratic terms. In the case of vector mesons, χPT motivated nonanalytic M_π^3-type terms were also used instead of M_π^4-type terms to estimate the systematic error. Following the example of the quenched CP-PACS calculation discussed in Sec. V.A, the physical light quark masses and the scale are defined via M_π and M_ρ, while two options M_K or M_ϕ were used to set the strange quark mass. The continuum limit is obtained by linear extrapolation in a.

The resulting light hadron spectrum is plotted in Fig. 16. Clearly the heavier baryon states are in good agreement with experiment while the lighter ones, especially the nucleon and the Δ, seem to be systematically too high. This does not come as a big surprise though since the extrapolation to the physical point is substantially more severe for the baryons containing more light valence quarks.

Similar efforts to that of the CP-PACS Collaboration were reported by the UKQCD and JLQCD Collaborations in Allton *et al.* (2002) and Aoki *et al.* (2003b). The UKQCD Collaboration worked at a single lattice spacing $a \sim 0.1$ fm that was set with r_0. The range of sea quark masses was chosen such that $M_\pi/M_\rho \sim 0.55$–0.9 and the spatial lattice extent was $L \sim 1.7$ fm. The JLQCD Collaboration worked at one single lattice spacing $a \sim 0.09$ fm at a spatial extent $L \sim 1.8$ fm using clover fermions on a Wilson gauge action and the same range of sea masses $M_\pi/M_\rho \sim 0.6$–0.8 than CP-PACS. The findings of both collaborations on the light hadron spectrum are in good agreement with the continuum CP-PACS results.

The conclusion from these two large scale projects regarding the feasibility of computations with light dynamical quarks was summarized in a plot that became known as the "Berlin wall plot" by Ukawa (2002). He conjectured that the cost of dynamical fermion simulations would rise toward the chiral limit essentially as $\propto M_\pi^6$ effectively rendering any dynamical calculations with Wilson-type fermions near the physical point impossible in the foreseeable future without

[21] We use the term nondegenerate here in the sense that no explicit term was added that breaks the flavor symmetry. In the case of staggered quarks the unavoidable taste splitting is of course present.

[22] See also Lesk *et al.* (2003).

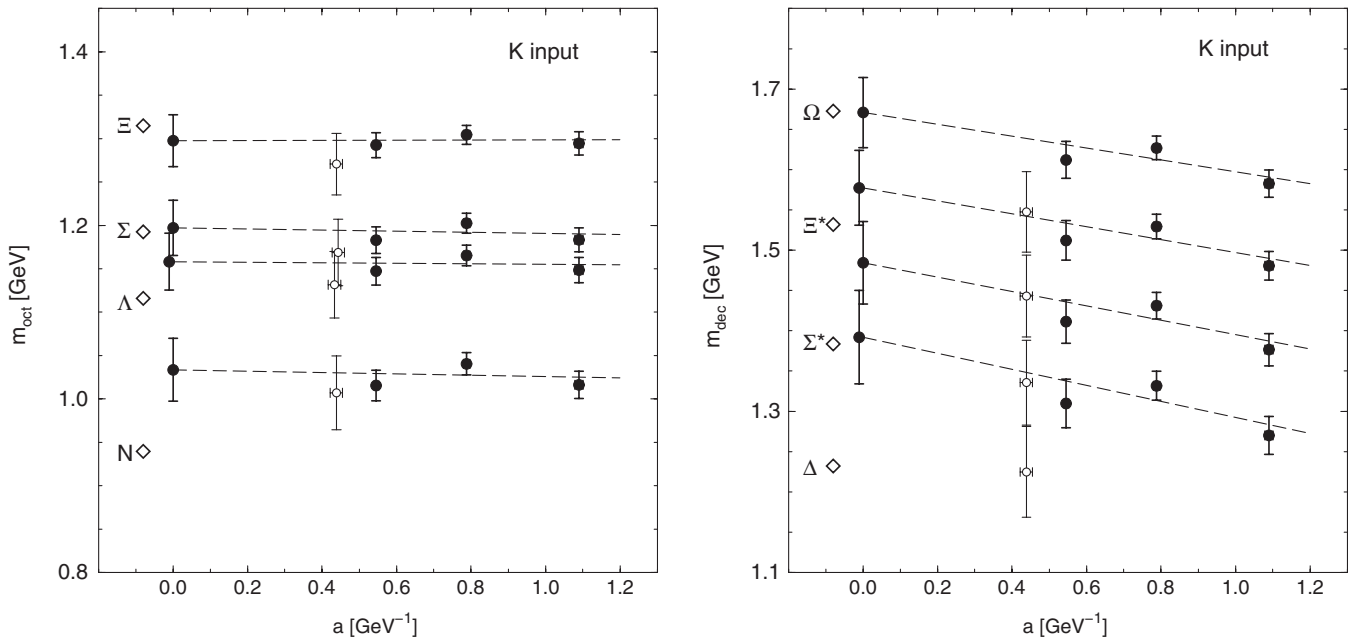

FIG. 16. Dynamical $N_f = 2$ lattice QCD prediction of the light baryon spectrum according to Ali Khan *et al.* (2002). The continuum extrapolation of the ground state light octet and decuplet baryon masses in the case where the strange mass was set via M_K are displayed. The continuum extrapolation was performed using three lattice spacings that are displayed with solid circles. Open circles represent a fourth, finer lattice which was not included in the analysis due to a too small volume. Figure courtesy of the CP-PACS Collaboration.

substantial algorithmic improvements. Because of their lower computational cost staggered fermions were able to push farther toward the chiral limit and already did so with also a dynamical strange quark (see Sec. V.C), but extracting especially baryonic states is less straightforward in this formulation (cf. Sec. III.A). For a more comprehensive review of these results see McNeile (2003).

Because the inclusion of a nondegenerate sea quark incurs little extra expense, from this point on, the main development in light hadron spectroscopy continued with the inclusion of a strange quark in addition to two degenerate light quarks. This is usually referred to as $N_f = 2 + 1$ and is discussed in Sec. V.C. The question of how much two-flavor calculations differ from experiment has not been answered as definitively as it has been for the quenched calculations discussed earlier. A number of $N_f = 2$ calculations of light hadron masses were still being performed, however, for a number of reasons such as algorithmic tests (Del Debbio *et al.*, 2007a, 2007b) or as a first step for formulations that allow an even number of quark flavors only (Alexandrou *et al.*, 2009). Similarly, flavor singlet spectroscopy that typically requires substantially more statistical precision was still investigated in $N_f = 2$ QCD (McNeile, Michael, and Sharkey, 2001; Allton *et al.*, 2004; Kunihiro *et al.*, 2004; Prelovsek *et al.*, 2004; Hart *et al.*, 2006; McNeile and Michael, 2006; McNeile, Michael, and Urbach, 2009). For a recent comprehensive review of these results, see McNeile (2007).

The ETM Collaboration (Alexandrou *et al.*, 2009) published results for the ground state light baryon spectrum with $N_f = 2$ twisted mass fermions.[23] They used $N_f = 2$ twisted mass fermions at maximal renormalized twist on a tree level Symanzik improved gauge action. Two lattice spacings ($a \sim 0.07$ and ~ 0.09 fm) were used with charged pion masses in the range 270–500 MeV.[24] The lattice spacing was set via the nucleon mass and chiral extrapolations were performed with a variety of different *Ansätze*. The valence strange quark mass is set by tuning the kaon mass to its physical value. The final result employs two different heavy baryon χPT *Ansätze* [$O(p^3)$, respectively, NLO SU(2)] for the extrapolation of baryons without, respectively, with valence strange quarks to the physical mass point. The continuum extrapolation was performed using a constant which was demonstrated to be sufficient at the given level of accuracy. Exponential finite-volume corrections were taken into account in the final fit form. Resonant state finite-volume corrections were not performed but are believed to be irrelevant in the region of parameter space covered by the simulations. Effects of the twisted mass isospin breaking were observed to be negligible except in the case of the Ξ where they amounted to a 6% correction. Their final result displayed in Fig. 17 shows good agreement with experiment at the level of precision of the calculation which is $\sim 5\%$. The ETM Collaboration also investigated the $\rho - \omega$ mass splitting and mixing (McNeile, Michael, and Urbach, 2009) excluding electromagnetic effects. While a clear signal and qualitatively correct behavior were found, the quantitative understanding of the experimentally observed splitting remains a challenging task.

Turning to excited states, the BGR Collaboration computed ground and excited state hadron spectra using $N_f = 2$ single step stout smeared chirally improved fermions on a

[23]Ses also Alexandrou *et al.* (2008) for some results with more lattice spacings and different scale setting.

[24]The isospin splitting of the pions is $M_{\pi^\pm}^2 - M_{\pi^0}^2 \sim$ (150–220 MeV)^2 (Baron *et al.*, 2010b).

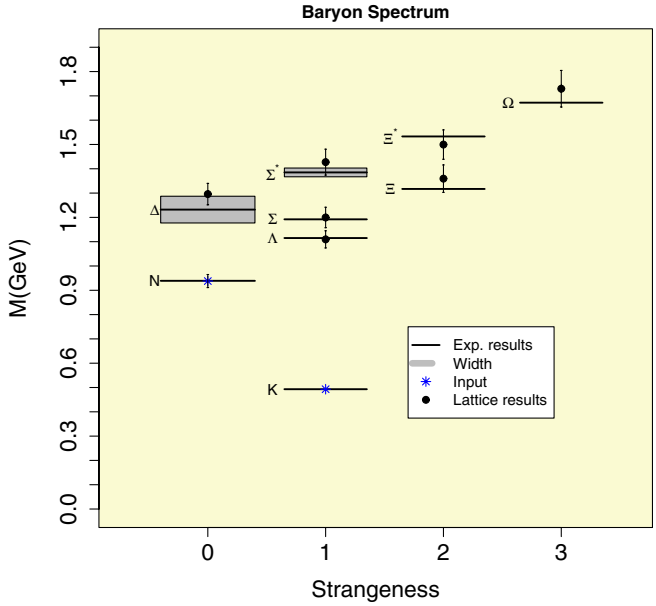

FIG. 17 (color online). Baryon spectrum obtained by the ETM Collaboration with $N_f = 2$ twisted mass fermions. From Alexandrou *et al.*, 2009, with permission of the ETM Collaboration.

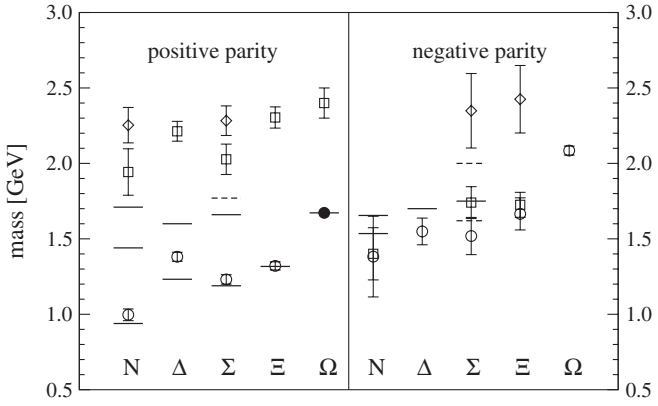

FIG. 18. Positive and negative baryon spectrum obtained by the BGR Collaboration with $N_f = 2$ chirally improved fermions. From Engel *et al.*, 2010, with permission of the BGR Collaboration.

tadpole improved Lüscher-Weisz gauge action at a singe lattice spacing $a \sim 0.15$ fm (Engel *et al.*, 2010; Prelovsek *et al.*, 2010). Three pion masses in the range 320–530 MeV were used and the scale was set with r_0. Gaussian smeared quark sources were used in combination with a variational method based on three interpolating operators to extract the energy levels. A chiral extrapolation linear in M_π was performed and the strange quark was introduced in a partially quenched setup. The results for positive and negative baryon states are plotted in Fig. 18. A good signal for the ground state was found but excited and scattering state signals were generally weak. Some evidence was also presented that the σ and κ resonances contain a sizable exotic admixture of a tetraquark ($\bar{q}\,\bar{q}\,qq$) state.

In an extension of the work of Melnitchouk *et al.* (2003) and Nemoto *et al.* (2003) in the quenched approximation, Takahashi and Oka (2010) studied the $\Lambda^*(1405)$ on $N_f = 2$ CP-PACS lattices and essentially reached the same conclusion as Melnitchouk *et al.* (2003) and Nemoto *et al.* (2003) that the $\Lambda^*(1405)$ cannot be reproduced using standard baryon octet and singlet interpolating operators.

C. Results with dynamical light and strange quarks

The first large scale computation of the light hadron spectrum with a pair of light and one strange sea quark was performed by the MILC Collaboration (Bernard *et al.*, 2001; Aubin *et al.*, 2004).[25] With asqtad fermions on a one-loop Symanzik improved gauge action, they reached Goldstone (i.e., taste pseudoscalar) pion masses down to $M_\pi \sim 260$ MeV on lattices of spatial size $L \sim 2.4$ and $\sim$3.4 fm at two values of the lattice spacing $a \sim 0.09$ and $\sim$0.12 fm. Finite-volume effects were explicitly checked for and found to be under control. The fermion update algorithm used was the R algorithm and explicit checks for the absence of step size dependent effects were performed. The scale was set via b-meson spectroscopy, in particular, the Υ $1P$-$1S$ mass splitting, and physical light and strange quark masses were defined by M_π and M_K. Ground state meson and some baryon masses were computed as well as the radially excited pseudoscalar meson state. The extrapolation to physical pion masses was performed using various heavy baryon χPT motivated fit functions and a continuum extrapolation was done using g^2a^2 terms where possible. An update of these results including data from finer lattices as well as a comprehensive review is available in Bazavov *et al.* (2010a). The resulting light hadron spectrum is displayed in Fig. 19. Note that due to the particular difficulties in extracting baryon masses in the staggered formulation (cf. Sec. III) there are only predictions for a subset of the ground state baryons. Again, the numbers result in good agreement with experiment.

A subset of the MILC ensembles with $a \sim 0.12$ fm and with the smallest pion mass of $\sim$290 MeV was studied by Walker-Loud *et al.* (2009) in a mixed action setup with domain wall valence quarks. Comparing different chiral fit forms for the nucleon mass it was demonstrated that a simple linear fit in M_π gives a good description of the given data set and extrapolates to the correct value at the physical point. In the same paper, this feature was also found in other collaborations data.

The PACS-CS Collaboration published results for the light hadron spectrum using both a chiral extrapolation (Aoki *et al.*, 2009) and a direct reweighting to the physical point (Aoki *et al.*, 2010). In both cases $N_f = 2 + 1$ nonperturbatively $O(a)$ improved cover fermions on an Iwasaki gauge action were used at a single lattice spacing $a \sim 0.09$ fm and a spatial lattice extent of $L \sim 2.9$ fm. Pion masses down to $\sim$150 MeV were directly simulated and a reweighting to the physical point was carried out with the lightest ensemble. In the extrapolated ensemble finite size effects on the pseudoscalar masses were corrected using SU(2) χPT at NLO. The small chiral extrapolation was performed linearly in the light quark mass and M_Ω was used to set the scale. More involved

[25] See also Davies *et al.* (2004), where the effects of unquenching are discussed for observables beyond the light hadron spectrum.

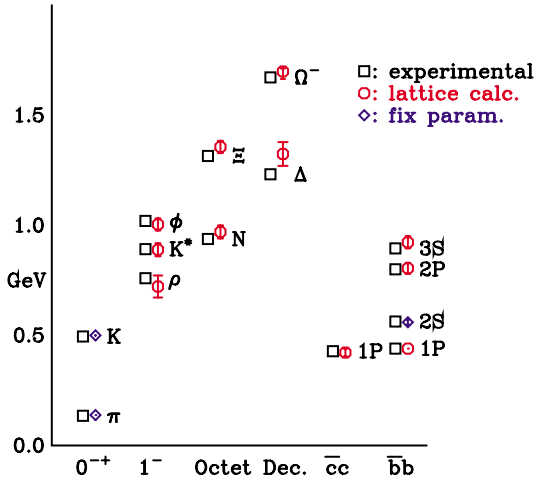

FIG. 19 (color online). Comparison of the $N_f = 2 + 1$ light hadron spectrum results from the MILC Collaboration (Bazavov *et al.*, 2010a) with experiment. The diamonds are input quantities while the circles are predictions. Experimental masses of hadrons from Amsler *et al.* (2008) are indicated by squares. Note that charmonium and bottomonium masses are also included with some of the later ones used to set the scale. Figure courtesy of the MILC Collaboration.

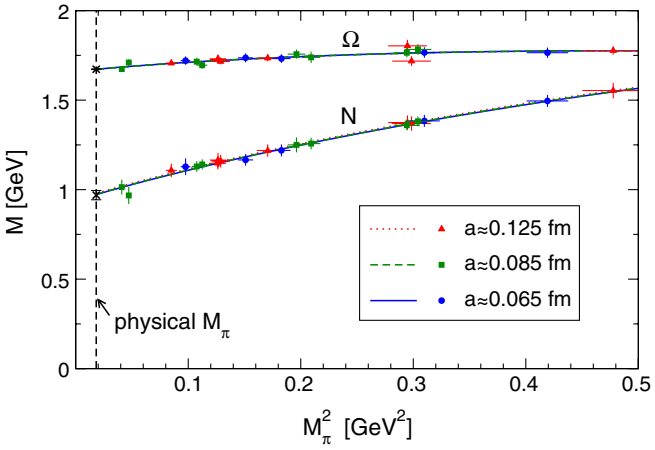

FIG. 21 (color online). Sample chiral and continuum extrapolation of the lattice hadron masses of Durr *et al.* (2008) at physical $M_K^2 - M_\pi^2/2$ in physical units. The scale setting variable M_Ω and the nucleon mass are plotted vs the square of the pion mass together with a fit of the data at every lattice spacing. The vertical dashed line represents the physical pion mass.

chiral forms were subsequently investigated by Ishikawa *et al.* (2009). Similarly in the reweighted ensemble the masses of the π, K, and Ω were used to tune to the physical point. The final result from the extrapolation method is plotted in Fig. 20. Similar results were found with the reweighting method as detailed by Aoki *et al.* (2010).

Full control over all systematic uncertainties at the few percent level was achieved in the light hadron spectrum calculation of the Budapest-Marseille-Wuppertal Collaboration (Durr *et al.*, 2008). They used tree level improved six-step stout smeared $N_f = 2 + 1$ clover fermions on a tree level Symanzik improved gauge action on lattices of spatial extent of $L \sim 2.0$–4.1 fm. Both the gauge and the fermion action are known to be in the correct universality classes and the updating algorithm is exact and free of possible ergodicity problems. Pion masses down to 190 MeV and three lattice spacings $a \sim 0.065$, ~ 0.85, and ~ 0.125 fm were used which allowed for a fully controlled extrapolation to the continuum and the physical point with various *Ansätze* for both. Possible contamination of the propagators from excited states was accounted for by varying the fit range. Finite-volume corrections were applied including energy shifts for resonant states (as described in Sec. IV.C.2) that allowed for a detailed treatment of resonant states, too. The continuum extrapolation was performed with a term linear in a or a^2 and chiral fits were done with both Taylor and NLO heavy baryon χPT with a free coefficient (see Fig. 21 for an example extrapolation to the physical point and continuum limit). The above procedure allowed for a fully controlled calculation of the systematic uncertainty via

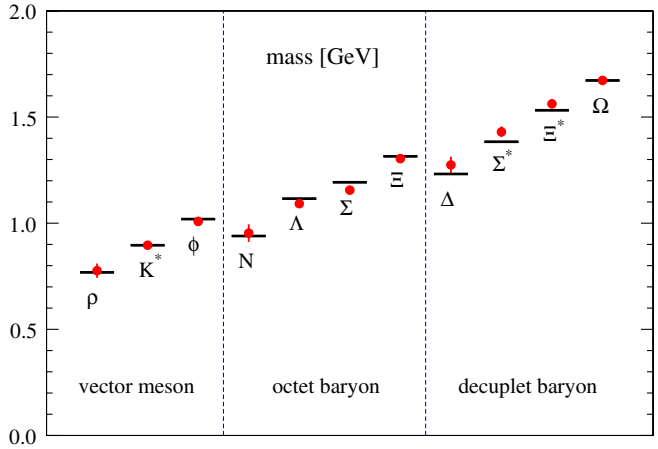

FIG. 20 (color online). The extrapolated $N_f = 2 + 1$ light hadron spectrum results from the PACS-CS Collaboration. Experimental data are from Amsler *et al.* (2008). From Aoki *et al.*, 2009, with permission of the PACS-CS Collaboration.

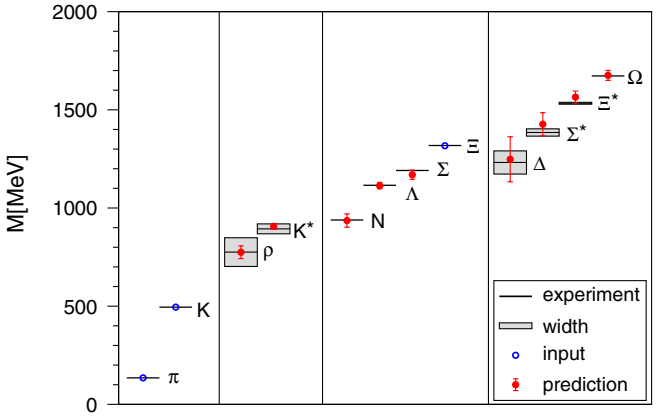

FIG. 22 (color online). Prediction of the light hadron spectrum in full $N_f = 2 + 1$ QCD according to Durr *et al.* (2008). Open circles are input quantities while filled circles are predictions. Experimental masses of hadrons that are stable in QCD are given with a vertical bar while for resonant states the box indicates the decay width. Experimental numbers are from Amsler *et al.*, 2008.

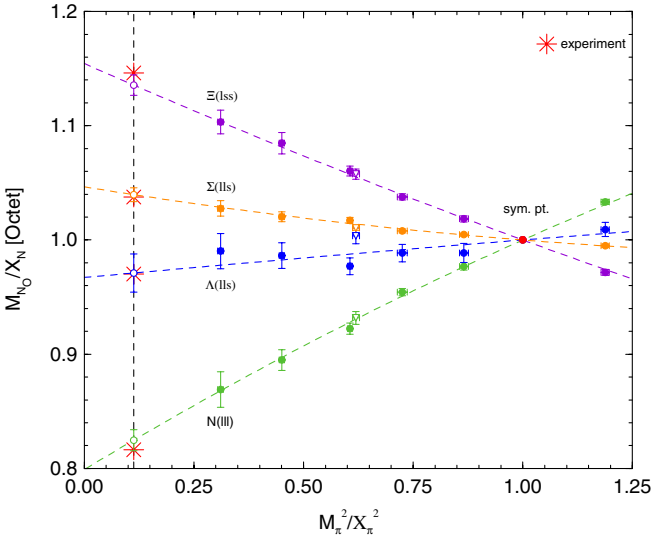

FIG. 23 (color online). Chiral behavior of the ratio of individual octet masses over the average octet mass $X_N = \frac{1}{3}(M_N + M_\Sigma + M_\Xi)$ vs the ratio of the square of the pion mass over the square average of pseudoscalar meson masses $X_\pi^2 = \frac{1}{3}(2M_K^2 + M_\pi^2)$ as obtained by the QCDSF-UKQCD Collaboration. From Bietenholz *et al.*, 2010a, with permission of the QCDSF-UKQCD Collaboration.

the spread of the results of all analyses weighted by the fit quality. The ground state light hadron spectrum was reproduced at the percent level (cf. Fig. 22).

The QCDSF-UKQCD Collaboration recently proposed a different approach to the physical point starting from an SU(3) symmetric theory and systematically expanding in the SU(3) breaking parameter while keeping $2M_K^2 + M_\pi^2$ constant (Bietenholz *et al.*, 2010a, 2010b, 2011). Preliminary results at a single lattice spacing of $a \sim 0.076$ fm and a spatial lattice extent of $L \sim 1.2$–2.5 fm are displayed in Fig. 23. They show a linear dependence of the octet and decuplet masses considered and a good agreement with the experimentally observed hadron spectrum. An $N_f = 2 + 1$ nonperturbatively improved single step stout smeared clover action on a tree level Symanzik improved gauge action was used for this study. Finite size corrections are not yet applied.

There is also an ongoing effort to compute ground state baryons with twisted mass fermions including a dynamical strange quark. As the twisted mass formalism necessitates an even number of fermion flavors (cf. Sec. II.D.3), these calculations also include a charm quark ($N_f = 2 + 1 + 1$). First preliminary results of this effort are reported by Drach *et al.* (2010).

The RBC-UKQCD Collaboration recently performed a pioneering calculation of the η and η' masses using $N_f = 2 + 1$ flavor domain wall ensembles on an Iwasaki gauge action (Christ *et al.*, 2010). Three pion masses in the range 400–700 MeV with a single lattice spacing $a \sim 0.11$ fm on latices with a spatial extent of $L \sim 1.8$ fm were used. A two operator basis with gauge fixed wall sources was used to extract the correlation functions. A mixing angle of $\Theta = -9.2(4.7)°$ and masses $M_\eta = 583(15)$ MeV and $M_{\eta'} = 853(123)$ MeV were found.

The Hadron Spectrum Collaboration used anisotropic lattices in order to obtain a fine time resolution of the propagators. These ensembles are mainly used to extract the highly excited baryon spectrum. The lattice spacing in the time direction is tuned to be smaller by a factor of $\xi \sim 3.5$ than the lattice spacing in the spatial directions (Edwards, Joo, and Lin, 2008). In their excited state spectroscopy studies (Lin *et al.*, 2009; Bulava *et al.*, 2010; Dudek *et al.*, 2011), they employed $N_f = 2 + 1$ anisotropic clover fermions on a tree level tadpole improved Symanzik gauge action. A single spatial lattice spacing $a_s \sim 0.12$ fm and three pion masses in the range 390–530 MeV are used. The scale is set with M_Ω. A variational method based on a large number (6–10) of specifically tailored interpolating operators is used to extract the tower of excited states in the different channels. Results are reported at three different pion masses and show a nice overall qualitative agreement with the experimentally observed excited hadron spectrum (see Fig. 24). They emphasize the need for multihadron interpolating operators in order to reliably identify scattering states. More recently, also the spins of nucleon and Δ excitations up to spin 7/2 were also identified by Edwards *et al.* (2011).

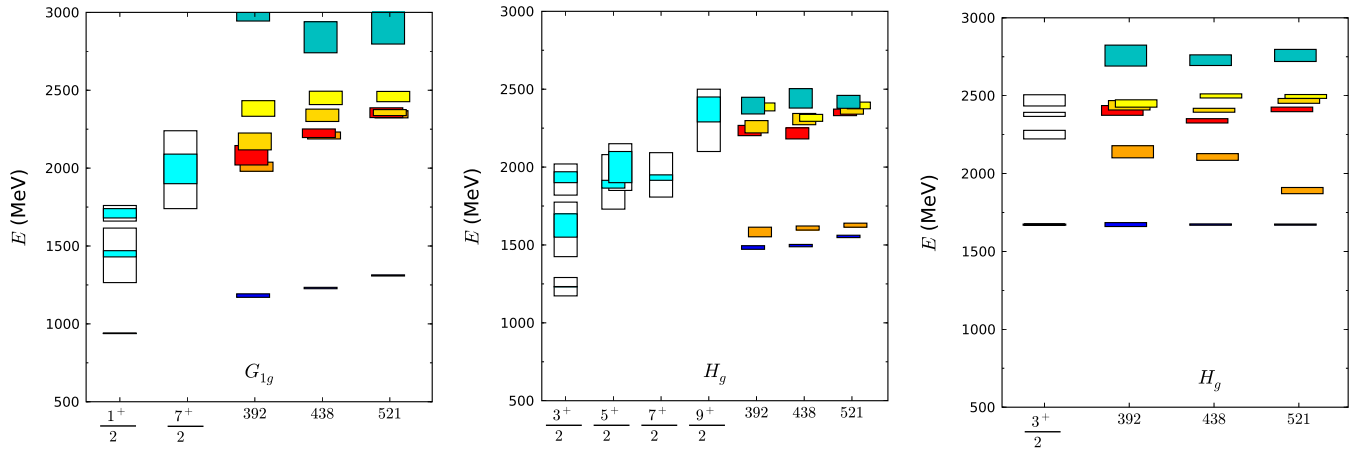

FIG. 24 (color online). Comparison of part of the excited state spectrum of nucleon (left) Δ (middle), and Ω (right) type baryons as computed by the Hadron Spectrum Collaboration at three different pion masses with experiment. More details can be found in the original paper. From Bulava *et al.*, 2010, with permission of the Hadron Spectrum Collaboration.

Ground and excited state meson spectra are also being studied with overlap valence on dynamical domain wall fermions. Some preliminary results can be found in Mathur *et al.* (2010).

The quenched studies of Mahbub *et al.* (2009b, 2010a) and Mahbub, Cais *et al.* (2010a) on the excited baryon spectrum, especially the excited states of the nucleon, were recently extended to $N_f = 2 + 1$ dynamical configurations by Mahbub *et al.*, 2010b; Mahbub *et al.*, 2010c). FLIC valence fermions were used on the PACS-CS dynamical ensembles discussed above. Large operator bases of up to eight were used and signals for up to three excited states were identified. The chiral behavior of both positive and negative nucleon excitations was studied and some evidence was found for the correct ordering of the negative parity ground state and the Roper resonance as one approaches physical pion masses.

VI. CONCLUDING REMARKS

Although it has taken over 30 years from the formulation of QCD as the theory of the strong force and Wilson's lattice regularization, it is fair to say that today we have a firm, quantitative understanding of the most relevant part of its particle content. It has taken so long to reach this level of understanding because low energy QCD is a very rich and nonperturbative theory. The mechanism of permanent quark confinement and the subsequent emergence of a particle spectrum that does not at all reflect the fundamental degrees of freedom required the development of an entirely new set of techniques that have now matured to a point where the experimentally observed spectrum of ground state, light nonsinglet hadrons can be reproduced to an accuracy of a few percent.

This quantitative understanding was gained in a process that spanned several decades. Although the fundamental theory and the general strategy toward its nonperturbative first-principles solution was clear from the beginning, it required a substantial amount of conceptual development and physical insight.

It is however still not a trivial task today to obtain a precise prediction with fully controlled uncertainties from QCD in the regime where it is a strongly coupled gauge theory. One needs to be careful of optimizing all aspects of the calculation to such a degree that no single one of them fully dominates the total error, while at the same time keeping the formalism simple and transparent enough that computations are manageable in a reasonable amount of time. While ground state nonsinglet hadron masses can be computed to a few percent accuracy today, reaching the same level of precision for excited states or singlet hadrons is still a challenging task. There has been substantial progress regarding the extraction of excited states and disconnected diagram contributions and the current understanding is approaching the precision level. A detailed treatment of resonant finite-volume effects, the continuum extrapolation, and even reaching the physical point is work currently in progress.

Lattice calculations of the ground state, nonsinglet hadron masses are currently trying to enter the subpercent level precision region. In order to reach this goal, the next challenges involve a first-principles treatment of electromagnetic and isospin breaking effects as well as an improved treatment of finite-volume effects in the case of resonant states.

In spite of these many open questions and future challenges, we believe, however, that the percent level understanding of relevant parts of the light hadron spectrum with fully controlled systematic uncertainties that has been achieved by lattice QCD is a milestone that marks the overall maturity of the method. While many interesting problems such as excited state spectroscopy still require substantial work, lattice QCD today represents a reliable tool of extracting from first-principles properties of a strongly coupled quantum field theory.

ACKNOWLEDGMENTS

We thank Stephan Dürr, Stefan Krieg, Thorsten Kurth, Laurent Lellouch, Alberto Ramos, Kalman Szabó, Balint Toth, and especially Craig McNeile for discussions and comments on the manuscript. This work was in part funded by the "Deutsche Forschungsgemeinschaft" under the Grant No. SFB-TR55.

REFERENCES

Adams, D. H., 2005, Phys. Rev. D **72**, 114512.
Adams, D. H., 2011, Phys. Lett. B **699**, 394.
Adler, S. L., 1969, Phys. Rev. **177**, 2426.
Adler, S. L., 1981, Phys. Rev. D **23**, 2901.
Adler, S. L., 1988, Phys. Rev. D **37**, 458.
Albanese, M., *et al.* (APE Collaboration), 1987, Phys. Lett. B **192**, 163.
Alexandrou, C., D. Christaras, A. O'Cais, and A. Strelchenko, 2010, Proc. Sci., LATTICE2010, 035.
Alexandrou, C., *et al.* (ETM Collaboration), 2008, Phys. Rev. D **78**, 014509.
Alexandrou, C., *et al.* (ETM Collaboration), 2009, Phys. Rev. D **80**, 114503.
Alford, M. G., I. T. Drummond, R. R. Horgan, H. Shanahan, and M. J. Peardon, 2001, Phys. Rev. D **63**, 074501.
Alford, M. G., T. R. Klassen, and G. P. Lepage, 1997, Nucl. Phys. **B496**, 377.
Ali Khan, A., *et al.* (CP-PACS Collaboration), 2002, Phys. Rev. D **65**, 054505.
Allton, C. R., *et al.* (UKQCD Collaboration), 1992, Phys. Lett. B **284**, 377.
Allton, C. R., *et al.* (UKQCD Collaboration), 1993, Phys. Rev. D **47**, 5128.
Allton, C. R., *et al.* (UKQCD Collaboration), 1994, Phys. Rev. D **49**, 474.
Allton, C. R., *et al.* (UKQCD Collaboration), 1999, Phys. Rev. D **60**, 034507.
Allton, C. R., *et al.* (UKQCD Collaboration), 2002, Phys. Rev. D **65**, 054502.
Allton, C. R., *et al.* (UKQCD Collaboration), 2004, Phys. Rev. D **70**, 014501.
Altmeyer, R., *et al.* (MT(c) Collaboration), 1993, Nucl. Phys. **B389**, 445.
Amsler, C., *et al.* (Particle Data Group), 2008, Phys. Lett. B **667**, 1.
Anisovich, A. V., and H. Leutwyler, 1996, Phys. Lett. B **375**, 335.
Anthony, S. J., C. H. Llewellyn Smith, and J. F. Wheater, 1982, Phys. Lett. **116B**, 287.

Antonio, D. J., *et al.* (RBC Collaboration), 2008, Phys. Rev. D **77**, 014509.
Aoki, S., 1984, Phys. Rev. D **30**, 2653.
Aoki, S., and O. Bar, 2004, Phys. Rev. D **70**, 116011.
Aoki, S., H. Fukaya, S. Hashimoto, and T. Onogi, 2007, Phys. Rev. D **76**, 054508.
Aoki, S., T. Kaneda, and A. Ukawa, 1997, Phys. Rev. D **56**, 1808.
Aoki, S., *et al.*, 1994, Phys. Rev. D **50**, 486.
Aoki, S., *et al.* (CP-PACS Collaboration), 2000, Phys. Rev. Lett. **84**, 238.
Aoki, S., *et al.* (CP-PACS Collaboration), 2003a, Phys. Rev. D **67**, 034503.
Aoki, S., *et al.* (JLQCD Collaboration), 2003b, Phys. Rev. D **68**, 054502.
Aoki, S., *et al.* (PACS-CS Collaboration), 2009, Phys. Rev. D **79**, 034503.
Aoki, S., *et al.* (PACS-CS Collaboration), 2010, Phys. Rev. D **81**, 074503.
Aoki, Y., *et al.*, 2009, J. High Energy Phys. 06, 088.
Aoki, Y., *et al.* (RBC Collaboration and UKQCD Collaboration), 2011, Phys. Rev. D **83**, 074508.
Arnold, G., B. Bunk, T. Lippert, and K. Schilling, 2003, Nucl. Phys. B, Proc. Suppl. **119**, 864.
Atiyah, M. F., and I. M. Singer, 1968, Ann. Math. **87**, 546.
Aubin, C., *et al.* (MILC Collaboration), 2004, Phys. Rev. D **70**, 114501.
Babich, R., *et al.*, 2006, J. High Energy Phys. 01, 086.
Babich, R., *et al.*, 2007, Phys. Rev. D **76**, 074021.
Bacilieri, P., *et al.*, 1988, Phys. Lett. B **214**, 115.
Bacilieri, P., *et al.*, 1990, Nucl. Phys. **B343**, 228.
Bacilieri, P., *et al.* (Ape Collaboration), 1989, Nucl. Phys. **B317**, 509.
Bailey, J. A., 2007, Phys. Rev. D **75**, 114505.
Bailey, J. A., 2008, Phys. Rev. D **77**, 054504.
Bali, G. S., S. Collins, and A. Schafer, 2010, Comput. Phys. Commun. **181**, 1570.
Bali, G. S., H. Neff, T. Duessel, T. Lippert, and K. Schilling (SESAM Collaboration), 2005, Phys. Rev. D **71**, 114513.
Bali, G. S., and K. Schilling, 1993a, Phys. Rev. D **47**, 661.
Bali, G. S., and K. Schilling, 1993b, Nucl. Phys. B, Proc. Suppl. **30**, 513.
Banks, T., L. Susskind, and J. B. Kogut, 1976, Phys. Rev. D **13**, 1043.
Bar, O., 2010, Phys. Rev. D **82**, 094505.
Bardeen, W. A., A. Duncan, E. Eichten, G. Hockney, and H. Thacker, 1998, Phys. Rev. D **57**, 1633.
Baron, R., *et al.*, 2010, J. High Energy Phys. 06, 111.
Baron, R., *et al.*, 2010a, Proc. Sci., LAT2010, 123.
Baron, R., *et al.* (ETM), 2010b, J. High Energy Phys. 08, 097.
Basak, S., *et al.*, 2005a, Phys. Rev. D **72**, 094506.
Basak, S., *et al.*, 2006, Nucl. Phys. B, Proc. Suppl. **153**, 242.
Basak, S., *et al.*, 2007, Phys. Rev. D **76**, 074504.
Basak, S., *et al.* (Lattice Hadron Physics (LHPC) Collaboration), 2005b, Phys. Rev. D **72**, 074501.
Basak, S., *et al.* (MILC Collaboration), 2008, Proc. Sci., LATTICE2008, 127.
Batrouni, G. G., *et al.*, 1985, Phys. Rev. D **32**, 2736.
Bazavov, A., *et al.*, 2010a, Rev. Mod. Phys. **82**, 1349.
Bazavov, A., *et al.* (MILC Collaboration), 2010b, Phys. Rev. D **82**, 074501.
Bazavov, A., *et al.* (MILC Collaboration), 2010c, Phys. Rev. D **81**, 114501.
Beane, S. R., K. Orginos, and M. J. Savage, 2007, Nucl. Phys.**B768**, 38.
Beane, S. R., and M. J. Savage, 2002, Nucl. Phys. **A709**, 319.
Becher, P., and H. Joos, 1982, Z. Phys. C **15**, 343.
Becher, T., and H. Leutwyler, 1999, Eur. Phys. J. C **9**, 643.
Bedaque, P. F., M. I. Buchoff, B. C. Tiburzi, and A. Walker-Loud, 2008, Phys. Lett. B **662**, 449.
Bell, J. S., and R. Jackiw, 1969, Nuovo Cimento A **60**, 47.
Benmerrouche, M., R. M. Davidson, and N. C. Mukhopadhyay, 1989, Phys. Rev. C **39**, 2339.
Berg, B., and D. Forster, 1981, Phys. Lett. **106B**, 323.
Bernard, C., 2005, Phys. Rev. D **71**, 094020.
Bernard, C., 2006, Phys. Rev. D **73**, 114503.
Bernard, C., C. E. DeTar, Z. Fu, and S. Prelovsek, 2007, Phys. Rev. D **76**, 094504.
Bernard, C., M. Golterman, and Y. Shamir, 2006, Phys. Rev. D **73**, 114511.
Bernard, C., M. Golterman, and Y. Shamir, 2008, Phys. Rev. D **77**, 074505.
Bernard, C., M. Golterman, Y. Shamir, and S. R. Sharpe, 2007, Phys. Lett. B **649**, 235.
Bernard, C. W., T. Draper, and K. Olynyk, 1983, Phys. Rev. D **27**, 227.
Bernard, C. W., *et al.*, 2001, Phys. Rev. D **64**, 054506.
Bernard, C. W., *et al.* (MILC Collaboration), 1998a, Phys. Rev. Lett. **81**, 3087.
Bernard, C. W., *et al.* (MILC Collaboration), 1998b, Phys. Rev. D **58**, 014503.
Bernard, V., N. Kaiser, J. Kambor, and U. G. Meissner, 1992, Nucl. Phys. **B388**, 315.
Bernard, V., M. Lage, U. G. Meissner, and A. Rusetsky, 2011, J. High Energy Phys. 01, 019.
Bernard, V., M. Lage, U.-G. Meissner, and A. Rusetsky, 2008, J. High Energy Phys. 08, 024.
Bernardson, S., P. McCarty, and C. Thron, 1994, Comput. Phys. Commun. **78**, 256.
Bhattacharya, T., R. Gupta, G. Kilcup, and S. R. Sharpe, 1996, Phys. Rev. D **53**, 6486.
Bietenholz, W., 1999, arXiv:hep-lat/9901005.
Bietenholz, W., 2008, Fortschr. Phys. **56**, 107.
Bietenholz, W., and U. Wiese, 1996, Nucl. Phys. **B464**, 319.
Bietenholz, W., *et al.*, 2010a, Proc. Sci., LATTICE2010, 122.
Bietenholz, W., *et al.*, 2010b, Phys. Lett. B **690**, 436.
Bietenholz, W., *et al.*, 2011, Phys. Rev. D **84**, 054509.
Bijnens, J., and K. Ghorbani, 2007, J. High Energy Phys. 11, 030.
Bijnens, J., and J. Prades, 1997, Nucl. Phys. **B490**, 239.
Billoire, A., and E. Marinari, 1987, Phys. Lett. B **184**, 381.
Billoire, A., E. Marinari, A. Morel, and J. P. Rodrigues, 1984, Phys. Lett. **148B**, 166.
Billoire, A., E. Marinari, and R. Petronzio, 1985, Nucl. Phys. **B251**, 141.
Bitar, K., A. D. Kennedy, R. Horsley, S. Meyer, and P. Rossi, 1989, Nucl. Phys. **B313**, 348.
Bitar, K. M., *et al.*, 1990a, Phys. Rev. D **42**, 3794.
Bitar, K. M., *et al.*, 1990b, Phys. Rev. Lett. **65**, 2106.
Bitar, K. M., *et al.*, 1992, Phys. Rev. D **46**, 2169.
Bitar, K. M., *et al.*, 1994, Phys. Rev. D **49**, 3546.
Blossier, B., M. Della Morte, G. von Hippel, T. Mendes, and R. Sommer, 2009a, J. High Energy Phys. 04, 094.
Blossier, B., *et al.* (ETM Collaboration), 2009b, J. High Energy Phys. 07, 043.
Blum, T., T. Doi, M. Hayakawa, T. Izubuchi, and N. Yamada, 2007, Phys. Rev. D **76**, 114508.
Blum, T., and A. Soni, 1997, Phys. Rev. D **56**, 174.
Blum, T., *et al.*, 1997, Phys. Rev. D **55**, R1133.
Blum, T., *et al.*, 2010, Phys. Rev. D **82**, 094508.

Bode, A., *et al.* (ALPHA Collaboration), 2001, Phys. Lett. B **515**, 49.
Borici, A., 2008, Phys. Rev. D **78**, 074504.
Borsanyi, S., *et al.* (Wuppertal-Budapest Collaboration), 2010, J. High Energy Phys. 09, 073.
Boucaud, P., *et al.* (ETM Collaboration), 2008, Comput. Phys. Commun. **179**, 695.
Bowler, K. C., G. S. Pawley, D. J. Wallace, E. Marinari, and F. Rapuano, 1983, Nucl. Phys. **B220**, 137.
Bowler, K. C., *et al.*, 1984, Nucl. Phys. **B240**, 213.
Bowler, K. C., *et al.*, 1985, Phys. Lett. **162B**, 354.
Bowler, K. C., *et al.*, 1986, Phys. Lett. B **179**, 375
Bowler, K. C., *et al.* (UKQCD Collaboration), 2000, Phys. Rev. D **62**, 054506.
Brandt, B. B., *et al.*, 2010, Proc. Sci., LATTICE2010, 164.
Brommel, D., *et al.* (Bern-Graz-Regensburg Collaboration), 2004, Phys. Rev. D **69**, 094513.
Brower, R., S. Chandrasekharan, J. W. Negele, and U. J. Wiese, 2003, Phys. Lett. B **560**, 64.
Brown, F. R., and T. J. Woch, 1987, Phys. Rev. Lett. **58**, 2394.
Brown, F. R., *et al.*, 1991, Phys. Rev. Lett. **67**, 1062.
Brueckner, K. A., 1952, Phys. Rev. **86**, 106.
Bulava, J., *et al.*, 2010, Phys. Rev. D **82**, 014507.
Burch, T., *et al.*, 2006a, Phys. Rev. D **74**, 014504.
Burch, T., *et al.*, 2006b, Phys. Rev. D **73**, 094505.
Burch, T., *et al.* (Bern-Graz-Regensburg Collaboration), 2004, Phys. Rev. D **70**, 054502.
Burgers, G., F. Karsch, A. Nakamura, and I. Stamatescu, 1988, Nucl. Phys. **B304**, 587.
Butler, F., H. Chen, J. Sexton, A. Vaccarino, and D. Weingarten, 1993, Phys. Rev. Lett. **70**, 2849.
Butler, F., H. Chen, J. Sexton, A. Vaccarino, and D. Weingarten, 1994, Nucl. Phys. **B430**, 179.
Cabasino, S., *et al.* (Ape Collaboration), 1991a, Phys. Lett. B **258**, 195.
Cabasino, S. *et al.* (APE Collaboration), 1991b, Phys. Lett. B **258**, 202.
Callan, J., Curtis, G., and J. A. Harvey, 1985, Nucl. Phys. **B250**, 427.
Callaway, D. J. E., and A. Rahman, 1982, Phys. Rev. Lett. **49**, 613.
Callaway, D. J. E., and A. Rahman, 1983, Phys. Rev. D **28**, 1506.
Campostrini, M., K. J. M. Moriarty, J. Potvin, and C. Rebbi, 1987, Phys. Lett. B **193**, 78.
Capitani, S., 2003, Phys. Rep. **382**, 113.
Capitani, S., M. Creutz, J. Weber, and H. Wittig, 2010, J. High Energy Phys. 09, 027.
Capitani, S., S. Durr, and C. Hoelbling, 2006, J. High Energy Phys. 11, 028.
Chadwick, J., 1932, Nature (London) **129**, 312.
Chen, J.-W., and M. J. Savage, 2002, Phys. Rev. D **65**, 094001.
Chen, P., 2001, Phys. Rev. D **64**, 034509.
Chiarappa, T., *et al.*, 2007, Eur. Phys. J. C **50**, 373.
Chodos, A., and J. B. Healy, 1977, Phys. Rev. D **16**, 387.
Christ, N. H., *et al.*, 2010, Phys. Rev. Lett. **105**, 241601.
Chung, Y., H. G. Dosch, M. Kremer, and D. Schall, 1982, Nucl. Phys. **B197**, 55.
Clark, M. A., and A. D. Kennedy, 2004, Nucl. Phys. B, Proc. Suppl. **129–130**, 850.
Clark, M. A., A. D. Kennedy, and Z. Sroczynski, 2005, Nucl. Phys. B, Proc. Suppl. **140**, 835.
Colangelo, G., and S. Durr, 2004, Eur. Phys. J. C **33**, 543.
Colangelo, G., S. Durr, and C. Haefeli, 2005, Nucl. Phys. **B721**, 136.
Colangelo, G., A. Fuhrer, and S. Lanz, 2010, Phys. Rev. D **82**, 034506.
Colangelo, G., S. Lanz, and E. Passemar, 2009, Proc. Sci., CD09, 047.
Colangelo, G., *et al.*, 2011, Eur. Phys. J. C **71**, 1695.
Collins, S., R. G. Edwards, U. M. Heller, and J. H. Sloan, 1997, Nucl. Phys. B, Proc. Suppl. **53**, 877.
Creutz, M., 1980a, Phys. Rev. Lett. **45**, 313.
Creutz, M., 1980b, Phys. Rev. D **21**, 2308.
Creutz, M., 1984, *Quarks, Gluons and Lattices* (Cambridge University Press, Cambridge, England).
Creutz, M., 1987, Phys. Rev. D **36**, 515.
Creutz, M., 2007a, Phys. Lett. B **649**, 241.
Creutz, M., 2007b, Phys. Lett. B **649**, 230.
Creutz, M., 2008, J. High Energy Phys. 04, 017.
Creutz, M., L. Jacobs, and C. Rebbi, 1979a, Phys. Rev. Lett. **42**, 1390.
Creutz, M., L. Jacobs, and C. Rebbi, 1979b, Phys. Rev. D **20**, 1915.
Creutz, M., L. Jacobs, and C. Rebbi, 1983, Phys. Rep. **95**, 201.
Csikor, F., Z. Fodor, and J. Heitger, 1998, Phys. Rev. D **58**, 094504.
Csikor, F., Z. Fodor, S. D. Katz, and T. G. Kovacs, 2003, J. High Energy Phys. 11, 070.
Csikor, F., *et al.*, 2004, J. High Energy Phys. 05, 046.
Cundy, N., *et al.*, 2009, Comput. Phys. Commun. **180**, 26.
Curci, G., P. Menotti, and G. Paffuti, 1983, Phys. Lett. **130B**, 205.
Daniel, D., R. Gupta, G. W. Kilcup, A. Patel, and S. R. Sharpe, 1992, Phys. Rev. D **46**, 3130.
Daniel, D., and T. D. Kieu, 1986, Phys. Lett. B **175**, 73.
Darnell, D., R. B. Morgan, and W. Wilcox, 2008, Linear Algebra Appl. **429**, 2415.
Das, T., G. S. Guralnik, V. S. Mathur, F. E. Low, and J. E. Young, 1967, Phys. Rev. Lett. **18**, 759.
Dashen, R. F., 1969, Phys. Rev. **183**, 1245.
Davies, C. T. H., E. Follana, I. D. Kendall, G. P. Lepage, and C. McNeile (HPQCD Collaboration), 2010, Phys. Rev. D **81**, 034506.
Davies, C. T. H., G. P. Lepage, F. Niedermayer, and D. Toussaint, 2005, Nucl. Phys. B, Proc. Suppl. **140**, 261.
Davies, C. T. H., *et al.* (HPQCD Collaboration), 2004, Phys. Rev. Lett. **92**, 022001.
de Divitiis, G. M., R. Frezzotti, M. Masetti, and R. Petronzio, 1996, Phys. Lett. B **382**, 393.
de Forcrand, P., 1996, Nucl. Phys. B, Proc. Suppl. **47**, 228.
de Forcrand, P., A. Kurkela, and M. Panero, 2010, Proc. Sci., LATTICE2010, 080.
de Forcrand, P., and T. Takaishi, 1997, Nucl. Phys. B, Proc. Suppl. **53**, 968.
de Forcrand, P., *et al.* (QCD-TARO Collaboration), 2000, Nucl. Phys. **B577**, 263.
DeGrand, T., and C. E. Detar, 2006, *Lattice Methods for Quantum Chromodynamics* (World Scientific, Singapore).
DeGrand, T. A., A. Hasenfratz, P. Hasenfratz, and F. Niedermayer, 1995, Nucl. Phys. **B454**, 587.
DeGrand, T. A., A. Hasenfratz, and T. G. Kovacs, 1999, Nucl. Phys. **B547**, 259.
DeGrand, T. A., A. Hasenfratz, and T. G. Kovacs, 2003, Phys. Rev. D **67**, 054501.
DeGrand, T. A., A. Hasenfratz, and T. G. Kovacs (MILC Collaboration), 1998, arXiv:hep-lat/9807002.
DeGrand, T. A., and U. M. Heller (MILC Collaboration), 2002, Phys. Rev. D **65**, 114501.
DeGrand, T. A., and R. D. Loft, 1991, Comput. Phys. Commun. **65**, 84.
DeGrand, T. A. (MILC Collaboration), 1998, Phys. Rev. D **58**, 094503.
DeGrand, T. A., and S. Schaefer, 2004, Comput. Phys. Commun. **159**, 185.

Del Debbio, L., L. Giusti, M. Luscher, R. Petronzio, and N. Tantalo, 2007a, J. High Energy Phys. 02, 056.
Del Debbio, L., L. Giusti, M. Luscher, R. Petronzio, and N. Tantalo, 2007b, J. High Energy Phys. 02, 082.
Del Debbio, L., H. Panagopoulos, and E. Vicari, 2002, J. High Energy Phys. 08, 044.
Della Morte, M., and A. Juttner, 2010, J. High Energy Phys. 11, 154.
Della Morte, M., *et al.* (ALPHA Collaboration), 2003, Nucl. Phys. B, Proc. Suppl. **119**, 439.
Detar, C. E., and J. B. Kogut, 1987a, Phys. Rev. D **36**, 2828.
Detar, C. E., and J. B. Kogut, 1987b, Phys. Rev. Lett. **59**, 399.
Di Pierro, M., 2000, arXiv:hep-lat/0009001.
Dirac, P. A. M., 1933, Phys. Z. Sowjetunion **3**, 64 [http://inspirehep.net/record/44918?ln=en].
Ditsche, C., B. Kubis, and U.-G. Meissner, 2009, Eur. Phys. J. C **60**, 83.
Dong, S.-J., and K.-F. Liu, 1994, Phys. Lett. B **328**, 130.
Donoghue, J. F., and A. F. Perez, 1997, Phys. Rev. D **55**, 7075.
Dorati, M., T. A. Gail, and T. R. Hemmert, 2008, Nucl. Phys. **A798**, 96.
Drach, V., K. Jansen, J. Carbonell, M. Papinutto, and C. Alexandrou, 2010, Proc. Sci., LATTICE2010, 101.
Draper, T., and C. McNeile, 1994, Nucl. Phys. B, Proc. Suppl. **34**, 453.
Draper, T., C. McNeile, and C. Nenkov, 1995, Nucl. Phys. B, Proc. Suppl. **42**, 325.
Drell, S. D., M. Weinstein, and S. Yankielowicz, 1976, Phys. Rev. D **14**, 1627.
Duane, S., 1985, Nucl. Phys. **B257**, 652.
Duane, S., A. D. Kennedy, B. J. Pendleton, and D. Roweth, 1987, Phys. Lett. B **195**, 216.
Duane, S., and J. B. Kogut, 1985, Phys. Rev. Lett. **55**, 2774.
Duane, S., and J. B. Kogut, 1986, Nucl. Phys. **B275**, 398.
Dudek, J. J., *et al.*, 2011, Phys. Rev. D **83**, 111502.
Duffy, W., G. Guralnik, and D. Weingarten, 1983, Phys. Lett. **125B**, 311.
Duncan, A., and E. Eichten, 2002, Phys. Rev. D **65**, 114502.
Duncan, A., E. Eichten, and H. Thacker, 1996, Phys. Rev. Lett. **76**, 3894.
Durr, S., 2006, Proc. Sci., LAT2005, 021.
Durr, S., Z. Fodor, C. Hoelbling, and T. Kurth, 2007, J. High Energy Phys. 04, 055.
Durr, S., and C. Hoelbling, 2004, Phys. Rev. D **69**, 034503.
Durr, S., and C. Hoelbling, 2005a, Phys. Rev. D **72**, 071501.
Durr, S., and C. Hoelbling, 2005b, Phys. Rev. D **71**, 054501.
Durr, S., and C. Hoelbling, 2006, Phys. Rev. D **74**, 014513.
Durr, S., C. Hoelbling, and U. Wenger, 2004, Phys. Rev. D **70**, 094502.
Durr, S., C. Hoelbling, and U. Wenger, 2005, J. High Energy Phys. 09, 030.
Durr, S., and G. Koutsou, 2011, Phys. Rev. D **83**, 114512.
Durr, S., *et al.*, 2010, Proc. Sci., LATTICE2010, 102.
Durr, S., *et al.*, 2011, Phys. Lett. B **701**, 265.
Durr, S., *et al.*, 2012, Phys. Rev. D **85**, 014509.
Durr, S., *et al.* (Budapest-Marseille-Wuppertal Collaboration), 2008, Science **322**, 1224.
Durr, S., *et al.* (Budapest-Marseille-Wuppertal Collaboration), 2009, Phys. Rev. D **79**, 014501.
Durr, S., *et al.* (Budapest-Marseille-Wuppertal Collaboration), 2011c, J. High Energy Phys. 08, 148.
Edwards, R. G., J. J. Dudek, D. G. Richards, and S. J. Wallace, 2011, Phys. Rev. D **84**, 074508.
Edwards, R. G., U. M. Heller, and T. R. Klassen, 1998, Phys. Rev. Lett. **80**, 3448.
Edwards, R. G., U. M. Heller, and R. Narayanan, 1999, Nucl. Phys. **B540**, 457.
Edwards, R. G., B. Joo, and H.-W. Lin, 2008, Phys. Rev. D **78**, 054501.
Egri, G. I., 2006, Proc. Sci., LAT2005, 290.
Eicker, N., *et al.* (TXL Collaboration), 1996, Phys. Lett. B **389**, 720.
Eicker, N., *et al.* (TXL Collaboration), 1998, Phys. Rev. D **59**, 014509.
El-Khadra, A. X., G. Hockney, A. S. Kronfeld, and P. B. Mackenzie, 1992, Phys. Rev. Lett. **69**, 729.
Engel, G. P., C. B. Lang, M. Limmer, D. Mohler, and A. Schafer (BGR (Bern-Graz-Regensburg) Collaboration), 2010, Phys. Rev. D **82**, 034505.
Engels, J., F. Karsch, and T. Scheideler, 2000, Nucl. Phys. **B564**, 303.
Espriu, D., and L. Tagliacozzo, 2003, Phys. Lett. B **557**, 125.
Farchioni, F., *et al.*, 2005a, Eur. Phys. J. C **42**, 73.
Farchioni, F., *et al.*, 2005b, Eur. Phys. J. C **39**, 421.
Ferrenberg, A. M., and R. H. Swendsen, 1988, Phys. Rev. Lett. **61**, 2635.
Ferrenberg, A. M., and R. H. Swendsen, 1989, Phys. Rev. Lett. **63**, 1195.
Feynman, R. P., 1948a, Phys. Rev. **74**, 939.
Feynman, R. P., 1948b, Rev. Mod. Phys. **20**, 367.
Feynman, R. P., 1949, Phys. Rev. **76**, 769.
Feynman, R. P., and A. R. Hibbs, 1965, *Quantum Mechanics and Path Integrals* (McGraw-Hill, New York).
Fleming, G. T., S. D. Cohen, H.-W. Lin, and V. Pereyra, 2009, Phys. Rev. D **80**, 074506.
Fodor, Z., and K. Jansen, 1994, Phys. Lett. B **331**, 119.
Fodor, Z., S. D. Katz, and K. K. Szabo, 2004, J. High Energy Phys. 08, 003.
Fodor, Z., K. K. Szabo, and B. C. Toth, 2007, J. High Energy Phys. 08, 092.
Foley, J., *et al.*, 2005, Comput. Phys. Commun. **172**, 145.
Follana, E., C. T. H. Davies, G. P. Lepage, and J. Shigemitsu (HPQCD Collaboration), 2008, Phys. Rev. Lett. **100**, 062002.
Follana, E., *et al.* (HPQCD Collaboration), 2007, Phys. Rev. D **75**, 054502.
Frezzotti, R., P. A. Grassi, S. Sint, and P. Weisz (Alpha Collaboration), 2001, J. High Energy Phys. 08, 058.
Frezzotti, R., and K. Jansen, 1997, Phys. Lett. B **402**, 328.
Frezzotti, R., and G. C. Rossi, 2004a, J. High Energy Phys. 08, 007.
Frezzotti, R., and G. C. Rossi, 2004b, Nucl. Phys. B, Proc. Suppl. **128**, 193.
Fritzsch, H., M. Gell-Mann, and H. Leutwyler, 1973, Phys. Lett. **47B**, 365.
Frolov, S. A., and A. A. Slavnov, 1993, Phys. Lett. B **309**, 344.
Frommer, A., B. Nockel, S. Gusken, T. Lippert, and K. Schilling, 1995, Int. J. Mod. Phys. C **6**, 627.
Fucito, F., E. Marinari, G. Parisi, and C. Rebbi, 1981, Nucl. Phys. **B180**, 369.
Fucito, F., K. J. M. Moriarty, C. Rebbi, and S. Solomon, 1986, Phys. Lett. B **172**, 235.
Fucito, F., *et al.*, 1982, Nucl. Phys. **B210**, 407.
Fukaya, H., *et al.* (JLQCD Collaboration), 2006, Phys. Rev. D **74**, 094505.
Fukugita, M., 1988, Nucl. Phys. B, Proc. Suppl., **4**, 105.
Fukugita, M., N. Ishizuka, H. Mino, M. Okawa, and A. Ukawa, 1993, Phys. Rev. D **47**, 4739.
Fukugita, M., T. Kaneko, and A. Ukawa, 1984, Nucl. Phys. **B230**, 62.
Fukugita, M., H. Mino, M. Okawa, G. Parisi, and A. Ukawa, 1992, Phys. Lett. B **294**, 380.

Fukugita, M., S. Ohta, Y. Oyanagi, and A. Ukawa, 1987, Phys. Lett. B **191**, 164.
Fukugita, M., Y. Oyanagi, and A. Ukawa, 1986, Phys. Rev. Lett. **57**, 953.
Fukugita, M., Y. Oyanagi, and A. Ukawa, 1987, Phys. Rev. D **36**, 824.
Fukugita, M., Y. Oyanagi, and A. Ukawa, 1988, Phys. Lett. B **203**, 145.
Galletly, D., *et al.*, 2007, Phys. Rev. D **75**, 073015.
Garden, J., J. Heitger, R. Sommer, and H. Wittig (ALPHA Collaboration), 2000, Nucl. Phys. **B571**, 237.
Gasser, J., and H. Leutwyler, 1982, Phys. Rep. **87**, 77.
Gasser, J., and H. Leutwyler, 1984, Ann. Phys. (N.Y.) **158**, 142.
Gasser, J., and H. Leutwyler, 1985, Nucl. Phys. **B250**, 465.
Gasser, J., and H. Leutwyler, 1987a, Phys. Lett. B **184**, 83.
Gasser, J., and H. Leutwyler, 1987b, Phys. Lett. B **188**, 477.
Gasser, J., and H. Leutwyler, 1988, Nucl. Phys. **B307**, 763.
Gasser, J., M. E. Sainio, and A. Svarc, 1988, Nucl. Phys. **B307**, 779.
Gattringer, C., 2001, Phys. Rev. D **63**, 114501.
Gattringer, C., and I. Hip, 1998, Nucl. Phys. **B536**, 363.
Gattringer, C., and C. B. Lang, 2010, *Quantum Chromodynamics on the Lattice* (Springer, Berlin).
Gattringer, C., and S. Solbrig, 2005, Phys. Lett. B **621**, 195.
Gattringer, C., *et al.* (BGR Collaboration), 2004, Nucl. Phys. **B677**, 3.
Gell-Mann, M., 1961, Report No. cTSL-20.
Gell-Mann, M., R. J. Oakes, and B. Renner, 1968, Phys. Rev. **175**, 2195.
Giedt, J., 2007, Nucl. Phys. **B782**, 134.
Gilchrist, J. P., G. Schierholz, H. Schneider, and M. Teper, 1984, Nucl. Phys. **B248**, 29.
Ginsparg, P. H., and K. G. Wilson, 1982, Phys. Rev. D **25**, 2649.
Giudice, P., D. McManus, and M. Peardon, 2010, Proc. Sci., LATTICE2010, 105.
Giusti, L., P. Hernandez, M. Laine, P. Weisz, and H. Wittig, 2004, J. High Energy Phys. 04, 013.
Giusti, L., C. Hoelbling, M. Luscher, and H. Wittig, 2003, Comput. Phys. Commun. **153**, 31.
Giusti, L., C. Hoelbling, and C. Rebbi, 2001, Phys. Rev. D **64**, 114508.
Glassner, U., *et al.*, 1996, arXiv:hep-lat/9605008.
Gliozzi, F., 1982, Nucl. Phys. **B204**, 419.
Gockeler, M., 1984, Phys. Lett. **142B**, 197.
Gockeler, M., *et al.*, 1997, Phys. Lett. B **391**, 388.
Gockeler, M., *et al.*, 1998a, Nucl. Phys. B, Proc. Suppl. **63**, 694.
Gockeler, M., *et al.*, 1998b, Phys. Rev. D **57**, 5562.
Gockeler, M., *et al.* (QCDSF Collaboration), 2002, Phys. Lett. B **532**, 63.
Goldstein, E., 1886, Berlin Akd. Monatsber. **2**, 691.
Golterman, M., and Y. Shamir, 2003, Phys. Rev. D **68**, 074501.
Golterman, M. F. L., 1986, Nucl. Phys. **B273**, 663.
Golterman, M. F. L., and J. Smit, 1984a, Phys. Lett. **140B**, 392.
Golterman, M. F. L., and J. Smit, 1984b, Nucl. Phys. **B245**, 61.
Golterman, M. F. L., and J. Smit, 1985, Nucl. Phys. **B255**, 328.
Gottlieb, S. A., 1997, Nucl. Phys. B, Proc. Suppl. **53**, 155.
Gottlieb, S. A., W. Liu, D. Toussaint, R. L. Renken, and R. L. Sugar, 1987a, Phys. Rev. Lett. **59**, 1513.
Gottlieb, S. A., W. Liu, D. Toussaint, R. L. Renken, and R. L. Sugar, 1987b, Phys. Rev. D **35**, 2531.
Grady, M. P., D. K. Sinclair, and J. B. Kogut, 1988, Phys. Lett. B **200**, 149.
Gross, D. J., and F. Wilczek, 1973, Phys. Rev. Lett. **30**, 1343.
Gross, M., G. P. Lepage, and P. E. L. Rakow, 1987, Phys. Lett. B **197**, 183.
Guagnelli, M., M. P. Lombardo, E. Marinari, G. Parisi, and G. Salina, 1992, Nucl. Phys. **B378**, 616.
Gupta, R., 1997, arXiv:hep-lat/9807028.
Gupta, R., G. Guralnik, G. W. Kilcup, and S. R. Sharpe, 1991, Phys. Rev. D **43**, 2003.
Gupta, R., G. W. Kilcup, A. Patel, and S. R. Sharpe, 1988, Phys. Lett. B **211**, 132.
Gupta, R., and A. Patel, 1983, Phys. Lett. **124B**, 94.
Gupta, R., *et al.*, 1987, Phys. Rev. D **36**, 2813.
Gupta, R., *et al.*, 1991, Phys. Rev. D **44**, 3272.
Gusken, S., 1990, Nucl. Phys. B, Proc. Suppl. **17**, 361.
Gutbrod, F., P. Hasenfratz, Z. Kunszt, and I. Montvay, 1983, Phys. Lett. **128B**, 415.
Hamber, H., and G. Parisi, 1981, Phys. Rev. Lett. **47**, 1792.
Hamber, H., and G. Parisi, 1983, Phys. Rev. D **27**, 208.
Hamber, H. W., 1987, Phys. Lett. B **193**, 292.
Hamber, H. W., and C. M. Wu, 1983, Phys. Lett. **133B**, 351.
Harada, J., A. S. Kronfeld, H. Matsufuru, N. Nakajima, and T. Onogi, 2001, Phys. Rev. D **64**, 074501.
Hart, A., C. McNeile, C. Michael, and J. Pickavance (UKQCD Collaboration), 2006, Phys. Rev. D **74**, 114504.
Hasenbusch, M., 2001, Phys. Lett. B **519**, 177.
Hasenbusch, M., and K. Jansen, 2003, Nucl. Phys. **B659**, 299.
Hasenfratz, A., and P. Hasenfratz, 1985, Annu. Rev. Nucl. Part. Sci. **35**, 559.
Hasenfratz, A., P. Hasenfratz, Z. Kunszt, and C. B. Lang, 1982, Phys. Lett. **117B**, 81.
Hasenfratz, A., and R. Hoffmann, 2006, Phys. Rev. D **74**, 014511.
Hasenfratz, A., R. Hoffmann, and S. Schaefer, 2007, J. High Energy Phys. 05, 029.
Hasenfratz, A., and F. Knechtli, 2001, Phys. Rev. D **64**, 034504.
Hasenfratz, P., V. Laliena, and F. Niedermayer, 1998, Phys. Lett. B **427**, 125.
Hasenfratz, P., and I. Montvay, 1983, Phys. Rev. Lett. **50**, 309.
Hasenfratz, P., and F. Niedermayer, 1994, Nucl. Phys. **B414**, 785.
Heatlie, G., G. Martinelli, C. Pittori, G. C. Rossi, and C. T. Sachrajda, 1991, Nucl. Phys. **B352**, 266.
Hernandez, P., K. Jansen, and M. Luscher, 1999, Nucl. Phys. **B552**, 363.
Hikasa, K., *et al.* (Particle Data Group), 1992, Phys. Rev. D **45**, S1.
Hoelbling, C., 2010, Proc. Sci., LATTICE2010, 011.
Hoelbling, C., 2011, Phys. Lett. B **696**, 422.
Hoffmann, R., A. Hasenfratz, and S. Schaefer, 2007, Proc. Sci., LAT2007, 104.
Horsley, R., H. Perlt, P. E. L. Rakow, G. Schierholz, and A. Schiller, 2008, Phys. Rev. D **78**, 054504.
Horvath, I., 1998, Phys. Rev. Lett. **81**, 4063.
Ilgenfritz, E.-M., W. Kerler, M. Muller-Preussker, A. Sternbeck, and H. Stuben, 2004, Phys. Rev. D **69**, 074511.
Ishikawa, K. I., *et al.* (PACS-CS Collaboration), 2009, Phys. Rev. D **80**, 054502.
Itoh, S., Y. Iwasaki, Y. Oyanagi, and T. Yoshie, 1986, Nucl. Phys. **B274**, 33.
Itoh, S., Y. Iwasaki, and T. Yoshie, 1986, Phys. Lett. **167B**, 443.
Iwasaki, Y., 1983, Report No. UTHEP-118.
Iwasaki, Y., *et al.* (QCDPAX Collaboration), 1996, Phys. Rev. D **53**, 6443.
Izubuchi, T., and C. Dawson (RBC Collaboration), 2002, Nucl. Phys. B, Proc. Suppl. **106–107**, 748.
Jegerlehner, B., 1996, arXiv:hep-lat/9612014.
Jenkins, E. E., and A. V. Manohar, 1991, Phys. Lett. B **255**, 558.
Jenkins, E. E., A. V. Manohar, J. W. Negele, and A. Walker-Loud, 2010, Phys. Rev. D **81**, 014502.
Jersak, J., C. Lang, and T. Neuhaus, 1996, Phys. Rev. D **54**, 6909.

Johnson, R., 1982, Phys. Lett. **114B**, 147.
Kambor, J., C. Wiesendanger, and D. Wyler, 1996, Nucl. Phys. **B465**, 215.
Kaplan, D. B., 1992, Phys. Lett. B **288**, 342.
Karsch, F., and I. Stamatescu, 1989, Phys. Lett. B **227**, 153.
Karsten, L. H., 1981, Phys. Lett. **104B**, 315.
Karsten, L. H., and J. Smit, 1981, Nucl. Phys. **B183**, 103.
Kennedy, A. D., and B. J. Pendleton, 1985, Phys. Lett. **156B**, 393.
Kerler, W., 1981, Phys. Rev. D **23**, 2384.
Kikukawa, Y., and A. Yamada, 1999, Nucl. Phys. **B547**, 413.
Kilcup, G. W., and S. R. Sharpe, 1987, Nucl. Phys. **B283**, 493.
Kim, S., and S. Ohta, 2000, Phys. Rev. D **61**, 074506.
Kim, S., and D. K. Sinclair, 1993, Phys. Rev. D **48**, 4408.
Kim, S., and D. K. Sinclair, 1995, Phys. Rev. D **52**, R2614.
Klassen, T. R., 1998, Nucl. Phys. **B533**, 557.
Klempt, E., and M. Richard, 2010, Rev. Mod. Phys. **82**, 1095.
Klempt, E., and A. Zaitsev, 2007, Phys. Rep. **454**, 1.
Kluberg-Stern, H., A. Morel, O. Napoly, and B. Petersson, 1983, Nucl. Phys. **B220**, 447.
Knechtli, F., and R. Sommer (ALPHA Collaboration), 1998, Phys. Lett. B **440**, 345.
Kogut, J. B., and C. G. Strouthos, 2005, Phys. Rev. D **71**, 094012.
Kogut, J. B., and L. Susskind, 1975, Phys. Rev. D **11**, 395.
Konig, A., K. H. Mutter, and K. Schilling, 1984, Phys. Lett. **147B**, 145.
Kovacs, T. G., 2003, Phys. Rev. D **67**, 094501.
Kunihiro, T., *et al.* (SCALAR Collaboration), 2004, Phys. Rev. D **70**, 034504.
Kunszt, Z., and I. Montvay, 1984, Phys. Lett. **139B**, 195.
Kuramashi, Y., M. Fukugita, H. Mino, M. Okawa, and A. Ukawa, 1993, Phys. Rev. Lett. **71**, 2387.
Kuramashi, Y., M. Fukugita, H. Mino, M. Okawa, and A. Ukawa, 1994, Phys. Rev. Lett. **72**, 3448.
Kurth, T., *et al.*, 2010, Proc. Sci., LATTICE2010, 232.
Kuti, J., 1982, Phys. Rev. Lett. **49**, 183.
Labrenz, J. N., and S. R. Sharpe, 1996, Phys. Rev. D **54**, 4595.
Lacock, P., A. McKerrell, C. Michael, I. M. Stopher, and P. W. Stephenson (UKQCD Collaboration), 1995, Phys. Rev. D **51**, 6403.
Lacock, P., C. Michael, P. Boyle, and P. Rowland (UKQCD Collaboration), 1996, Phys. Rev. D **54**, 6997.
Lacock, P., and C. Michael (UKQCD Collaboration), 1995, Phys. Rev. D **52**, 5213.
Lagae, J. F., and D. K. Sinclair, 1998, Phys. Rev. D **59**, 014511.
Landau, L. D., 1955, in *Niels Bohr and the Development of Physics*, edited by W. Pauli (Pergamon Press, London).
Lang, C. B., 2008, Prog. Part. Nucl. Phys. **61**, 35.
Langacker, P., and H. Pagels, 1974, Phys. Rev. D **10**, 2904.
Langguth, W., and I. Montvay, 1984, Phys. Lett. **145B**, 261.
Lasscock, B. G., *et al.*, 2007, Phys. Rev. D **76**, 054510.
Lattes, C. M. G., H. Muirhead, G. P. S. Occhialini, and C. Powell, 1947, Nature (London) **159**, 694.
Lee, W.-J., and D. Weingarten, 1999, Phys. Rev. D **61**, 014015.
Leinweber, D. B., 1995, Phys. Rev. D **51**, 6383.
Leinweber, D. B., T. Draper, and R. M. Woloshyn, 1992, Phys. Rev. D **46**, 3067.
Leinweber, D. B., W. Melnitchouk, D. G. Richards, A. G. Williams, and J. M. Zanotti, 2005, Lect. Notes Phys. **663**, 71.
Lellouch, L., 2009, Proc. Sci., LATTICE2008, 015.
Lepage, G. P., 1999, Phys. Rev. D **59**, 074502.
Lepage, G. P., and P. B. Mackenzie, 1993, Phys. Rev. D **48**, 2250.
Lepage, P., 1998, Nucl. Phys. B, Proc. Suppl. **60**, 267.
Lesk, V. I., *et al.* (CP-PACS Collaboration), 2003, Phys. Rev. D **67**, 074503.
Leutwyler, H., 1996, Phys. Lett. B **378**, 313.
Lin, H.-W., *et al.* (Hadron Spectrum), 2009, Phys. Rev. D **79**, 034502.
Lipps, H., G. Martinelli, R. Petronzio, and F. Rapuano, 1983, Phys. Lett. **126B**, 250.
Loschmidt, J. J., 1865, Sitzungsberichte der kaiserlichen Akademie der Wissenschaften Wien **52**, 395.
Luscher, M., 1986a, Commun. Math. Phys. **104**, 177.
Luscher, M., 1986b, Commun. Math. Phys. **105**, 153.
Luscher, M., 1991a, Nucl. Phys. **B364**, 237.
Luscher, M., 1991b, Nucl. Phys. **B354**, 531.
Luscher, M., 1994, Nucl. Phys. **B418**, 637.
Luscher, M., 1998, Phys. Lett. B **428**, 342.
Luscher, M., 2003, J. High Energy Phys. 05, 052.
Luscher, M., 2004, Comput. Phys. Commun. **156**, 209.
Luscher, M., 2005, Comput. Phys. Commun. **165**, 199.
Luscher, M., 2007, J. High Energy Phys. 07, 081.
Luscher, M., 2010, Proc. Sci., LATTICE2010, 015.
Luscher, M., S. Sint, R. Sommer, P. Weisz, and U. Wolff, 1997, Nucl. Phys. **B491**, 323.
Luscher, M., R. Sommer, P. Weisz, and U. Wolff, 1994, Nucl. Phys. **B413**, 481.
Luscher, M., and P. Weisz, 1985a, Phys. Lett. **158B**, 250.
Luscher, M., and P. Weisz, 1985b, Commun. Math. Phys. **98**, 433.
Luscher, M., and P. Weisz, 1985c, Commun. Math. Phys. **97**, 59.
Luscher, M., and P. Weisz, 1996, Nucl. Phys. **B479**, 429.
Luscher, M., and U. Wolff, 1990, Nucl. Phys. **B339**, 222.
Mahbub, M. S., A. O. Cais, W. Kamleh, D. B. Leinweber, and A. G. Williams, 2010, Phys. Rev. D **82**, 094504.
Mahbub, M. S., W. Kamleh, D. B. Leinweber, A. O. Cais, and A. G. Williams, 2010a, Phys. Lett. B **693**, 351.
Mahbub, M. S., W. Kamleh, D. B. Leinweber, P. J. Moran, and A. G. Williams, 2010b, Proc. Sci., LATTICE2010, 112.
Mahbub, M. S., W. Kamleh, D. B. Leinweber, P. J. Moran, and A. G. Williams (CSSM Lattice Collaboration), 2010c, arXiv:1011.5724.
Mahbub, M. S., *et al.*, 2009a, Phys. Rev. D **80**, 054507.
Mahbub, M. S., *et al.*, 2009b, Phys. Lett. B **679**, 418.
Marinari, E., G. Parisi, and C. Rebbi, 1981a, Phys. Rev. Lett. **47**, 1795.
Marinari, E., G. Parisi, and C. Rebbi, 1981b, Nucl. Phys. **B190**, 734.
Martinelli, G., C. Omero, G. Parisi, and R. Petronzio, 1982, Phys. Lett. **117B**, 434.
Martinelli, G., C. T. Sachrajda, and A. Vladikas, 1991, Nucl. Phys. **B358**, 212.
Mathieu, V., N. Kochelev, and V. Vento, 2009, Int. J. Mod. Phys. E **18**, 1.
Mathur, N., *et al.*, 2005, Phys. Lett. B **605**, 137.
Mathur, N., *et al.*, 2007, Phys. Rev. D **76**, 114505.
Mathur, N., *et al.*, 2010, Proc. Sci., LATTICE2010, 114.
Mawhinney, R., 2010 (private communication).
McNeile, C., 2003, arXiv:hep-lat/0307027.
McNeile, C., 2007, Proc. Sci., LAT2007, 019.
McNeile, C., 2009, Nucl. Phys. B, Proc. Suppl. **186**, 264.
McNeile, C., C. Michael, and K. J. Sharkey (UKQCD Collaboration), 2001, Phys. Rev. D **65**, 014508.
McNeile, C., and C. Michael (UKQCD Collaboration), 2000, Phys. Lett. B **491**, 123.
McNeile, C., and C. Michael (UKQCD Collaboration), 2001, Phys. Rev. D **63**, 114503.
McNeile, C., and C. Michael (UKQCD Collaboration), 2006, Phys. Rev. D **74**, 014508.
McNeile, C., C. Michael, and C. Urbach (ETM Collaboration), 2009, Phys. Lett. B **674**, 286.

Meissner, U.-G., K. Polejaeva, and A. Rusetsky, 2011, Nucl. Phys. **B846**, 1.
Melnitchouk, W., *et al.*, 2003, Phys. Rev. D **67**, 114506.
Metropolis, N., A. W. Rosenbluth, M. N. Rosenbluth, A. H. Teller, and E. Teller, 1953, J. Chem. Phys. **21**, 1087.
Michael, C., 1985, Nucl. Phys. **B259**, 58.
Michael, C., and J. Peisa (UKQCD Collaboration), 1998, Phys. Rev. D **58**, 034506.
Mitra, P., 1983, Phys. Lett. **123B**, 77.
Mitra, P., and P. Weisz, 1983, Phys. Lett. **126B**, 355.
Montvay, I., 1984, Phys. Lett. **139B**, 70.
Montvay, I., 1987, Rev. Mod. Phys. **59**, 263.
Montvay, I., and G. Munster, 1994, *Cambridge Monographs on Mathematical Physics* (Cambridge University Press, Cambridge, England), p. 491.
Morningstar, C., and M. J. Peardon, 2004, Phys. Rev. D **69**, 054501.
Morningstar, C., *et al.*, 2010, AIP Conf. Proc. **1257**, 779.
Morningstar, C., *et al.*, 2011, Phys. Rev. D **83**, 114505.
Morrin, R., A. O. Cais, M. Peardon, S. M. Ryan, and J.-I. Skullerud, 2006, Phys. Rev. D **74**, 014505.
Naik, S., 1989, Nucl. Phys. **B316**, 238.
Nakamura, K., *et al.* (Particle Data Group), 2010, J. Phys. G **37**, 075021.
Narayanan, R., and H. Neuberger, 1993a, Phys. Rev. Lett. **71**, 3251.
Narayanan, R., and H. Neuberger, 1993b, Phys. Lett. B **302**, 62.
Narayanan, R., and H. Neuberger, 1994, Nucl. Phys. **B412**, 574.
Narayanan, R., and H. Neuberger, 1995, Nucl. Phys. **B443**, 305.
Necco, S., and R. Sommer, 2002, Nucl. Phys. **B622**, 328.
Neff, H., N. Eicker, T. Lippert, J. W. Negele, and K. Schilling, 2001, Phys. Rev. D **64**, 114509.
Nemoto, Y., N. Nakajima, H. Matsufuru, and H. Suganuma, 2003, Phys. Rev. D **68**, 094505.
Neuberger, H., 1998a, Phys. Rev. Lett. **81**, 4060.
Neuberger, H., 1998b, Phys. Lett. B **417**, 141.
Neuberger, H., 1998c, Phys. Lett. B **427**, 353.
Nielsen, H. B., and M. Ninomiya, 1981a, Nucl. Phys. **B185**, 20.
Nielsen, H. B., and M. Ninomiya, 1981b, Nucl. Phys. **B193**, 173.
Nielsen, H. B., and M. Ninomiya, 1981c, Phys. Lett. **105B**, 219.
Noaki, J., *et al.* (TWQCD Collaboration), Proc. Sci., LAT2009, 096.
Omelyan, I. P., I. M. Mryglod, and R. Folk, 2002a, Phys. Rev. E **66**, 026701.
Omelyan, I. P., I. M. Mryglod, and R. Folk, 2002b, Phys. Rev. E **65**, 056706.
Omelyan, I. P., I. M. Mryglod, and R. Folk, 2003, Comput. Phys. Commun. **151**, 272.
Orginos, K., and D. Toussaint (MILC Collaboration), 1998, Phys. Rev. D **59**, 014501.
Orginos, K., D. Toussaint, and R. L. Sugar (MILC Collaboration), 1999, Phys. Rev. D **60**, 054503.
Otto, S. W., and J. D. Stack, 1984, Phys. Rev. Lett. **52**, 2328.
Parisi, G., 1980, *Recent Progresses in Gauge Theories*, Lecture Note Phys. Vol. 49 (World Scientific, Singapore), p. 349.
Patel, A., R. Gupta, G. W. Kilcup, and S. R. Sharpe, 1989, Phys. Lett. B **225**, 398.
Peardon, M., *et al.* (Hadron Spectrum), 2009, Phys. Rev. D **80**, 054506.
Pena, C., S. Sint, and A. Vladikas, 2004, J. High Energy Phys. 09, 069.
Pietarinen, E., 1981, Nucl. Phys. **B190**, 349.
Polchinski, J., 1998, *String Theory. Vol. 1: An Introduction to the Bosonic String* (Cambridge University Press, Cambridge, England).
Politzer, H. D., 1973, Phys. Rev. Lett. **30**, 1346.
Politzer, H. D., 1984, Nucl. Phys. **B236**, 1.
Polonyi, J., and H. W. Wyld, 1983, Phys. Rev. Lett. **51**, 2257.
Portelli, A., *et al.* (Budapest-Marseille-Wuppertal Collaboration), 2010, Proc. Sci., LATTICE2010, 121.
Prelovsek, S., 2006, Phys. Rev. D **73**, 014506.
Prelovsek, S., C. Dawson, T. Izubuchi, K. Orginos, and A. Soni, 2004, Phys. Rev. D **70**, 094503.
Prelovsek, S., *et al.*, 2010, Phys. Rev. D **82**, 094507.
Press, W. H., S. A. Teukolsky, W. T. Vetterling, and B. P. Flannery, 2007, *Numerical Recipes: The Art of Scientific Computing* (Cambridge University Press, Cambridge, England), 3rd ed.
Prout, W., 1815, Annals of Philosophy **6**, 321.
Rebbi, C., 1987, Phys. Lett. B **186**, 200.
Rochester, G. D., and C. C. Butler, 1947, Nature (London) **160**, 855.
Rothe, H. J., 2005, *Lattice Gauge Theories: An Introduction* (World Scientific, Singapore).
Rummukainen, K., and S. A. Gottlieb, 1995, Nucl. Phys. **B450**, 397.
Rutherford, E., 1911, Philos. Mag. **21**, 669, Series 6.
Rutherford, E., 1919, Philos. Mag. **37**, 581, Series 6.
Sasaki, K., and S. Sasaki, 2005, Phys. Rev. D **72**, 034502.
Sasaki, K., S. Sasaki, and T. Hatsuda, 2005, Phys. Lett. B **623**, 208.
Sasaki, S., T. Blum, and S. Ohta, 2002, Phys. Rev. D **65**, 074503.
Savage, M. J., 2002, Nucl. Phys. **A700**, 359.
Scalapino, D. J., and R. L. Sugar, 1981, Phys. Rev. Lett. **46**, 519.
Schaefer, S., R. Sommer, and F. Virotta (ALPHA Collaboration), 2011, Nucl. Phys. **B845**, 93.
Schierholz, G., 2010 (private communication).
Scorzato, L., 2004, Eur. Phys. J. C **37**, 445.
Seriff, A. J., R. B. Leighton, C. Hsiao, E. W. Cowan, and C. D. Anderson, 1950, Phys. Rev. **78**, 290.
Setoodeh, R., C. T. H. Davies, and I. M. Barbour, 1988, Phys. Lett. B **213**, 195.
Sexton, J. C., and D. H. Weingarten, 1992, Nucl. Phys. **B380**, 665.
Shamir, Y., 1993, Nucl. Phys. **B406**, 90.
Shamir, Y., 2007, Phys. Rev. D **75**, 054503.
Sharatchandra, H. S., H. J. Thun, and P. Weisz, 1981, Nucl. Phys. **B192**, 205.
Sharpe, S. R., 2006, Proc. Sci., LAT2006, 022.
Sharpe, S., and R. Singleton, Jr., 1998, Phys. Rev. D **58**, 074501.
Sheikholeslami, B., and R. Wohlert, 1985, Nucl. Phys. **B259**, 572.
Shindler, A. A., 2008, Phys. Rep. **461**, 37.
Slavnov, A. A., 1996, Phys. Lett. B **366**, 253.
Smit, J., 2002, *Introduction to Quantum Fields on a Lattice: A Robust Mate* (Cambridge University Press, Cambridge, England).
Smit, J., and J. C. Vink, 1987, Nucl. Phys. **B286**, 485.
Sommer, R., 1994, Nucl. Phys. **B411**, 839.
Sommer, R., F. Tekin, and U. Wolff, 2010, Proc. Sci., LATTICE2010, 241.
Stathopoulos, A., and K. Orginos, 2007, arXiv:0707.0131.
Stephenson, M., C. E. Detar, T. A. DeGrand, and A. Hasenfratz, 2000, Phys. Rev. D **63**, 034501.
Sternbeck, A., E.-M. Ilgenfritz, W. Kerler, M. Muller-Preussker, and H. Stuben, 2004, Nucl. Phys. B, Proc. Suppl. **129–130**, 898.
Susskind, L., 1977, Phys. Rev. D **16**, 3031.
Symanzik, K., 1983a, Nucl. Phys. **B226**, 187.
Symanzik, K., 1983b, Nucl. Phys. **B226**, 205.
Takahashi, T. T., and M. Oka, 2010, Phys. Rev. D **81**, 034505.
Takaishi, T., 1996, Phys. Rev. D **54**, 1050.
Takaishi, T., and P. de Forcrand, 2006, Phys. Rev. E **73**, 036706.
Tekin, F., R. Sommer, and U. Wolff (ALPHA Collaboration), 2010, Nucl. Phys. **B840**, 114.
Teper, M. J., 1998, arXiv:hep-th/9812187.
Thomson, J. J., 1907, Philos. Mag. **13**, 561, Series 6.
't Hooft, G., and M. J. G. Veltman, 1972, Nucl. Phys. **B44**, 189.

Ukawa, A. (CP-PACS and JLQCD Collaborations), 2002, Nucl. Phys. B, Proc. Suppl. **106–107**, 195.
Umeda, T., *et al.* (CP-PACS Collaboration), 2003, Phys. Rev. D **68**, 034503.
Urech, R., 1995, Nucl. Phys. **B433**, 234.
van den Doel, C., and J. Smit, 1983, Nucl. Phys. **B228**, 122.
van den Eshof, J., A. Frommer, T. Lippert, K. Schilling, and H. A. van der Vorst, 2002, Comput. Phys. Commun. **146**, 203.
Van Nieuwenhuizen, P., 1981, Phys. Rep. **68**, 189.
Vink, J. C., 1988, Nucl. Phys. **B307**, 549.
Vranas, P. M., 2006, Phys. Rev. D **74**, 034512.
Wada, H., *et al.*, 2007, Phys. Lett. B **652**, 250.
Walker-Loud, A., *et al.*, 2009, Phys. Rev. D **79**, 054502.
Weinberg, S., 1979, Physica A (Amsterdam) **96**, 327.
Weingarten, D., 1982, Phys. Lett. **109B**, 57.
Weingarten, D., 1983, Nucl. Phys. **B215**, 1.
Weingarten, D. H., and D. N. Petcher, 1981, Phys. Lett. **99B**, 333.
Weisz, P., 1983, Nucl. Phys. **B212**, 1.
Wien, W., 1902, Ann. Phys. (Leipzig) **313**, 244.
Wilcox, W., 1999, arXiv:hep-lat/9911013.
Wilczek, F., 1987, Phys. Rev. Lett. **59**, 2397.
Wilson, K. G., 1974, Phys. Rev. D **10**, 2445.
Wilson, K. G., 1975, *Proceedings of the First Half of the 1975 International School of Subnuclear Physics, Erice, Sicily*, edited by A. Zichichi (Plenum Press, New York), p. 69.
Wilson, K. G., 2005, Nucl. Phys. B, Proc. Suppl. **140**, 3.
Wohlert, R., 1987, Report No. DESY 87/069.
Zanotti, J. M., *et al.* (CSSM Lattice Collaboration), 2002, Phys. Rev. D **65**, 074507.